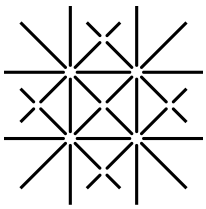

Towards an Understanding of CFTR Regulation by ATP Hydrolysis

INAUGURALDISSERTATION

zur

Erlangung der Würde eines Doktors der Philosophie

vorgelegt der Philosophisch-Naturwissenschaftlichen Fakultät

der Universität Basel

von

Matthias Zwick

aus Straubing, Deutschland

Basel 2012

Genehmigt von der Philosophisch-Naturwissenschaftlichen Fakultät auf Antrag von

Prof. Dr. Anna Seelig

Prof. Dr. Timm Maier

Basel, den 21.2.2012

_____

Prof. Dr. Martin Spiess (Dekan)

Table of Contents

Summary

The cystic fibrosis transmembrane conductance regulator (CFTR) belongs to the protein family of ATP binding cassette (ABC) transporters. However, its function is unique. CFTR has not been described as a transporter of large molecules like for example P-glycoprotein (Pgp) but instead functions as an anion channel allowing passive diffusion of mainly chloride and bicarbonate. Channel opening depends on the phosphorylation state of a regulatory domain and is additionally stimulated in the presence of ATP. The nucleotide binding domains of CFTR can bind this ATP and it has been shown that CFTR hydrolyzes ATP. While a lot is known about the channel conductance only little data about ATPase activity is available and therefore the coupling of both functions is not yet well understood. The general aim of this thesis was to measure CFTR-ATPase in living cells employing microphysiometry. As the main advantage, protein function in this assay is monitored in a native environment where cellular regulation mechanisms are kept intact and artifacts due to purification and reconstitution of the protein can be excluded. However, microphysiometry provides an indirect measurement and only changes in ATPase activity can be monitored. In the first part of the current study, we investigated how the phosphorylation process via protein kinase A (PKA) is reflected in this assay. For that we compared the effect of a cell permeable cyclic adenosine-monophosphate (cAMP) analogon and stimulation of cellular cAMP production on Chinese hamster ovary (CHO) and baby hamster kidney (BHK) cell lines overexpressing functional and defective human *CFTR* variants. We detected an increased ATP consumption that depends on the presence of functional CFTR and is sensitive to protein kinase A inhibition. Furthermore the results could be fitted with an equation describing PKA activation and an apparent $K_{d,app}$ value consistent with findings for purified PKA. We therefore concluded that we indeed monitor the activation of CFTR by phosphorylation. However, we could not clarify whether we are monitoring mainly ATP consumption by PKA or by CFTR itself. Nevertheless, we could show in this part that microphysiometry can be used to detect the presence of functional CFTR. As two thirds of all cystic fibrosis cases are caused by a mutation, *ΔF508*, resulting in impaired trafficking to the membrane and rapid degradation of CFTR, reliable label-free assays for detection of functional CFTR are of great interest. Microphysiometry could therefore prove useful in the search for CFTR trafficking correctors.

In the second part of this thesis, we focused on inhibitors and so called potentiators of CFTR chloride conductance. These compounds supposedly bind directly to CFTR and are at least partially known as substrates of other ABC transporters. We found that channel inhibitors cause concentration dependent changes in ATP consumption that are again specific for the presence of functional CFTR. In contrast to the phosphorylation agents investigated in the first part, an indirect mechanism via PKA could be excluded. The observed effects could be well described by a two-site binding model developed earlier for the Pgp-ATPase activity. These findings suggested that we were indeed monitoring ATPase activity of CFTR. The results for potentiators were ambiguous, as the readout was dominated by unspecific effects. However, we could conclude that ATPase activity was probably not stimulated. As our assumptions are based on similarities between ABC transporters, knowledge about the ATPase modulation of other transporters by the tested compounds was essential. Although some of the tested compounds had been identified as ABC transporter substrates before, only little information was available about the modulation of ATPase activity in these cases. Furthermore the supposedly specific CFTR inhibitors, CFTRinh-172 and PPQ-102, had not even been described as transporter substrates before. Therefore we studied their influence on ATPase activity of Pgp and the breast cancer resistance protein (BCRP) in inside-out membrane vesicles. All of these compounds indeed caused bell-shaped ATPase-activity stimulation in at least one of the tested transporters and supported earlier findings that amphiphilic neutral compounds stimulate Pgp-ATPase whereas non-amphiphilic compounds inhibit. Substrate binding in these transporters is a two-step process and compounds need to partition first into the membrane where they bind to the transporter from the cytosolic leaflet of the lipid bilayer. To be able to distinguish between these binding steps, we measured air-water partition coefficients, K_{aw}, in surface activity measurements and predicted the cross-sectional area A_D of the molecules in the most amphiphilic conformation, i.e. the conformation that is adopted for entry into the membrane. From these parameters we could calculate the lipid water partition coefficient, K_{lw}. The apparent transporter-water binding constant, K_{tw}, under steady-state conditions could be estimated from the concentrations of half-maximum activation of ATP hydrolysis. These parameters and the corresponding free enthalpies allowed us to calculate also the actual transporter-lipid binding constant, K_{tl}. Based on these parameters we could show that the observed effects on CFTR can be reasonably explained by the same mechanism for substrate-transporter interaction as in Pgp and that CFTR inhibitors are amphiphilic compounds while most potentiators are rather non-amphiphilic. We therefore proposed a model for ATPase activity modulation of

CFTR and suggested that CFTR resembles Pgp as the ATPase is stimulated by amphiphilic compounds whereas activity is inhibited by non-amphiphilic compounds. However, Pgp and CFTR differ concerning binding of charged molecules as Pgp does not transport anionic compounds. From a comparison with effects on channel conductance, we could furthermore conclude that stimulation of ATPase activity might be the common mechanism for inhibition by the structurally divergent inhibitors. The proposed two-site binding model could also well explain earlier findings that high concentrations of potentiators had inhibitory effects. In the last part of the current study we employed the microphysiometry assay to investigate the effect of steroid hormones on CFTR. Both potentiation and inhibition of CFTR currents had been reported for 17β-estradiol and the estrogen receptor antagonist tamoxifen before, while no data was available for cortisol and progesterone. However, all of these compounds are known as Pgp substrates. We could distinguish between CFTR specific ATPase stimulation, reversible unspecific effects and an additional irreversible cytotoxic effect only seen for tamoxifen. Therefore high concentrations of the latter could not be tested but no effects were observed at low concentrations. Cortisol and progesterone resembled CFTR inhibitors as stimulation of CFTR-ATPase exhibited a bell-shaped concentration dependency. Measurements with estradiol also revealed a slightly stimulating effect but results were dominated by reversible unspecific effects as seen before for potentiators. The findings support the soundness of our assumptions made above, as again more pronounced specific stimulation of CFTR-ATPase was observed for more amphiphilic compounds. Assuming that hydrogen bonds determine interaction between modulators and CFTR, the effects of steroid hormones showed that not only hydrogen bond acceptors but also hydrogen bond donors, i.e. hydroxyl groups, of modulator molecules are important. Based on our results we proposed that cortisol and progesterone could be inhibitors while estradiol potentiates at low and inhibits at high concentrations, which is in line with the aforementioned findings for estradiol.

In conclusion we could establish label-free assays to monitor phosphorylation of CFTR and CFTR-ATPase activity in living cells. We could show that modulators most likely bind to CFTR via similar mechanisms as described before for the interaction between substrates and other ABC transporters. Comparison of the results with effects on channel conductance finally allowed us to propose that the action of CFTR potentiators and inhibitors is based on drug induced ATPase activity changes and can be explained with the same two-site binding model introduced earlier for Pgp.

1 Introduction

1.1 ABC Transporters

ATP **b**inding **c**assette (ABC) transporters are one of the largest protein families. The PFAM database currently lists 237000 sequences from almost 5000 species that contain the ABC transporter signature domain (1). They can be found in virtually all species from archaea to mammals and can transport a wide variety of substrates (2-4). The family contains importers as well as exporters and also proteins that have not been associated with a transport function so far. Some of the latter seem to act only as regulators of other proteins, as for example the sulfonylurea receptors (SUR1 and SUR2) that influence the function of potassium channels (5). Despite their differing function, ABC transporters share a similar domain architecture. All of them comprise at least one **n**ucleotide **b**inding **d**omain (NBD) and a **t**rans**m**embrane **d**omain (TMD). Proteins with such a minimal ABC transporter architecture, like for example Sav1866 from *S. aureus,* most likely function only as a dimer (6,7). More evolved ABC transporters, however, contain 2 NBDs and 2 TMDs on a single polypeptide chain (3), resulting in a TMD1-NBD1-TMD2-NBD2 domain arrangement, with the NBDs oriented towards the cytoplasm. While the NBD sequence is highly conserved among these proteins (8), the TMD sequences differ drastically reflecting the differences in substrate specificity. The ABC transporters were therefore classified according to a conserved motif in the NBDs, the ABC transporter signature motif LSGGQ. Besides this unique motif, the sequence contains the Walker A and B motifs known from other ATPases that are also highly conserved and important for ATP hydrolysis. ATP binding and hydrolysis at the NBDs has been well characterized for many ABC transporters and was shown to drive conformational changes in the TMDs which are most likely involved in the transport process (3).

In humans, 49 ABC transporters (9) are known to date that have been classified into seven families (A-G) by the human genome organization (10). Two of these families, ABCE and ABCF, are most likely not involved in any transport as they lack the presence of transmembrane regions. ABCD comprises transporters only expressed in the peroxisomes and involved in fatty acid export. Subfamily A contains ABCA1 which is involved in cholesterol homeostasis and the formation of HDL lipoprotein particles. The most prominent member of the ABCB family is P-glycoprotein (Pgp, ABCB1). It is well characterized as an exporter with a broad specificity conferring multidrug

resistance to cancer cells and contributing to the blood-brain barrier. A similar function was also attributed to ABCG2, the **b**reast **c**ancer **r**esistance **p**rotein (BCRP). The ABCC subfamily finally contains also proteins characterized as contributors to multidrug resistance. In contrast to the other classes, these exporters have been mainly described as specific for large organic anions and drug-glutathione conjugates. The subfamily also comprises the aforementioned sulfonylurea receptors (3). In this study we will focus on a member of the ABCC family with another unique function, the **c**ystic **f**ibrosis **t**ransmembrane **c**onductance **r**egulator (CFTR, ABCC7).

1.2 Structure and Function of CFTR

The *CFTR* gene codes for a 1480 amino acid protein and was first identified as the gene mutated in patients suffering from cystic fibrosis (11). It is the only member of the ABCC family known so far that functions as a chloride channel (12). Different domain architectures can be found among ABCC proteins. Some comprise the TMD1-NBD1-TMD2-NBD2 architecture described above (MRP4-7 and CFTR) others contain an additional TMD (MRP1-3) that does not seem to be involved in transport. CFTR, however, is the only example among the entire ABC superfamily known to date that contains an additional regulatory domain (RD) resulting in the domain organization TMD1-NBD1-RD-TMD2-NBD2 (Fig. 1). As in most human ABC transporters, the TMDs comprise 6 transmembrane helices each. The RD contains several phosphorylation sites and these sites are mainly phosphorylated by cAMP dependent protein kinase A (PKA) although other kinases might play a role as well (13,14). No high-resolution structure of CFTR is available to date. However, X-ray structures of the isolated NBDs have been resolved (15,16) as well as a low-resolution electron-crystallography structure of the holoenzyme (17). From these fragments and from molecular models based on the recently crystallized Sav1866 or MsbA (18-20) several conclusions could be drawn. Overall, it has been found that the architecture of CFTR is indeed similar to other ABC transporters like Pgp.

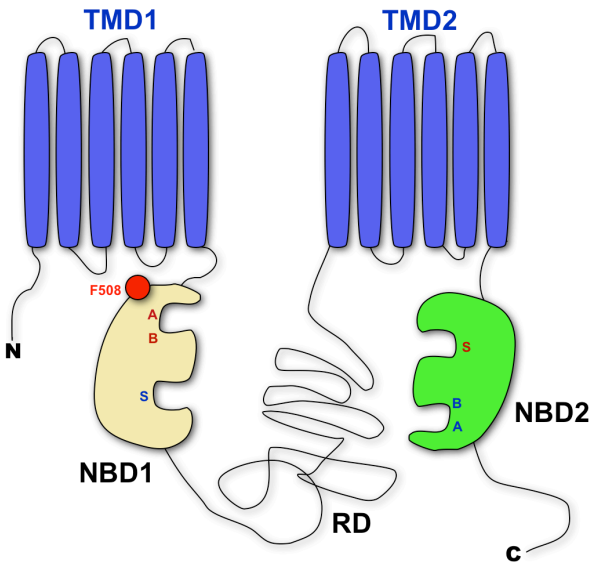

Figure 1: Domain architecture of CFTR. TMD1-NBD1 and TMD2-NBD2 are connected by the disordered RD. The NBDs form two nucleotide binding pockets. Each NBD contributes to both pockets with either the signature motif (S) or the Walker motifs (A, B). However, one binding pocket bears mutations in catalytically important residues (indicated by red letters). The position of phenylalanine 508 that is deleted in the *CFTR* gene of many cystic fibrosis patients (see section 1.5) is also shown.

The overlap with other ABC transporters includes a head-to-tail arrangement of the NBDs where each nucleotide binding site bears contributions from both NBDs i.e. each site is composed of the Walker motifs of one NBD and the signature motif of the other. Similar to all other ABCC proteins one of the sites lacks important catalytic residues in all motifs resulting in only one catalytically active site while the other only binds ATP without hydrolyzing it (21). Due to the similarities, it was speculated that the inward-facing and outward-facing conformations seen before for ABC transporters like P-glycoprotein could correspond to the closed and open state of CFTR (22). Electron crystallography and homology models furthermore support the hypothesis of a pore formed by the transmembrane domains. In mutational studies several of these TMD residues that influence chloride conductance have been identified and might therefore be involved in pore formation. Cationic residues on the intracellular (R303, R352) (23) and extracellular end (R104, R117, R334, K335) (24,25) of the putative pore were found to play an important role for ion conductance. In contrast to the relatively clear picture of the NBDs and TMDs, less information is available about the structure of the RD. It has been proposed to be a largely disordered region and this could be confirmed by NMR studies (26). A recent molecular modeling study suggested that the RD adopts

a more defined conformation upon phosphorylation, and that this conformational change might drive a change in the TMDs towards the open conformation (27).
Besides chloride conductance, several other functions have been attributed to CFTR. First of all, CFTR seems to be a rather unspecific anion channel. Although primarily identified as a chloride channel, conductance was also observed for other anions. Most notably, CFTR was identified as a bicarbonate channel (28) and the conductance for iodide can be exploited for functional studies. A translocation of larger charged molecules like glutathione (29) or ATP was also reported (30). In addition to the channel functions, CFTR also regulates several other proteins like for example the epithelial Na^+ channel (ENaC) that is inhibited by CFTR. However, it is not yet fully understood whether this regulation occurs due to direct interactions or via an effect of altered chloride concentrations (31). Nevertheless, interaction of CFTR with other proteins is probably mainly mediated by a C-terminal PDZ-binding domain (32). Such direct interactions were shown for example with the family of Na^+/H^+ exchanger regulatory factors (NHERFs) (33).

1.3 Regulation of CFTR Channel Conductance

It has been found that the gating of CFTR is regulated by two processes: phosphorylation of the RD and ATP binding to the NBDs. The dependency of CFTR gating on the presence of ATP has been studied extensively. While for isolated NBDs adenylate kinase activity has been observed, full-length CFTR hydrolyzes ATP. As suggested from the sequence, ATP is probably only hydrolyzed at one nucleotide binding site, while the other site only binds ATP tightly (34). Most of the data correlating ATP binding and hydrolysis is not generated from direct measurements of ATPase activity, but inferred from single channel patch-clamp experiments. It was suggested that ATP binding induces channel opening. However, there are contradictory results, whether both sites take part in this process (35) or not (36). ATP hydrolysis and subsequent ADP dissociation on the other hand are involved in rapid channel closure as shown by inhibition of the hydrolytic cycle with vanadate or non-hydrolyzable nucleotide analogs (37). This corresponds also well with findings for the hydrolysis deficient mutant E1371S showing a prolonged channel open time (38). From these findings, a catalytic cycle as shown in Fig. 2 was proposed.

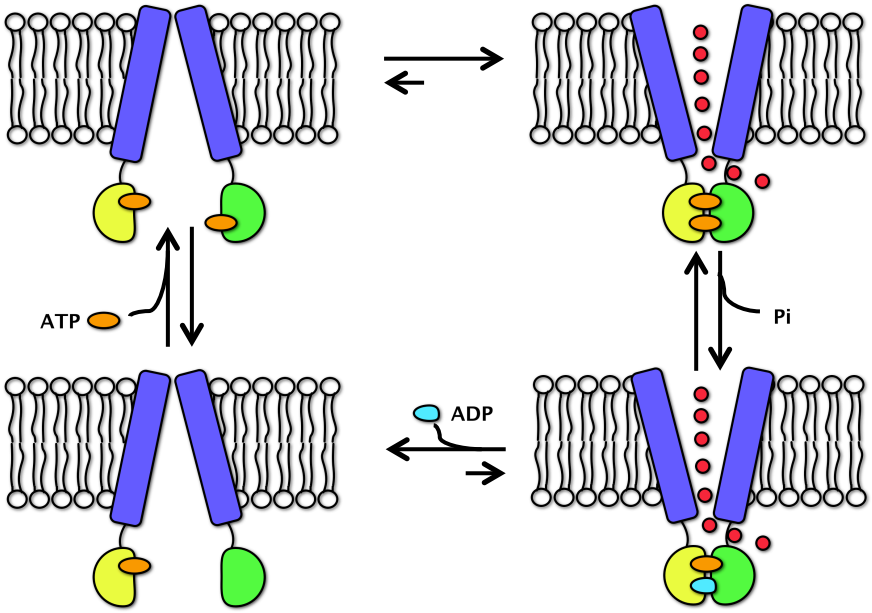

Figure 2: Mechanism of ATP dependent channel gating. The red circles symbolize chloride ions flowing down their gradient. It was assumed that two ATP molecules (orange) have to be present to induce dimerization of NBDs (yellow and green), but hydrolysis and subsequent dissociation of ADP (light blue) takes place only in one binding site, and the other ATP remains stably bound. The figure was adapted from (22).

Channel regulation via this catalytic cycle only takes place after preceding phosphorylation of CFTR in the RD. It is assumed that the unphosphorylated RD inhibits channel conductance. The hypothesis is supported by studies on a CFTR mutant lacking a large part of the RD. Csanády and colleagues could show that the corresponding channels are constitutively active (39). Although the actual mechanism is still unknown several characteristics of CFTR activation by phosphorylation have been described. The negative charges introduced via phosphorylation seem to be crucial as exchange of the serines and threonines in phosphorylation sites to negatively charged amino acids resulted again in constitutively opened channels (40). Moreover, the contribution of single phosphorylation sites seems to be additive. The removal of only single phosphorylation sites has little influence on channel conductance, and removal of several sites leads to different levels of activity (41). The contribution of the individual positions, however, seems to vary and it was even shown that some of the sites (S737 and S768) have inhibitory effects on channel conductance upon phosphorylation (42,43).

1.4 Tissue Distribution and Physiological Role of CFTR

CFTR is expressed in the apical membrane of exocrine epithelial cells. It is therefore found in a wide variety of organs. In the lung, CFTR is involved in maintaining proper fluidity of the airway surface liquid (ASL). The ASL consists of an outer layer, the viscous mucus, and a low-viscosity layer that separates the mucus from the cell surface. This second layer is called pericilliary liquid (PCL), as the cilia of lung epithelial cells are surrounded by this liquid (44). While the mucus acts as a trap for particles, ciliary motion is an important factor in actual clearance. Thus, maintenance of the low viscosity is crucial as it supports beating of the cilia (45). Chloride efflux through CFTR and inhibited sodium absorption due to CFTR dependent inhibition of ENaC as described above, leads to an increased salt concentration on the cell surface. As the epithelial cells are water permeable, water is therefore secreted into the ASL due to osmosis (46). A similar interplay between CFTR and ENaC was also found for sweat glands and thus maintenance of the correct salt concentration in excreted sweat (47,48).

The epithelial cells in the pancreatic duct secrete an alkaline fluid containing high concentrations of bicarbonate and CFTR has been identified as an important factor also in this secretion (49). However, it is still unclear whether this is a direct process due to its bicarbonate conductance or an effect of chloride gradients on bicarbonate/chloride exchangers (50). In colonic epithelial cells, an involvement of CFTR in both salt secretion and absorption is assumed (51) and CFTR is also expressed in gallbladder epithelia (52) and in the liver.

Apart from this well studied expression in epithelial cells, there is increasing evidence that it also plays a role in other cell types including for example macrophages (53) and even neurons (54).

1.5 CFTR Defects and Related Disorders

Considering the ubiquitous presence of CFTR, it is not surprising that defects of the protein lead to multifactorial disorders. The best known among these is cystic fibrosis (CF) which is one of the most common hereditary diseases among the Caucasian population. Although multiple organs are affected, pulmonary problems are among the most prominent symptoms of this disorder. Impaired chloride efflux through CFTR and probably also increased sodium influx through ENaC lead to a reduced PCL height. Therefore ciliary motion is impaired and the mucus is no longer separated from the epithelial cells. Both symptoms create an optimal environment for pathogen infection.

It is thus not surprising that mortality in CF is mainly associated with pulmonary disease and chronic inflammation caused by *P. aeruginosa* or *S. aureus.* (55). More than 95 % of the patients also suffer from pancreatic insufficiency, i.e. a lack of digestive enzymes, (56) and among male patients infertility due to obstructed or absent *vas deferens* can be often found. About two thirds of the CF cases are caused by a 3-base-pair deletion in exon 10 that leads to the lack of phenylalanine F508. This mutation leads to CFTR with defective folding, trafficking and decreased function. Although ΔF508 is probably the best investigated mutation, the cystic fibrosis mutation database (57) currently lists 1900 genetic variations associated with CF. To organize this vast amount of mutations a classification of mutations in the *CFTR* gene was introduced (58). Class I contains nonsense and frame-shift mutations leading to impaired protein production. Therefore only truncated versions or no CFTR at all is produced in that case. The above mentioned mutation ΔF508 belongs to class II, containing CFTR variants with impaired trafficking to the membrane. In the case of ΔF508 disruption of a contact between the NBDs and an intracellular loop of the TMDs (see Fig. 2) probably leads to incorrect folding. The protein is therefore rapidly degraded after translation through endoplasmic reticulum associated processes involving ubiquitinylation and the following proteasome pathway (59,60). Although ΔF508 also shows impaired function when reaching the membrane, CF symptoms are mainly caused due to the absence of functional protein in the membrane for these two classes. Class III mutations, in contrast, are characterized by the production of correctly folded CFTR that is present in the membrane but no longer regulated by ATP or cAMP. This class comprises several mutations in the nucleotide binding domains, including the signature motif variants G551D and G1349D. Class IV mutations result in CFTR with impaired ion conductance and are located mainly within the TMDs. Several of these mutations affect arginine residues (for example R334) that might contribute to the channel (61). Class V mutations lead to reduced levels of fully functional CFTR due to affected promoter and splicing regions. Lukacs and colleagues suggested an additional class VI comprising CFTR variants truncated at the C-terminus that are fully functional but are degraded 5-6 times faster than wildtype CFTR (62). Apart from CF, several other diseases were attributed to CFTR mutations despite the absence of classical CF symptoms. It was suggested recently that these diseases should be named CFTR related disorders (63). The most important of these disorders are congenital bilateral absence of *vas deferens*, pancreatitis and disseminated bronchiectasis.

While all of these diseases are related to impaired CFTR function, also fully functional CFTR is of clinical interest. As described above, CFTR in enterocytes plays a major role

in intestinal chloride and subsequent fluid secretion. In secretory diarrheas (64), such as cholera, intestinal fluid secretion is drastically increased. Evidence was found that cholera toxin from *V. cholerae* or STa toxin from *E. coli* stimulates CFTR dependent chloride secretion through the cAMP/PKA pathway (65). Besides diarrhea, an involvement of CFTR was also found for autosomal polycystic kidney disease. Patients with this disorder develop cysts in both kidneys that lead to enlarged dysfunctional kidneys. It has been described that cyst formation in that case is driven by fluid influx mediated through the same CFTR dependent mechanisms as described above (66).

1.6 Small Molecules as CFTR Modulators

Due to its involvement in the mentioned diseases, CFTR is an interesting drug target. CF research mainly focuses on two classes of CFTR modulators as potential drugs: correctors and potentiators. The former group comprises substances that can overcome the trafficking defect of class II mutants. Therefore at least two general mechanisms of action are possible: direct interaction with CFTR as a chemical chaperone and therefore stabilization of the correct conformation or indirect effects like upregulation of chaperones or inhibition of ubiquitinylation and therefore hindered degradation of misfolded CFTR. Many investigated substances seem to act through one of the latter mechanisms, as they have been shown to work in a cell type dependent manner (67). Only two correctors were identified so far that act independent of the cellular background: VRT-325 and Corr4a (Fig. 3) (67).

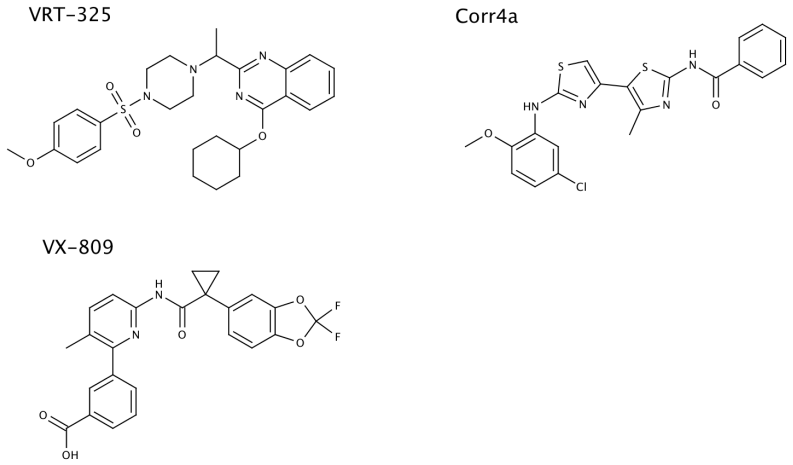

Figure 3: Structures of CFTR correctors

For the former, action as a chemical chaperone through direct interaction was suggested due to parallels to Pgp. In that case it was identified as a directly interacting inhibitor that also showed the potency to rescue misfolded Pgp (68). Similarly, interaction between corr4a and CFTR could only be shown indirectly in experiments where cross-linking of several residues in the TMDs was inhibited in the presence of corr4a (69). Interestingly, also additive effects of these compounds were found (70) which might either point to binding to different sites or effects on different steps in the maturation process. Correction through such pathways was for example suggested for the dietary compound curcumin. There is evidence that curcumin might act due to its ability to inhibit the sarcoplasmic/endoplasmic reticulum calcium pump (71) or through the keratin 18 network (72). However, the observed correction effects *in vitro* could not yet be shown in *in vivo* (73). The most promising compound is probably VX-809 (Fig. 3) that is currently in clinical trial phase IIa (74). First results, however, show that little beneficial effects were only observed for sweat chloride concentration, while other biomarkers and most notably lung function remained unaffected (75). This illustrates again a general problem in current corrector search, as most of the observed effects *in vitro* might be either too small or, as mentioned, highly cell type specific (67).

In contrast to correctors, potentiators increase the chloride conductance of CFTR present in the membrane. These compounds (examples shown in Fig. 4) are needed for class II and III mutations, as the former often results not only in hindered trafficking but also functional defects. Several dietary compounds have been identified with this function. Among these were capsaicin, several flavonoids like apigenin or genistein and again curcumin. Flavonoids and capsaicin are supposed to act via an equal mechanism (76). For genistein a direct interaction with CFTR was suggested (77) whereas an action via activation of kinases or inhibition of phosphatases could be excluded (78).

Such indirect mechanisms could be possible for potentiators and were shown for example for 3-isobutyl-1-methylxanthine (79). For flavonoids, furthermore a bell-shaped activation profile of chloride currents, i.e. activation at low and inhibition at high concentration was observed. Thus, flavonoids might act through more than one binding site (80,81). In general, it was concluded from electrophysiology data that potentiation occurs due to prolonged open time of the channel. Thus, for genistein and similar compounds a mechanism involving inhibited ATP hydrolysis was proposed and a drug binding site within the NBDs was suggested (82). However, there is no direct evidence from ATPase measurements to date. Interestingly, all of these compounds also interact with other ABC transporters. Apart from these natural compounds, recent advances have been made in high throughput screens. Two novel classes of

potentiators were identified: phenylglycines and sulfonamides (83,84). These compounds showed even higher affinity for CFTR than flavonoids and reduced the time between single-channel openings in CFTRΔF508. The most promising potentiator is probably ivacaftor (VX-770). It is currently in phase III clinical trials and beneficial effects have been detected for sweat chloride concentration and also for lung function of CF patients bearing the G551D mutation (85).

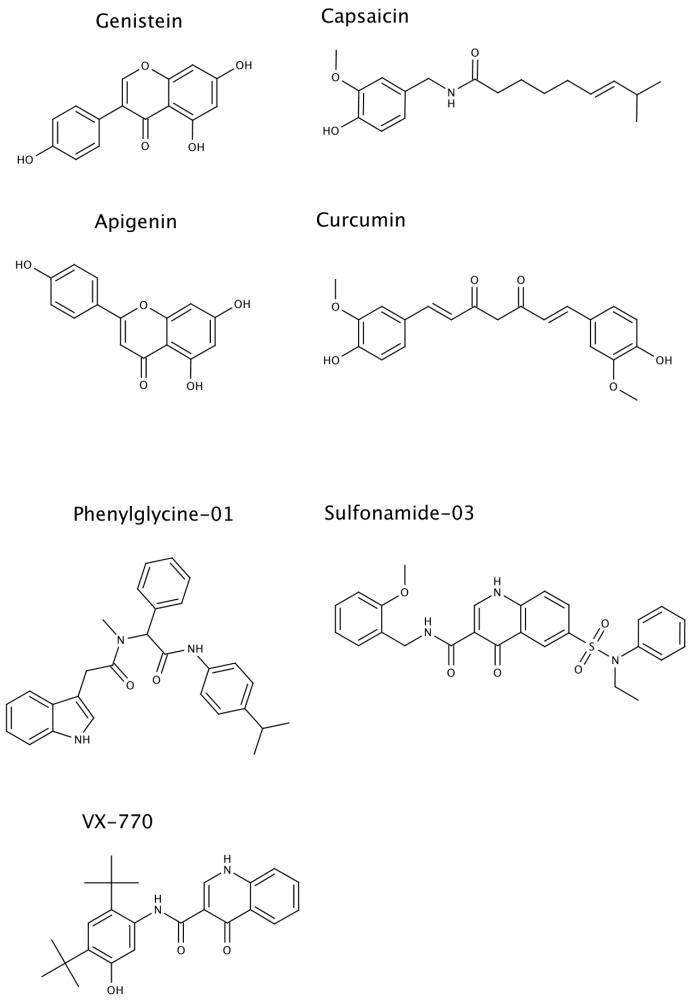

Figure 4: Structures of CFTR potentiators

Also CFTR inhibitors (examples shown in Fig. 5) are thoroughly investigated due to their proposed beneficial action in other CFTR related disorders. Additionally, CFTR inhibitors constitute useful tools in CF research. Two general principles of inhibitor action have been described so far. One compound, the glycine hydrazide GlyH-101, identified in a high-throughput screen (86), was found to most likely bind from the extracellular side to the open pore. It was furthermore supposed that GlyH-101 simply occludes the pore. Simple pore occlusion seems also likely for inhibitors acting on

multiple chloride channels like diphenylamine-2-carboxylate (87). For other CFTR inhibitors an allosteric mechanism was suggested (88). This class includes sulfonylurea compounds like glibenclamide or glipizide (89) and the recently identified more specific CFTR inhibitors CFTRinh-172 and PPQ-102 (90,91). CFTRinh-172 is probably the best investigated among these. It has been shown that the inhibitory action is most likely due to a reduction of mean channel open time (92) and that a residue within the TMDs, R347, is involved in binding of the inhibitor (93). While CFTRinh-172 and PPQ-102 are assumed to be rather specific for CFTR, sulfonylurea compounds have been shown to interact with several ABC transporters including Pgp (94), MRPs (95) and BCRP (96). Also the MRP substrates taurolithocholate-3-sulfate and 17-beta-estradiolglucuronide were identified as CFTR channel blockers.

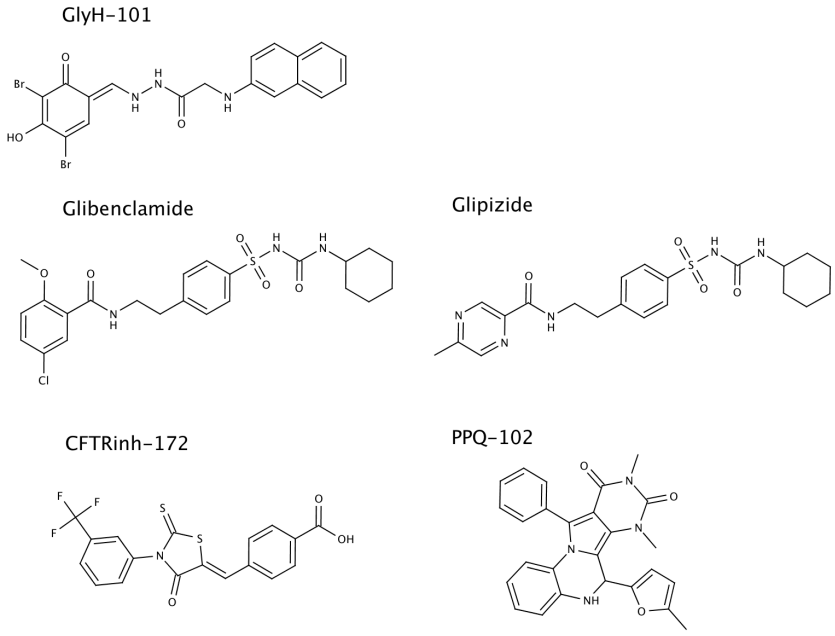

Figure 5: Structures of CFTR inhibitors

In summary, despite great efforts in identifying new modulators of CFTR function in recent years mainly in high throughput screenings, there is still a lack of understanding the mechanisms of action.

1.7 Substrate Binding to ABC Transporters

The interaction of substrates with Pgp has been investigated intensively. Various studies suggest that binding of substrates takes place in the cytosolic leaflet of the lipid bilayer (97-99). A recently solved medium resolution crystal structure indeed revealed a "portal" open to this part of the membrane in the nucleotide free conformation (100). Thus, compounds which bind to Pgp need to partition into the membrane first, a step favoring hydrophobic compounds. However, Pgp does not only transport hydrophobic compounds but also rather hydrophilic ones. It was shown by means of surface activity measurements that amphiphilicity of the molecules rather than hydrophobicity is the important factor (101). In these measurements partition of molecules into the air-water interface is detected. This interface is a good model for partitioning into a lipid membrane as the dielectric constant of air ($\varepsilon \approx 1$) is similar to the dielectric constant of a lipid environment ($\varepsilon \approx 2$). Substrate-transporter interaction within the lipid-bilayer leads to several implications for the actual binding step. First of all, drugs will accumulate in the lipid membrane depending on their hydrophobicity. Thus, the same bulk concentration of different compounds can lead to different concentrations in the membrane and binding from the aqueous phase to the transporter has to be viewed as a two-step mechanism comprising the lipid-water partitioning and the binding from the lipid phase to the transporter. Furthermore, compounds will be oriented along their amphiphilicity axis in a way that the hydrophobic part inserts into the membrane while the hydrophilic part interacts with the lipid head groups. As a third implication from binding events in the hydrophobic environment, electrostatic interactions will be greatly enhanced. Thus, even weak interactions such as between cations and the π-electrons of an aromatic ring become important. Also hydrogen bonds will significantly contribute to binding processes (102,103). A recent study on interaction of polyoxyethylene alkyl ethers with Pgp showed that the interaction with the transporter can be even exclusively due to hydrogen bonds and suggests that the hydrophobic part of a compound remains in the lipid while the hydrophilic part binds to the cavity of Pgp (104).

Despite the described evidence for the underlying mechanism of substrate-transporter interaction an actual substrate binding site could not be unambiguously localized. Most of the studies, however, agree that the binding occurs within the TMDs and that especially transmembrane helices TM5, TM6, TM11 and TM12 could be involved (105,106). Interactions of substrates with even more transmembrane helices were inferred from the recently solved crystal structure (100). The amino acid composition of putative binding sites furthermore supports the importance of hydrogen-bonding as

25 percent of the identified residues were aromatic (F, W, Y ,H) and about one third contained hydrogen bond donor groups (S, T, Y, W, Q, N) (107). The wide variety of substrates furthermore raises the question whether multiple binding sites exist. Two, three or even four binding sites were suggested by several research groups (108,109). In line, Pgp-ATPase activity is stimulated at low and inhibited at high-concentrations. This observation also points towards binding to different sites (110). In contrast to this mode of action, a different model was suggested assuming larger binding regions. Here, different substrates would create their own binding site by interaction with different residues within the transmembrane region (111). The idea of multiple, at least partially overlapping binding sites was also supported by the aforementioned study on substrate-transporter interaction with polyoxyethylene alkyl ethers. The study showed that the entry of the second molecule into the cavity was counteracted by steric effects that increased with the size of the molecules (104).

As mentioned in section 1.6, substrate specificity overlaps between different ABC transporters have been observed. This raises the question whether the principles of compound-transporter interaction described for Pgp might hold true for other ABC transporters as well. Several studies suggest that this could indeed be the case not only within the ABCB subfamily but throughout the entire group of ABC transporters. Contribution of TM1, TM2, TM3, TM5 and TM6 to substrate binding was for example observed for BCRP (ABCG2) (112,113) and charged residues within or close to TM6, TM7, TM8 and TM11 were identified as crucial for substrate binding to MRP1 (ABCC1) (114). A recent comparison between Pgp, SUR1 and SUR2 suggested not only similar binding region, but even a functional homology in terms of ATPase modulation although no transport by SUR1 and SUR2 has been observed (94).

1.8 Microphysiometry

In the current study we employed an approach based on the concept of microphysiometry introduced by McConnell and colleagues (115). Employing this technique, essentially the cell metabolism is detected with sensors integrated in a silicon chip. The most common parameter detected in such measurements is the extracellular acidification rate (ECAR). More recent approaches also exploit for example oxygen consumption rates (OCR) and cell adhesion (116). Measurements, however, are in principle always performed in the same way, independent of the actual readout. Cells are continuously flushed with medium or buffer. In certain time intervals

pumps are stopped for a few seconds to several minutes depending on the metabolic activity of the cell line, and the ECAR or OCR are recorded (Fig. 6).

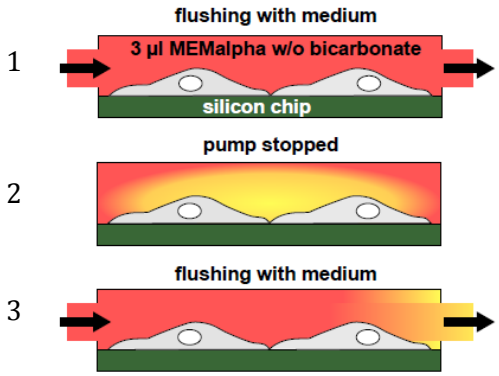

Figure 6: Schematic view of the microphysiometry assay. Cells are flushed with culture medium in a small chamber where $5 \cdot 10^6$ cells are surrounded by only approx. 3 µL medium with low buffer capacity (1). When the flow is stopped (2), the medium in the chamber gets acidified rapidly (yellow) and the pH change can be detected by sensors in the silicon chip. To maintain cell viability the acidified medium has to be flushed away (3).

In the case of ECAR detection, it is essential that a low buffer capacity of the flow medium is maintained, as the detected pH changes are low (below 0.1 pH unit) (115). It has been shown that the ECAR readout correlates to ATP production which is mainly due to glycolysis in cultured cells under mostly anaerobic conditions (117). This technique has been used successfully in the study of receptor mediated effects on cell metabolism (118) and it has been shown in our group that it can be used to detect the ATPase activity of P-glycoprotein (119).

2 Rationale and Aims of Research

As described in the introduction, CFTR is an important chloride channel in many tissues and is involved in salt excretion or uptake. As salt gradients can lead to osmosis driven water movements across cell membranes, CFTR controls the viscosity of mucus layers on epithelial cells in the lung or the colon (section 1.4). Thus, malfunction due to either mutations or to upregulation of CFTR function by extrinsic factors leads to multifactorial disorders like CF or secretory diarrheas (section 1.5). However, more than 20 years after the discovery of CFTR no CF drug targeting CFTR is available (section 1.6). Although the function of CFTR is known, regulation of channel gating by its ATPase function is still poorly understood. One reason for this could be that most of the measurements on channel function are performed in living cells and thus in a native environment, while the little amount of ATPase data available so far is generated employing reconstituted purified protein. Membrane proteins in general are, however, strongly influenced by their membrane environment and especially CFTR might behave differently when native regulation by protein kinases and phosphatases is kept intact. The aim of this study was to establish an ATPase assay for CFTR in a native-like environment and to investigate whether a correlation of ATPase activity and channel conductance can be inferred from the results. We therefore tested the applicability of an assay based on microphysiometry. The framework of the assay has been developed earlier in our group to measure Pgp-ATPase (119) and is based on the finding that an upregulation of ATP consumption is tightly coupled to an increase in cell metabolism that can be monitored by an elevated extracellular acidification. As described above (section 1.2), phosphorylation is a crucial step in the activation of CFTR. Therefore our first goal was to investigate whether this step can be monitored by microphysiometry in different cell lines overexpressing CFTR variants and whether CFTR specific signals can be distinguished from unspecific effects (summarized in 3.1, full report in 7.1). For that, we perfused the cells with compounds used in CFTR research to stimulate protein kinase A dependent phosphorylation and investigated whether the combination of ECAR and OCR measurements can help to exclude artifacts due to unspecific effects.

While little is known about the modulation of CFTR-ATPase by potentiators and inhibitors, the effect of substrates on the ATPase of P-glycoprotein is well understood and ATPase activity measured as a function of substrate concentrations leads to bell-shaped activity profiles (120). Our aim was to investigate whether compounds directly interacting with CFTR alter the ATPase activity and whether a similar effect as for

other ABC transporters can be observed. For that, we focused on CFTR inhibitors and potentiators that had been identified as ABC transporter substrates before (section 1.6) and tested whether supposedly specific CFTR modulators are in turn also substrates for the ABC transporters Pgp and BCRP (summarized in 3.2, full report in 7.2). This study revealed similarities between modulation of Pgp-ATPase and CFTR-ATPase. The similarities suggest that binding occurs due to the same mechanisms as for Pgp. Thus, the compounds probably need to enter the lipid membrane before binding to CFTR. Another goal of this study was therefore to distinguish between lipid binding and transporter binding of the tested compounds. Intrinsic binding constants and free enthalpies should be calculated and therefore air-water partition coefficients K_{aw} were measured by means of surface activity measurements and cross-sectional areas were predicted in order to calculate lipid-water partition coefficients K_{lw}. Considering the calculated binding constants and free enthalpies we can judge whether a similar involvement of hydrogen bonds in drug-transporter interaction, as seen for Pgp, is plausible.

In order to gain insight into the regulation of channel conductance by the observed ATPase modulation, it was also our aim to establish an assay that can be used to detect chloride conductance under similar conditions as used in the microphysiometer. An iodide efflux assay employing an iodide selective electrode was identified as an approach fulfilling these requirements and was thus used as described in section 3.1 and 3.2 (full reports in 7.1 and 7.2).

Finally, we tested whether we can use our approach to understand the action of compounds that are not yet well investigated in their effect on CFTR but known as substrates of Pgp or other ABC transporters. Steroid hormones for which effects in CF patients had been reported earlier and which are known as Pgp substrates, were characterized with respect to lipid-binding and stimulation of CFTR-ATPase as described above (summarized in 3.3, full report in 8.1).

3 Summary of Research Addressed

3.1 Monitoring CFTR Phosphorylation and ATPase Activity in Living Cells

The channel function of CFTR is regulated by phosphorylation of the RD and by ATP binding and hydrolysis at the NBDs (section 1.3 for details). Only little is known so far about the ATPase activity of CFTR, especially in its native environment. However, phosphorylation seems to be crucial for CFTR function. As it was the aim of the current study to establish an ATPase assay in living cells, we first of all investigated how different cell lines overexpressing CFTR variants respond to stimulation of protein kinase A and thus the basal activation step for CFTR. For that we studied the effects of the protein kinase A activating agents forskolin and 8-(4-Chlorophenylthio)-adenosine-3',5'-cyclic monophosphate (CPT-cAMP). The latter is a membrane permeable analog of cAMP and thus directly causes the dissociation of regulatory and catalytic subunits of PKA. Forskolin, in contrast, acts indirectly by stimulating adenylate cyclase and thus cAMP synthesis. In both cases two processes can cause a signal change in a microphysiometry measurement: (i) the ATP consumption due to the phosphogroup transferase activity of PKA (ATP + CFTR → phospho-CFTR + ADP) and (ii) ATP hydrolysis by CFTR. Production of cAMP by adenylate cyclase (ATP → cAMP + PP_i) might be detected as well, when forskolin is used. ATP consumption was measured as described in section 1.8 in a Cytosensor microphysiometer or the recently developed Bionas 2500 cell analyzer. While the former is only capable of ECAR measurements, the latter can additionally detect OCR but the sensitivity for ECAR recordings is lower. We could show that we can detect increased ATP consumption that is dependent on the concentration of CPT-cAMP or forskolin respectively and is, at least for low concentrations of the phosphorylation agents, exclusively observed in Chinese hamster ovary (CHO) or baby hamster kidney (BHK) cells overexpressing functional CFTR. Higher concentrations of both CPT-cAMP and forskolin also affect the ECAR of control cells, i.e. non-transfected cells and cells overexpressing the defective mutants *CFTR-ΔF508* and *CFTR-E1371S*. The absence of specific effects in measurements with these mutants allowed us to exclude that ECAR was stimulated due to altered cell metabolism potentially caused by the transfection. The results raised the question whether the observed ECAR changes reflect stimulation of CFTR via PKA or whether we monitor stimulation of ATPase due to direct binding of phosphorylation agents to CFTR. The observed signal was sensitive to PKA inhibition and the results could be

described by a model for PKA activation with a similar apparent $K_{d,app}$ as observed earlier for purified PKA. Therefore, we concluded that we indeed monitor CFTR phosphorylation. As PKA inhibition did not abolish the signal completely, we investigated whether a direct interaction of the phosphorylation agents with CFTR would be possible due to the principles of substrate binding to ABC transporters described in section 1.7. For that surface activity measurements and predictions of cross-sectional area and amphiphilicity were performed. We could show that a direct interaction between CFTR and these agents would be plausible based on compound properties. However, the determined values for the lipid-water partition coefficient K_{lw} are not consistent with the observed high concentrations of half-maximal activation for CPT-cAMP. Thus, we could not exclude that these interactions are involved, however the measurements were again more in favor of our assumption that we were monitoring mainly CFTR activation via phosphorylation. We also observed strong inhibition of ECAR especially at high concentrations of forskolin. As this effect correlated with earlier findings that forskolin inhibits glucose import under these conditions, we tested whether it is possible to identify this kind of unspecific effects on the basis of oxygen consumption measurements. We could indeed show that cells switch from glycolysis to oxygen consumption under these conditions.
In summary, this part showed that microphysiometry could be used to monitor the activation of functional CFTR via phosphorylation in a label-free non-invasive way. The absence of signals in cells expressing *CFTR*-Δ*F508* suggests that this assay can also help to detect the presence of functional CFTR in the membrane and therefore could prove useful in corrector screening. In this study, the results were used as a basis for measurements of more specific CFTR modulators and CHO cells were chosen due to the greater signals and thus better signal to noise ratio (section 3.2 and 6.2).

The results are described in detail in the following unpublished manuscript in section 7.1 (p. 41): *Zwick M., Hellstern M., Seelig A: "Monitoring Phosphorylation of CFTR in Living Cells via Microphysiometry"*

3.2 CFTR-ATPase Activity Modulated by Inhibitors and Potentiators

In this section, we investigated the effects of compounds directly interacting with CFTR on the ECAR of CHO-CFTR after preceding phosphorylation. For that, known inhibitors and potentiators of CFTR were chosen. We focused especially on compounds that were known to interact with other ABC transporters (flavonoids, curcumin, capsaicin,

glibenclamide, glipizide) but also included two potentially specific inhibitors of CFTR (CFTRinh-172, PPQ-102). ECAR measurements were carried out upon prestimulation with CPT-cAMP (5 – 100 µM). While all of the inhibitors lead to CFTR specific bell-shaped ECAR vs. inhibitor concentration profiles, measurements with potentiators were dominated by unspecific effects on both transfected and control cell lines. As ECAR changes correspond to ATP consumption, we detected a CFTR specific ATP consumption caused by compounds that are not affecting the PKA pathway but are known to interact directly with CFTR. As these effects furthermore resembled the bell-shaped ATPase-activity profiles seen for ABC transporters, we assumed that we were indeed monitoring CFTR-ATPase. Moreover, the concentration of half-maximum activation, K_1, was shifted depending on the CPT-cAMP concentration. This observation is in line with earlier findings on CFTR modulators by others. As substrate specificities of ABC transporters often overlap, one would expect that these compounds also influence ATPase activity of other ABC transporters. However, two of the tested compounds have not yet been described as transporter substrates and for most of the others no data on actual ATPase activity modulation of Pgp and BCRP was available. Therefore we characterized these compounds by means of Pgp- and BCRP-ATPase activity assays in inside-out vesicles. We could show that all of them, potentiators and inhibitors, were indeed modulating the ATPase activity of at least one of these transporters. Since binding to Pgp and BCRP involves two steps, i.e. partitioning into the membrane followed by the actual binding to the transporter (section 1.7), we carried out surface activity measurements and predictions of the cross-sectional area and amphiphilicity of the investigated compounds. Based on these parameters, we were able to separate ΔG_{tl} (free enthalpy of transporter-lipid binding) and ΔG_{lw} (free enthalpy of lipid-water partitioning) and we could show that a similar interaction determined by amphiphilicity and partially also by hydrogen-bonding can account for the observed effects on CFTR-ATPase activity. The modulator interaction with CFTR resembles substrate binding to Pgp in terms of amphiphilicity and to MRPs in terms of charge. The amphiphilic inhibitors thus activate ATPase activity while the non-amphiphilic potentiators inhibit. However, while Pgp only accepts neutral or cationic compounds as substrates, CFTR can bind neutral or anionic compounds. In order to develop a model for channel regulation by ATP hydrolysis, we needed to correlate our ATPase data to channel conductance. We compared our data to results on channel conductance found in literature and carried out iodide efflux experiments under conditions that have not yet been tested before. We were especially interested how activation and inhibition of ATPase activity influences channel conductance. Our

results show that the inhibitory branch of the activation curves corresponds to channel blocking. The increase in ATPase activity at lower inhibitor concentrations could not be attributed to a stimulation of channel conductance, as either no effect was observed on iodide efflux or even inhibition had been reported earlier under these conditions. Therefore we proposed the following model: In analogy to Pgp, amphiphilic inhibitors bind to the closed state of channel and induce opening at low concentrations when only the first binding site is occupied. They are easily flopped over the membrane and dissociate rapidly leading to fast resetting of the channel to the closed state and thus no stimulation of chloride conductance or even inhibition occurs. Non-amphiphilic potentiators similarly induce opening due to binding but are flopped slowly and therefore CFTR remains open for a longer time span. These findings are in accordance with earlier hypotheses proposing that inhibition involves accelerated channel closure and thus ATP hydrolysis in our working model and that potentiators cause stalling of the channel in an open state. At higher concentrations, inhibitor or potentiator occupation of the second binding site is increased and might either lock CFTR in the closed state or the compound could block the channel due to protrusion into the pore. This could also explain why some potentiators have inhibitory effects at high concentrations.

The results are described in detail in the following unpublished manuscript in section 7.2 (p. 73): *Zwick M., Müller R., Seelig A: "CFTR-ATPase Modulation by Inhibitors and Potentiators"*

3.3 Steroid Hormones Modulate the ATPase Activity of CFTR

The approach described in section 3.2 and 6.2, was applied in this part of the thesis to study the interaction of steroid hormones with CFTR. Steroids had been shown earlier to modulate ATPase activity of P-glycoprotein and both, inhibition and potentiation of CFTR function had been suggested for 17β-estradiol. We investigated the effects of 17β-estradiol, cortisol, progesterone and the 17β-estradiol antagonist tamoxifen. Titration of CHO-CFTR cells with cortisol and progesterone over a broad concentration range in the presence of phosphorylation agents yielded bell-shaped ATPase activity curves. In the case of estradiol also slightly stimulating effects could be observed, but the measurements were dominated by unspecific reversible metabolic effects due to reduced glucose import. We observed a similar shift in concentration of half maximum activation, $K_{1,}$ of the bell-shaped activity curves as described before (section 3.2 and

7.2) not only in the presence of different CPT-cAMP concentrations but also different forskolin concentrations. Tamoxifen had no effects on either control cells or transfected cells at low concentrations. High concentrations were not accessible due to an irreversible ECAR reduction indicating cytotoxic effects. Characterization of the compounds by means of surface activity measurements revealed an overall low surface activity of the steroid hormones, with estradiol being the least amphiphilic compound. In summary, our findings support the model proposed in section 3.2 and 7.2. CFTR-ATPase was again stimulated by the more amphiphilic compounds progesterone and cortisol which therefore might be inhibitors, whereas the non-amphiphilic estradiol rather resembles a CFTR potentiator. However, effects were generally small compared to the more specific inhibitors described before. The observed interactions furthermore support the hypothesis that modulator binding to CFTR is not only determined by hydrogen bond acceptors but also hydrogen bond donors, i.e. hydroxyl groups.

The results are described in detail in the following unpublished manuscript in section 8.1 (p. 121): *Zwick M., Hellstern M., Seelig A: "Steroid Hormones Modulate the ATPase Activity of CFTR"*

4 Acknowledgment

This work was carried out in the laboratories of Prof. Anna Seelig at the Biozentrum of the University of Basel and was financially supported by the Werner Siemens Foundation and the SNF.

I want to thank

my PhD supervisor Prof. Anna Seelig for giving me the opportunity to work on this challenging project. Thank you for your inspiring ideas and for the freedom I had in shaping the project.

Prof. Joachim Seelig for a lot of valuable suggestions (not only) as a member of my PhD advisory committee and for initiating the Werner Siemens stipend program and the excursions (especially the last one)

all members of the Seelig group. It was a pleasure to meet all of you and I really enjoyed the time here. In particular, thank you Rita Müller and Xiaochun Li-Blatter for your help especially with the last-minute experiments. Many thanks to Manuel Hellstern who did a great job during his Bachelor thesis. Thank you Cinzia Esposito for your help with the microscope and for our monthly minutes of fresh air. Thank you Andy Beck for taking care of me in my first weeks in the lab and I really appreciate sharing an office with Christian Müller.

Prof. Dagmar Klostermeier for the chance to work in her lab during my lab rotation and I want to thank all the members of the Klostermeier group for the great atmosphere on the 6th floor. I really had a fun time with you, not only in the lab but far beyond. Thank you, Manuel Hilbert and Martin Linden, for making my start in Basel so easy and for your friendship.

my parents and my sister for their continuous support and for always encouraging me.

Anne Karow for proofreading, supervising my lab rotation and co-running the coffee corner. Thank you so much for always being there for me. This would not have been possible without you.

Prof. Kaspar Vogt as a member of my PhD advisory committee and for the chance to carry out patch-clamp experiments in his lab

Lydia Barth for help with patch-clamp experiments

Prof. Jack Riordan and Dr. Jürgen Reinhardt for the supply with various cell lines

Prof. Timm Maier for working as a referee for this thesis

Angie Klarer, for everything she does for us PhD students of the Biozentrum

5 References

1. http://pfam.sanger.ac.uk.
2. Lee, S. J., Bohm, A., Krug, M., and Boos, W. (2007) *Trends Microbiol* **15**, 389-397
3. Dean, M., Hamon, Y., and Chimini, G. (2001) *J Lipid Res* **42**, 1007-1017
4. Linton, K. J., and Higgins, C. F. (2007) *Pflugers Arch* **453**, 555-567
5. Aittoniemi, J., Fotinou, C., Craig, T. J., de Wet, H., Proks, P., and Ashcroft, F. M. (2009) *Philos Trans R Soc Lond B Biol Sci* **364**, 257-267
6. Velamakanni, S., Yao, Y., Gutmann, D. A., and van Veen, H. W. (2008) *Biochemistry* **47**, 9300-9308
7. Dawson, R. J., and Locher, K. P. (2006) *Nature* **443**, 180-185
8. Davidson, A. L., and Chen, J. (2004) *Annu Rev Biochem* **73**, 241-268
9. http://nutrigene.4t.com/humanabc.htm.
10. http://www.genenames.org.
11. Riordan, J. R., Rommens, J. M., Kerem, B., Alon, N., Rozmahel, R., Grzelczak, Z., Zielenski, J., Lok, S., Plavsic, N., Chou, J. L., and et al. (1989) *Science* **245**, 1066-1073
12. Bear, C. E., Li, C. H., Kartner, N., Bridges, R. J., Jensen, T. J., Ramjeesingh, M., and Riordan, J. R. (1992) *Cell* **68**, 809-818
13. Seavilleklein, G., Amer, N., Evagelidis, A., Chappe, F., Irvine, T., Hanrahan, J. W., and Chappe, V. (2008) *Am J Physiol Cell Physiol* **295**, C1366-1375
14. Luz, S., Kongsuphol, P., Mendes, A. I., Romeiras, F., Sousa, M., Schreiber, R., Matos, P., Jordan, P., Mehta, A., Amaral, M. D., Kunzelmann, K., and Farinha, C. M. (2011) *Mol Cell Biol* **31**, 4392-4404
15. Lewis, H. A., Buchanan, S. G., Burley, S. K., Conners, K., Dickey, M., Dorwart, M., Fowler, R., Gao, X., Guggino, W. B., Hendrickson, W. A., Hunt, J. F., Kearins, M. C., Lorimer, D., Maloney, P. C., Post, K. W., Rajashankar, K. R., Rutter, M. E., Sauder, J. M., Shriver, S., Thibodeau, P. H., Thomas, P. J., Zhang, M., Zhao, X., and Emtage, S. (2004) *Embo J* **23**, 282-293
16. Thibodeau, P. H., Brautigam, C. A., Machius, M., and Thomas, P. J. (2005) *Nat Struct Mol Biol* **12**, 10-16
17. Rosenberg, M. F., O'Ryan, L. P., Hughes, G., Zhao, Z., Aleksandrov, L. A., Riordan, J. R., and Ford, R. C. (2011) *J Biol Chem* **286**, 42647-42654
18. Serohijos, A. W., Hegedus, T., Aleksandrov, A. A., He, L., Cui, L., Dokholyan, N. V., and Riordan, J. R. (2008) *Proc Natl Acad Sci U S A* **105**, 3256-3261
19. Mornon, J. P., Lehn, P., and Callebaut, I. (2009) *Cell Mol Life Sci* **66**, 3469-3486
20. Mornon, J. P., Lehn, P., and Callebaut, I. (2008) *Cell Mol Life Sci* **65**, 2594-2612
21. Basso, C., Vergani, P., Nairn, A. C., and Gadsby, D. C. (2003) *J Gen Physiol* **122**, 333-348
22. Muallem, D., and Vergani, P. (2009) *Philos Trans R Soc Lond B Biol Sci* **364**, 247-255
23. Aubin, C. N., and Linsdell, P. (2006) *J Gen Physiol* **128**, 535-545
24. Gong, X., and Linsdell, P. (2003) *J Physiol* **549**, 387-397
25. Zhou, J. J., Fatehi, M., and Linsdell, P. (2008) *Pflugers Arch* **457**, 351-360
26. Baker, J. M., Hudson, R. P., Kanelis, V., Choy, W. Y., Thibodeau, P. H., Thomas, P. J., and Forman-Kay, J. D. (2007) *Nature structural & molecular biology* **14**, 738-745
27. Hegedus, T., Serohijos, A. W., Dokholyan, N. V., He, L., and Riordan, J. R. (2008) *J Mol Biol* **378**, 1052-1063

28. Ishiguro, H., Steward, M. C., Naruse, S., Ko, S. B., Goto, H., Case, R. M., Kondo, T., and Yamamoto, A. (2009) *J Gen Physiol* **133**, 315-326
29. Kogan, I., Ramjeesingh, M., Li, C., Kidd, J. F., Wang, Y., Leslie, E. M., Cole, S. P., and Bear, C. E. (2003) *Embo J* **22**, 1981-1989
30. Kanno, T., and Nishizaki, T. (2011) *Mol Pain* **7**, 72
31. Boucherot, A., Schreiber, R., and Kunzelmann, K. (2001) *Biochim Biophys Acta* **1515**, 64-71
32. Guggino, W. B. (2004) *Proc Am Thorac Soc* **1**, 28-32
33. Seidler, U., Singh, A. K., Cinar, A., Chen, M., Hillesheim, J., Hogema, B., and Riederer, B. (2009) *Ann N Y Acad Sci* **1165**, 249-260
34. Cui, L., Aleksandrov, L., Hou, Y. X., Gentzsch, M., Chen, J. H., Riordan, J. R., and Aleksandrov, A. A. (2006) *J Physiol* **572**, 347-358
35. Vergani, P., Nairn, A. C., and Gadsby, D. C. (2003) *J Gen Physiol* **121**, 17-36
36. Zhou, Z., Wang, X., Liu, H. Y., Zou, X., Li, M., and Hwang, T. C. (2006) *J Gen Physiol* **128**, 413-422
37. Gunderson, K. L., and Kopito, R. R. (1994) *J Biol Chem* **269**, 19349-19353
38. Csanady, L., Vergani, P., and Gadsby, D. C. (2010) *Proc Natl Acad Sci U S A* **107**, 1241-1246
39. Csanady, L., Chan, K. W., Seto-Young, D., Kopsco, D. C., Nairn, A. C., and Gadsby, D. C. (2000) *J Gen Physiol* **116**, 477-500
40. Rich, D. P., Berger, H. A., Cheng, S. H., Travis, S. M., Saxena, M., Smith, A. E., and Welsh, M. J. (1993) *J Biol Chem* **268**, 20259-20267
41. Hegedus, T., Aleksandrov, A., Mengos, A., Cui, L., Jensen, T. J., and Riordan, J. R. (2009) *Biochim Biophys Acta* **1788**, 1341-1349
42. Vais, H., Zhang, R., and Reenstra, W. W. (2004) *Am J Physiol Cell Physiol* **287**, C737-745
43. Csanady, L., Seto-Young, D., Chan, K. W., Cenciarelli, C., Angel, B. B., Qin, J., McLachlin, D. T., Krutchinsky, A. N., Chait, B. T., Nairn, A. C., and Gadsby, D. C. (2005) *J Gen Physiol* **125**, 171-186
44. Knowles, M. R., and Boucher, R. C. (2002) *J Clin Invest* **109**, 571-577
45. Wanner, A., Salathe, M., and O'Riordan, T. G. (1996) *Am J Respir Crit Care Med* **154**, 1868-1902
46. Boucher, R. C. (2004) *Eur Respir J* **23**, 146-158
47. Reddy, M. M., and Quinton, P. M. (2003) *Pflugers Arch* **445**, 499-503
48. Reddy, M. M., and Quinton, P. M. (1996) *Am J Physiol* **270**, C474-480
49. Pallagi, P., Venglovecz, V., Rakonczay, Z., Jr., Borka, K., Korompay, A., Ozsvari, B., Judak, L., Sahin-Toth, M., Geisz, A., Schnur, A., Maleth, J., Takacs, T., Gray, M. A., Argent, B. E., Mayerle, J., Lerch, M. M., Wittmann, T., and Hegyi, P. (2011) *Gastroenterology* **141**, 2228-2239 e2226
50. Kim, D., and Steward, M. C. (2009) *J Med Invest* **56 Suppl**, 336-342
51. Kunzelmann, K., and Mall, M. (2002) *Physiol Rev* **82**, 245-289
52. Dray-Charier, N., Paul, A., Veissiere, D., Mergey, M., Scoazec, J. Y., Capeau, J., Brahimi-Horn, C., and Housset, C. (1995) *Lab Invest* **73**, 828-836
53. Di, A., Brown, M. E., Deriy, L. V., Li, C., Szeto, F. L., Chen, Y., Huang, P., Tong, J., Naren, A. P., Bindokas, V., Palfrey, H. C., and Nelson, D. J. (2006) *Nat Cell Biol* **8**, 933-944
54. Weyler, R. T., Yurko-Mauro, K. A., Rubenstein, R., Kollen, W. J., Reenstra, W., Altschuler, S. M., Egan, M., and Mulberg, A. E. (1999) *Am J Physiol* **277**, C563-571
55. Buchanan, P. J., Ernst, R. K., Elborn, J. S., and Schock, B. (2009) *Biochem Soc Trans* **37**, 863-867
56. Rowntree, R. K., and Harris, A. (2003) *Ann Hum Genet* **67**, 471-485
57. http://www.genet.sickkids.on.ca/cftr.
58. Welsh, M. J., and Smith, A. E. (1993) *Cell* **73**, 1251-1254

59. Ward, C. L., Omura, S., and Kopito, R. R. (1995) *Cell* **83**, 121-127
60. Turnbull, E. L., Rosser, M. F., and Cyr, D. M. (2007) *BMC Biochem* **8 Suppl 1**, S11
61. Vankeerberghen, A., Wei, L., Teng, H., Jaspers, M., Cassiman, J. J., Nilius, B., and Cuppens, H. (1998) *FEBS Lett* **437**, 1-4
62. Haardt, M., Benharouga, M., Lechardeur, D., Kartner, N., and Lukacs, G. L. (1999) *J Biol Chem* **274**, 21873-21877
63. Bombieri, C., Claustres, M., De Boeck, K., Derichs, N., Dodge, J., Girodon, E., Sermet, I., Schwarz, M., Tzetis, M., Wilschanski, M., Bareil, C., Bilton, D., Castellani, C., Cuppens, H., Cutting, G. R., Drevinek, P., Farrell, P., Elborn, J. S., Jarvi, K., Kerem, B., Kerem, E., Knowles, M., Macek, M., Jr., Munck, A., Radojkovic, D., Seia, M., Sheppard, D. N., Southern, K. W., Stuhrmann, M., Tullis, E., Zielenski, J., Pignatti, P. F., and Ferec, C. (2011) *J Cyst Fibros* **10 Suppl 2**, S86-102
64. Gabriel, S. E., Brigman, K. N., Koller, B. H., Boucher, R. C., and Stutts, M. J. (1994) *Science* **266**, 107-109
65. Thiagarajah, J. R., and Verkman, A. S. (2003) *Curr Opin Pharmacol* **3**, 594-599
66. Terryn, S., Ho, A., Beauwens, R., and Devuyst, O. (2011) *Biochim Biophys Acta* **1812**, 1314-1321
67. Pedemonte, N., Tomati, V., Sondo, E., and Galietta, L. J. (2010) *Am J Physiol Cell Physiol* **298**, C866-874
68. Loo, T. W., Bartlett, M. C., and Clarke, D. M. (2005) *Mol Pharm* **2**, 407-413
69. Wang, Y., Loo, T. W., Bartlett, M. C., and Clarke, D. M. (2007) *J Biol Chem* **282**, 33247-33251
70. Wang, Y., Loo, T. W., Bartlett, M. C., and Clarke, D. M. (2007) *Biochem J* **406**, 257-263
71. Egan, M. E., Pearson, M., Weiner, S. A., Rajendran, V., Rubin, D., Glockner-Pagel, J., Canny, S., Du, K., Lukacs, G. L., and Caplan, M. J. (2004) *Science* **304**, 600-602
72. Lipecka, J., Norez, C., Bensalem, N., Baudouin-Legros, M., Planelles, G., Becq, F., Edelman, A., and Davezac, N. (2006) *J Pharmacol Exp Ther* **317**, 500-505
73. Grubb, B. R., Gabriel, S. E., Mengos, A., Gentzsch, M., Randell, S. H., Van Heeckeren, A. M., Knowles, M. R., Drumm, M. L., Riordan, J. R., and Boucher, R. C. (2006) *Am J Respir Cell Mol Biol* **34**, 355-363
74. Van Goor, F., Hadida, S., Grootenhuis, P. D., Burton, B., Stack, J. H., Straley, K. S., Decker, C. J., Miller, M., McCartney, J., Olson, E. R., Wine, J. J., Frizzell, R. A., Ashlock, M., and Negulescu, P. A. (2011) *Proc Natl Acad Sci U S A* **108**, 18843-18848
75. Clancy, J. P., Rowe, S. M., Accurso, F. J., Aitken, M. L., Amin, R. S., Ashlock, M. A., Ballmann, M., Boyle, M. P., Bronsveld, I., Campbell, P. W., De Boeck, K., Donaldson, S. H., Dorkin, H. L., Dunitz, J. M., Durie, P. R., Jain, M., Leonard, A., McCoy, K. S., Moss, R. B., Pilewski, J. M., Rosenbluth, D. B., Rubenstein, R. C., Schechter, M. S., Botfield, M., Ordonez, C. L., Spencer-Green, G. T., Vernillet, L., Wisseh, S., Yen, K., and Konstan, M. W. (2012) *Thorax* **67**, 12-18
76. Ai, T., Bompadre, S. G., Wang, X., Hu, S., Li, M., and Hwang, T. C. (2004) *Mol Pharmacol* **65**, 1415-1426
77. Weinreich, F., Wood, P. G., Riordan, J. R., and Nagel, G. (1997) *Pflugers Arch* **434**, 484-491
78. French, P. J., Bijman, J., Bot, A. G., Boomaars, W. E., Scholte, B. J., and de Jonge, H. R. (1997) *Am J Physiol* **273**, C747-753
79. Al-Nakkash, L., and Hwang, T. C. (1999) *Pflugers Arch* **437**, 553-561
80. Moran, O., and Zegarra-Moran, O. (2005) *FEBS Lett* **579**, 3979-3983
81. Illek, B., Lizarzaburu, M. E., Lee, V., Nantz, M. H., Kurth, M. J., and Fischer, H. (2000) *Am J Physiol Cell Physiol* **279**, C1838-1846
82. Moran, O., Galietta, L. J., and Zegarra-Moran, O. (2005) *Cell Mol Life Sci* **62**, 446-460

83. Pedemonte, N., Sonawane, N. D., Taddei, A., Hu, J., Zegarra-Moran, O., Suen, Y. F., Robins, L. I., Dicus, C. W., Willenbring, D., Nantz, M. H., Kurth, M. J., Galietta, L. J., and Verkman, A. S. (2005) *Mol Pharmacol* **67**, 1797-1807
84. Caputo, A., Hinzpeter, A., Caci, E., Pedemonte, N., Arous, N., Di Duca, M., Zegarra-Moran, O., Fanen, P., and Galietta, L. J. (2009) *J Pharmacol Exp Ther* **330**, 783-791
85. Accurso, F. J., Rowe, S. M., Clancy, J. P., Boyle, M. P., Dunitz, J. M., Durie, P. R., Sagel, S. D., Hornick, D. B., Konstan, M. W., Donaldson, S. H., Moss, R. B., Pilewski, J. M., Rubenstein, R. C., Uluer, A. Z., Aitken, M. L., Freedman, S. D., Rose, L. M., Mayer-Hamblett, N., Dong, Q., Zha, J., Stone, A. J., Olson, E. R., Ordonez, C. L., Campbell, P. W., Ashlock, M. A., and Ramsey, B. W. (2010) *N Engl J Med* **363**, 1991-2003
86. Muanprasat, C., Sonawane, N. D., Salinas, D., Taddei, A., Galietta, L. J., and Verkman, A. S. (2004) *J Gen Physiol* **124**, 125-137
87. Schultz, B. D., Singh, A. K., Devor, D. C., and Bridges, R. J. (1999) *Physiol Rev* **79**, S109-144
88. Verkman, A. S., and Galietta, L. J. (2009) *Nat Rev Drug Discov* **8**, 153-171
89. Cui, G., Song, B., Turki, H. W., and McCarty, N. A. (2011) *Pflugers Arch*
90. Ma, T., Thiagarajah, J. R., Yang, H., Sonawane, N. D., Folli, C., Galietta, L. J., and Verkman, A. S. (2002) *J Clin Invest* **110**, 1651-1658
91. Tradtrantip, L., Sonawane, N. D., Namkung, W., and Verkman, A. S. (2009) *J Med Chem* **52**, 6447-6455
92. Taddei, A., Folli, C., Zegarra-Moran, O., Fanen, P., Verkman, A. S., and Galietta, L. J. (2004) *FEBS Lett* **558**, 52-56
93. Caci, E., Caputo, A., Hinzpeter, A., Arous, N., Fanen, P., Sonawane, N., Verkman, A. S., Ravazzolo, R., Zegarra-Moran, O., and Galietta, L. J. (2008) *Biochem J* **413**, 135-142
94. Bessadok, A., Garcia, E., Jacquet, H., Martin, S., Garrigues, A., Loiseau, N., Andre, F., Orlowski, S., and Vivaudou, M. (2011) *J Biol Chem* **286**, 3552-3569
95. Klokouzas, A., Wu, C. P., van Veen, H. W., Barrand, M. A., and Hladky, S. B. (2003) *Eur J Biochem* **270**, 3696-3708
96. Gedeon, C., Anger, G., Piquette-Miller, M., and Koren, G. (2008) *Placenta* **29**, 39-43
97. Shapiro, A. B., and Ling, V. (1997) *Eur J Biochem* **250**, 122-129
98. Shapiro, A. B., Fox, K., Lam, P., and Ling, V. (1999) *Eur J Biochem* **259**, 841-850
99. Chen, Y., Pant, A. C., and Simon, S. M. (2001) *Cancer Res* **61**, 7763-7769.
100. Aller, S. G., Yu, J., Ward, A., Weng, Y., Chittaboina, S., Zhuo, R., Harrell, P. M., Trinh, Y. T., Zhang, Q., Urbatsch, I. L., and Chang, G. (2009) *Science* **323**, 1718-1722
101. Fischer, H., Gottschlich, R., and Seelig, A. (1998) *J Membr Biol* **165**, 201-211
102. Seelig, A., Landwojtowicz, E., Fischer, H., and Li Blatter, X. (2003) Towards P-glycoprotein structure-activity relationships. in *Drug Bioavailability/Estimation of Solubility, Permeability and Absorption* (Waterbeemd, v. d., Lennernäs, and Artursson eds.), Wiley/VCH, Weinheim. pp 461-492
103. Seelig, A. (1998) *Eur J Biochem* **251**, 252-261.
104. Li-Blatter, X., and Seelig, A. (2010) *Biophys J* **99**, 3589-3598
105. Loo, T. W., Bartlett, M. C., and Clarke, D. M. (2009) *J Biol Chem* **284**, 24074-24087
106. Bruggemann, E. P., Currier, S. J., Gottesman, M. M., and Pastan, I. (1992) *J Biol Chem* **267**, 21020-21026
107. Shilling, R. A., Venter, H., Velamakanni, S., Bapna, A., Woebking, B., Shahi, S., and van Veen, H. W. (2006) *Trends Pharmacol Sci* **27**, 195-203
108. Dey, S., Ramachandra, M., Pastan, I., Gottesman, M. M., and Ambudkar, S. V. (1997) *Proc Natl Acad Sci U S A* **94**, 10594-10599

109. Martin, C., Berridge, G., Higgins, C. F., Mistry, P., Charlton, P., and Callaghan, R. (2000) *Mol Pharmacol* **58**, 624-632.
110. Litman, T., Zeuthen, T., Skovsgaard, T., and Stein, W. D. (1997) *Biochim Biophys Acta* **1361**, 169-176
111. Loo, T. W., Bartlett, M. C., and Clarke, D. M. (2003) *J Biol Chem* **278**, 13603-13606
112. Miwa, M., Tsukahara, S., Ishikawa, E., Asada, S., Imai, Y., and Sugimoto, Y. (2003) *Int J Cancer* **107**, 757-763
113. Ni, Z., Bikadi, Z., Cai, X., Rosenberg, M. F., and Mao, Q. (2010) *Am J Physiol Cell Physiol* **299**, C1100-1109
114. Haimeur, A., Conseil, G., Deeley, R. G., and Cole, S. P. (2004) *Mol Pharmacol* **65**, 1375-1385
115. McConnell, H. M., Owicki, J. C., Parce, J. W., Miller, D. L., Baxter, G. T., Wada, H. G., and Pitchford, S. (1992) *Science* **257**, 1906-1912
116. Thedinga, E., Kob, A., Holst, H., Keuer, A., Drechsler, S., Niendorf, R., Baumann, W., Freund, I., Lehmann, M., and Ehret, R. (2007) *Toxicol Appl Pharmacol* **220**, 33-44
117. Gebhardt, R., Bellemann, P., and Mecke, D. (1978) *Experimental Cell Research* **112**, 431-441
118. Hafner, F. (2000) *Biosens Bioelectron* **15**, 149-158
119. Landwojtowicz, E., Nervi, P., and Seelig, A. (2002) *Biochemistry* **41**, 8050-8057.
120. Gatlik-Landwojtowicz, E., Aanismaa, P., and Seelig, A. (2006) *Biochemistry* **45**, 3020-3032

6 List of Abbreviations

ABC	ATP binding cassette
ADP	adenosine 5´-diphosphate
ASL	airway surface liquid
ATP	adenosine 5´-triphosphate
api	apigenin
BHK	baby hamster kidney
BCRP	breast cancer resistance protein
cAMP	adenosine 3´5´-cyclic monophosphate
caps	capsaicin
CPTcAMP	8-(4-chlorophenylthio)- adenosine 3´5´-cyclic monophosphate
CF	cystic fibrosis
CFTR	cystic fibrosis transmembrane conductance regulator
CFTRinh-172	4-[[4-Oxo-2-thioxo-3-[3-trifluoromethyl)phenyl]-5-thiazolidinylidene]methyl]benzoic acid
CHO	chinese hamster ovary
CMC	critical micellar concentration
curc	curcumin
DMEM	Dulbecco´s modified Eagle´s medium
DMSO	dimethyl sulfoxide
DPBS	Dulbecco´s phosphate buffered saline
DTT	Dithiothreitol
EC_{50}	half maximal effective concentration
ECAR	extracellular acidification rate
E. coli	*Escherichia coli*
EDTA	*N,N,N',N'*-ethylenediamine-tetraacetic disodium salt
EGTA	ethyleneglycol-bis(2-aminoethylether)-*N,N,N',N'*-tetraacetic disodium salt
ENaC	epithelial Na+ channel
FBS	fetal bovine serum
fsk	forskolin
FRT	Fisher rat thyroid
gen	genistein
glib	glibenclamide

glipz	glipizide
H-89	N-[2-(p-Bromocinnamylamino)ethyl]-5-isoquinolinesulfonamide dihydrochloride
HBA	hydrogen bond acceptor pattern
HEPES	4-(2-hydroxyethyl)piperazine-1-ethanesulfonic acid
MEMa	minimum essential medium alpha
MTX	methotrexate
MRP	multidrug resistance protein
NAD	nicotinamide adenine dinucleotide
NBD	nucleotide binding domain
NIH/3T3	mouse embryo fibroblasts
NHERF	Na+/H+ exchanger regulatory factor
OCR	oxygen consumption rate
PBS	phosphate buffered saline
PCL	periciliary layer
P. aeruginosa	*Pseudomonas aeruginosa*
Pgp	P-glycoprotein
PKA	protein kinase A
PKC	protein kinase C
PKI(14-22)	protein kinase A inhibitor fragment 14-22
PP_i	pyrophosphate
PPQ-102	7,9-Dimethyl-11-phenyl-6-(5-methylfuran-2-yl) -5,6-dihydro-pyrimido-[4,´5-´3,4]pyrrolo[1,2-a] quinoxaline-8,10-(7H,9H)-dione
RD	regulatory domain
S. aureus	*Staphylococcus aureus*
SDS	sodium dodecyl sulfate
SUR	sulfonylurea receptor
Tris	tris-(hydroxymethyl)aminomethane
TMD	transmembrane domain
TM	transmembrane helix
V. cholera	*Vibrio cholerae*

7 Submitted Manuscripts

7.1 Monitoring CFTR Phosphorylation in Living Cells via Microphysiometry

Matthias Zwick, Manuel Hellstern and Anna Seelig*

Submitted to Biochemistry

Biophysical Chemistry, Biozentrum, University of Basel, Klingelbergstrasse 50/70, CH-4056 Basel, Switzerland, Phone: +41-61-267 2206, FAX: +41-61-267 2189, e-mail: anna.seelig@unibas.ch

*Corresponding author

Introduction

Cystic fibrosis is caused by a mutation in the gene coding for the protein cystic fibrosis transmembrane conductance regulator (CFTR) (1). CFTR belongs to the protein family of ATP binding cassette (ABC) transporters and has been shown to bind and hydrolyze ATP (2). Similar to other ABC transporters ATP binding and hydrolysis at the nucleotide binding domains induces conformational changes in the transmembrane domains and drives opening and closing of the channel (3-5). In contrast to all other characterized members of this family no transporter function has been observed so far for CFTR. It is a channel for anions, especially chloride (6) and bicarbonate. A strict coupling between ATP hydrolysis and channel gating has recently been deduced from the kinetics of channel gating in excised patches (7). Channel opening seems to be regulated by phosphorylation (8) which mediates conformational changes in the regulatory domain of CFTR (9). There is evidence that phosphorylation by protein kinase A (PKA) can promote dimerization of the nucleotide binding domains (10). This raised the question whether phosphorylation enhances or reduces the ATPase activity of CFTR. However, reconstitution experiments yielded so far contradictory results (2,11).

To our knowledge, monitoring of ATP hydrolysis has so far been possible only in assays using reconstituted channels (12), while the channel function of CFTR can be measured in living cells in a label-free and non-invasive way for example by means of Ussing chamber measurements (reviewed in ref. (13)) or cell-attached patch-clamp experiments (14). The poor understanding of the correlation between phosphorylation, ATP hydrolysis and channel gating might thus be due to the differences in measuring conditions required to resolve the different processes. As demonstrated for another ABC transporter, P-glycoprotein, Pgp, (15-17) the ATPase activity can be measured in living cells by means of microphysiometry (18,19) which has a higher sensitivity than conventional techniques (Joseph Zolnerciks, Kenneth Linton, submitted). Membrane transporters are moreover influenced by the nature of the surrounding membrane (20). Particularly CFTR might behave differently, when cellular regulation mechanisms by kinases and phosphatases remain intact. Therefore methods where channel function and ATPase activity or phosphorylation can be monitored under similar conditions could be helpful to get deeper insight into the regulation and function of CFTR.

The aim of the present investigation was therefore to establish an ATPase assay using CFTR transfected cells using a Cytosensor® microphysiometer and the recently developed Bionas Discovery 2500® cell analyzer. To this purpose we studied the effects of the protein kinase A activating agents forskolin and 8-(4-Chlorophenylthio)-adenosine-3',5'-cyclic monophosphate (CPT-cAMP). While CPT-cAMP directly causes the dissociation of regulatory and catalytic subunits of PKA, forskolin acts indirectly by stimulating cAMP synthesis through adenylate cyclase. In both cases two processes might be reflected in our readout: (i) ATP consumption due to the phosphogroup transferase activity of PKA (ATP + CFTR → phospho-CFTR + ADP) and (ii) ATP hydrolysis by CFTR. Production of cAMP by adenylate cyclase (ATP → cAMP + PP_i) might be detected as well, when forskolin is used. To distinguish between these effects we carried out experiments with PKA inhibitors H-89 and myristoylated PKI(14-22) and studied the CFTR variant E1371S which exhibits reduced ATP hydrolysis. Furthermore we investigated the correlation between ATP consumption and channel opening detected in iodide efflux experiments. Our results show that microphysiometry can be used to detect the presence of functional CFTR. The readout could be the basis for drug screening assays. ECAR measurements by means of microphysiometry provide additional information on potential metabolic side effects. Simultaneous ECAR and oxygen consumption rate (OCR) measurements were used to identify whether these effects are caused by impaired glucose import.

Materials and Methods:

Compound preparation

8-(4-Chlorophenylthio)-adenosine 3′,5′-cyclic monophosphate (CPT-cAMP), forskolin, methotrexate and H-89 were obtained from Sigma-Aldrich (St. Louis, Missouri, USA). Myristoylated PKI(14-22), minimum essential medium, Dulbecco's phosphate buffered saline (DPBS), fetal bovine serum (FBS) and other chemicals needed for cell culture were purchased from LuBioScience (Luzern, Switzerland). CPT-cAMP, PKI(14-22) and H-89 stock solutions were prepared in water, forskolin solution in DMSO. Methotrexate for cell culture was prepared as 100 mg/ml stock in sterile 1 N NaOH.

Cell lines

CHO and BHK cell lines stably transfected with the human *CFTR* (CHO-CFTR, BHK-CFTR), *CFTRΔF508* (CHO-ΔF, BHK-ΔF) or *CFTRE1371S* (BHK-E1371S) gene were a generous gift from Dr. J. R. Riordan (University of North Carolina, USA) and Dr. Jürgen Reinhardt (Novartis, Switzerland).

Cell culture

Untransfected CHO cells were grown in minimum essential medium alpha (MEMα) without ribonucleosides/deoxyribonucleosides containing 10 % heat inactivated fetal bovine serum (FBS) at 37 °C and 5 % CO_2. Stably transfected cell lines expressing either functional *CFTR* or *CFTRΔF508* were cultured in the same medium supplemented with 50 µM methotrexate (MTX). The cells were split 1:15 and passaged every 2 - 3 days. BHK cell lines expressing *CFTR* variants were grown in DMEM/F12 1:1 supplemented with 10% FBS and 500 µM MTX under the same conditions as CHO cells.

Microphysiometry

The Cytosensor® microphysiometer (Molecular Devices) consists of eight light-addressable potentiometric sensors. Cells are grown as a layer on 3.0 µm polycarbonate membranes (Ø 12 mm, Corning) on the bottom of a flow chamber. This flow chamber is placed above the sensors which can measure voltage changes that are linearly correlated to pH changes. Calibration experiments showed that 61 mV correspond to 1 pH unit. Cells were seeded to reach a final number of $n = 5 \cdot 10^5$ cells / membrane and incubated either for 4 hours or overnight. Commercially available dry powder MEMα without sodium bicarbonate (for CHO cells) or DMEM without sodium bicarbonate (for BHK cells) was used for flow medium preparation. The absence of

sodium bicarbonate is necessary to maintain a very low buffer capacity and to avoid bubble formation during the measurements. Sodium chloride was used as a substitute to preserve osmotic balance. The pH was always adjusted to 7.4 at 37 °C. For some experiments medium was replaced by various buffers as described below. Cells were continuously flushed with fresh flow medium at a flow rate of 100 µl/min. Extracellular acidification rates were calculated using Molecular Devices Cytosoft® and the slope between 5 seconds after stopping and 2 seconds before restarting the pump was evaluated to avoid artifacts caused by pump switching. The Cytosensor® offers a second tubing system that was filled with CPT-cAMP or forskolin containing medium prior to application. The stimulating agents could therefore be applied with little delay, as a valve close to the measurement chamber can be switched between the two channels. Additional oxygen consumption data was obtained in a Bionas Discovery® 2500 cell analyzing system. Cells were seeded on Bionas SC1000 metabolic chips with oxygen, pH and impedance sensors, to reach a final number of $n = 3 \cdot 10^5$ cells / chip. The same flow medium as described above was used and the flow rate was 110 µL/min. The Bionas Discovery lacks a second channel for substance supply therefore actual presence of drug in the measurement chamber was either calculated from the tubing length or could be directly deduced from changes in impedance values. All measurements were carried out at 37 °C.

Lactate quantification

Experiments in the Cytosensor microphysiometer were carried out as described, but flow medium was replaced by phosphate buffer (0.3 mM $CaCl_2$, 0.6 mM $MgCl_2$, 0.5 mM KH_2PO_4, 3 mM KCl, 0.5 mM Na_2HPO_4, 130 mM NaCl, 10 mM Glucose). The buffer was collected after the measurement chamber. The samples where lyophyllized and solved again in 3 ml buffer at pH 9.5 (1 M glycine, 0.6 M hydrazine, 5.6 mM EDTA). Lactate-dehydrogenase (5000 U / ml) and NAD (2.5 mM) were added to the buffer and the absorbance increase at 340 nm was monitored. Lactate concentrations where calculated from the stable absorption at 340 nm reached at the end of the reaction.

Iodide efflux measurements

Iodide efflux measurements were carried out according to Chen et al. (21) with small modifications. CHO cells were grown to 90% confluency in 60 mm culture dishes and were washed three times with 2.5 ml loading buffer pH 7.4 (136 mM NaI, 3 mM KNO_3, 2 mM $Ca(NO_3)_2$, 11 mM Glucose, 20 mM HEPES/NaOH). After incubation for 2 – 3h in the dark at 37 °C, cells were washed carefully 30 times with 2.5 ml efflux buffer pH 7.4

(136 mM $NaNO_3$, 3 mM KNO_3, 2 mM $Ca(NO_3)_2$, 11 mM Glucose, 20 mM HEPES/NaOH) to remove excess iodide. For measurements, efflux buffer was exchanged in one minute intervals. After 5 minutes, efflux buffer was replaced by stimulation buffer (i.e., efflux buffer containing forskolin or CPT-cAMP). Samples were collected and stored in the dark at room temperature. An iodide selective electrode (Mettler Toledo, perfectIon® combination I-) was used to measure voltages of the samples. Iodide concentrations were calculated using a calibration curve. The calibration curve was recorded using efflux buffer containing various concentrations of NaI. All experiments were carried out at 37 °C.

Air-Water and Lipid- Water Partition Coefficient.

Measurements of the surface pressure, π, as a function of CPT-cAMP and forskolin concentration, C, were performed with a Fromherz Teflon trough (20 mL) connected to a Wilhelmi balance (22). Experiments were carried out at T = 27 °C in buffer containing at pH 7.4 (50 mM Tris/HCl and 114 mM NaCl). Final DMSO concentration in measurements with forskolin was below 5%. Therefore the surface activity of DMSO could be neglected. Serial aliquots of the stock solution were added to the monolayer trough filled with buffer. The surface pressure, π, was recorded as a function of time until equilibrium was reached. The Gibbs adsorption isotherm i.e. the surface pressure at equilibrium as a function of the solute concentration, C, was measured. This allowed assessing the air-water partition coefficient, K_{aw}, the cross-sectional area of the molecule at the air-water interface, A_D, and the critical micelle concentration, CMC_D, which coincides with the concentration at the solubility limit, C_{sol}, for many drugs (23). Data were evaluated as described in detail elsewhere (23,24). The lipid-water partition coefficient, K_{lw}, was derived from the air-water partition coefficient, K_{aw},

$$K_{lw} = K_{aw} * e^{\frac{-\pi_M A_D}{kT}}, \qquad (1)$$

where $\pi_M \cdot A_D = \Delta W$ corresponds to the work required to create a hole in the lipid membrane with a given packing density, π_M, that is large enough to accommodate the molecule with the cross-sectional area A_D (25), and k is the Boltzmann constant.

Results

Influence of CPT-cAMP on the ECAR of CHO-CFTR, CHO-ΔF and CHO-K1 cells

CHO-CFTR, CHO-ΔF and CHO-K1 cells were seeded onto polycarbonate membranes either 17 h or 4 h before a measurement to reach a final number of approx. $5 \cdot 10^5$ cells / membrane, corresponding to 80 - 90% confluency. Each chamber was flushed with flow medium exhibiting a low buffer capacity until a stable basal ECAR and thus a stable metabolism was reached. In a next step, the second medium supply tubing of each measurement chamber was flushed for 10 minutes with flow medium containing CPT-cAMP, to ensure that the entire tubing up to the valve had been filled. After switching the valve to the drug channel, cells were exposed to CPT-cAMP. At low concentrations, C(CPT) ≤ 100 µM stimulations were carried out for 20 minutes until a steady state was reached (Fig. 1A, B), at concentrations, C(CPT) > 100 µM stimulation periods were extended up to 50 minutes to monitor the ECAR decrease which occurred after an initial ECAR increase (Fig 1 C). Subsequently cells were again flushed with pure flow medium until the ECAR returned to the basal level. To quantify the observed ECAR changes, four measurement points at the end of each drug exposure period were averaged and normalized to the average of the last four points of basal ECAR before substance application. The ECAR of CHO-CFTR cells as a function of the CPT-cAMP concentration is shown in Fig. 1D. CPT-cAMP induced a response which reached a maximum of 166 ± 18 % at C(CPT) = 100 µM. After the ECAR increased during the first 10 minutes a second ECAR-reducing effect appeared at high CPT-cAMP concentrations (Fig. 1C). Disregarding the second effect, the ECAR vs. Log concentration curve could be well fitted with an apparent $K_{d,app}$(CPT) = 12 µM using an equation proposed earlier (26),

$$ECAR = 100 + (ECAR_{max} - 100)\left(\frac{C(CPT)}{K_{d,app}+C(CPT)}\right)^4 . \qquad (2)$$

The term in brackets describes the activation of protein kinase A by binding of 4 cAMP molecules to the regulatory subunit and subsequent dissociation of regulatory and catalytic subunits. The resulting curve corresponded well with maximal ECAR reached for C(CPT-cAMP) ≥ 100 µM before slow ECAR reduction set in (Fig. 1C and D). CHO-K1 cells showed no changes in ECAR at low concentrations, however, at higher concentrations (C(CPT) ≥ 200 µM) an ECAR increase up to 142 ± 9 % was visible. At

these high concentrations CHO-ΔF cells behaved in the same manner as CHO-K1 cells (not shown).

To clarify whether the ECAR changes due to CPT-cAMP addition reflect increased lactate export, CHO-CFTR cells were stimulated with 50 µM CPT-cAMP for 2 hours in a Cytosensor experiment. The medium was collected after having passed the measurement chamber. Lactate in the collected medium was quantified as described above. The observed increase by a factor of 1.9, however, is somewhat higher than the observed increase in measured ECAR to approximately 150 -170 %. This might indicate, that additional alkalinization processes counteract the measured signal. Basal acidification rates of CHO cells were determined to be $4 \cdot 10^6$ H^+ s^{-1} per cell and the expression level was estimated to be between $5 \cdot 10^4$ and $1 \cdot 10^6$ molecules of CFTR per cell (communication from Novartis, Switzerland). Based on these numbers, one can estimate an ECAR per molecule CFTR between 70 and 135 H^+ s^{-1}.

Fig. 1 A-D

Effect of forskolin on the ECAR of CHO-CFTR, CHO-ΔF and CHO-K1 cells

Titrations with forskolin in the concentration range of C(fsk) = (0.1 - 100) µM were carried out as described above for CPT-cAMP. To obtain an ECAR vs. concentration curve, the last four points of the stimulation period were again averaged and normalized to the average basal ECAR 10 minutes before drug application. The activity increased at low concentrations up to a maximum of 195 ± 20 % at a concentration C(fsk) = 1 µM. At concentrations C(fsk) < 1 µM (Fig. 2A) a stimulatory effect was observed only with CHO-CFTR cells while CHO-K1 cells remained at the level of the basal ECAR rate. In the concentration range, C(fsk) = (1 – 10) µM, (Fig. 2D) the stimulation of ECAR in CHO-CFTR cells decreased while the ECAR in control cells still slightly increased (125 ± 18 %). As soon as forskolin was removed from the medium the ECAR of CHO-CFTR cells increased again to 180-200% (Fig. 2B). Upon further flushing, the latter signal decreased only very slowly and required up to 2 h, depending on the concentration, to return to the basal level. At concentrations C(fsk) ≥ 10 µM a decrease in ECAR was observed in CHO-CFTR and CHO-K1 cells. At the highest concentration of forskolin tested (C(fsk) = 100 µM) a decrease of the ECARs down to 30 % of the basal level of CHO-CFTR and 50 % of the basal level of control cells, was observed. Even at these high concentrations, CHO-CFTR cells reached higher ECARs immediately after removal of forskolin, compared to control cells (Fig. 2B-C). CHO-ΔF

cells behaved in the same manner as CHO-K1 cells (not shown) in the presence of forskolin and CPT-cAMP.

Fig. 2 A-D

Effect of CPT-cAMP and forskolin on BHK cells overexpressing CFTR variants

As CHO-K1 and CHO-ΔF cells behaved in the same manner we could exclude that the observed effects on ECAR where due to the presence of misfolded CFTR or to processes induced by the presence of methotrexate in the cell culture medium. To test whether the effect of forskolin and CPT-cAMP stimulation was CHO cell-specific we also investigated *CFTR* overexpressed in BHK cells. To test moreover whether the ECAR observed upon stimulation was due to ATP hydrolysis by CFTR, we investigated the effects of phosphorylation agents on BHK cells overexpressing the ATPase deficient mutant *CFTRE1371S*. All experiments were carried out under the conditions described above for CHO cells, except that DMEM without bicarbonate was used as flow medium instead of MEMα to preserve the conditions used for cell culture. The response of BHK-CFTR cells to stimulation with CPT-cAMP was qualitatively similar to that of CHO-CFTR cells. However, the maximum ECAR was only 123 ± 7 % at C(CPT) = 100 µM (Fig. 3A). BHK-E1371S cells showed no increase but even a slight decrease in the ECAR with a minimum of 84 ± 4 % at C(CPT) = 50 µM. The ECAR as a function of the CPT-cAMP concentration on CHO-CFTR could be again described by equation 1 with a maximum ECAR of 125 % and an apparent $K_{d,app}$(CPT) = 3.7 µM.

The ECAR in BHK cells upon stimulation with forskolin was qualitatively similar to that in CHO cells but again lower as seen above for CPT-cAMP. A maximal stimulation of 117 ± 4 % was reached around C(fsk) = 0.5 µM (Fig. 3B). In contrast to CHO cells, no ECAR decrease in BHK-CFTR cells between C(fsk) = 1 µM and C(fsk) = 10 µM was observed. For BHK-E1371S cells, again a small ECAR decrease was observed with a minimum of 91 ± 3 % at C(fsk) = 0.5 µM. At concentrations C(fsk) > 10 µM, again an unspecific ECAR decrease in ECAR for both cell lines was observed resulting in a minimum ECAR of 65 ± 12 % for BHK-CFTR and 40 ± 5 % for BHK-E1371S at a concentration of C(fsk) = 100 µM.

Fig. 3 A, B

Effect of forskolin and CPT-cAMP on the oxygen consumption rate (OCR)

The conditions are essentially anaerobic in the Cytosensor®, but not in the Bionas Discovery® 2500 measuring chambers. To get further insight into the inhibitory effect of high forskolin concentrations, the experiments were repeated in a Bionas Discovery® 2500 cell analysis system which in addition to the ECAR also detects the OCR and the cell impedance. All measurements were carried out at 37 °C in the same flow medium as described above. Pump cycles comprised 2 min go and 2 minutes stop which lead to a two times lower time resolution than obtained in the Cytosensor. Changes in ECAR and OCR were parallel upon CPT-cAMP exposure however, with a delay in the OCR response. Effects on OCR were observed only at high concentrations, i.e. at C(CPT) ≥ 200 µM in the case of CHO-K1 (Fig. 4A), and at C(CPT) ≥ 50 µM in the case of CHO-CFTR cells (Fig. 4B).

Fig. 4 A, B

Titrating CHO-K1 cells with forskolin (Fig. 5A) induced a slight ECAR increase at forskolin concentrations, C(fsk) > 50 µM and a slight ECAR decrease at the highest forskolin concentrations (C(fsk) > 50 µM) as described above (Fig. 2). The OCR remained close to basal values at low concentrations of forskolin (C(fsk) < 10 µM) and increased slightly under conditions where the ECAR decreased. In CHO-CFTR cells the ECAR increase was observed already at low concentrations (Fig. 5B). The ECAR reached a maximum and decreased again at high concentrations as seen above (Fig. 2). The OCR decreased slightly at lower forskolin concentrations, under conditions of increasing ECAR, but clearly increased at high forskolin concentrations under conditions of decreasing ECAR (Fig. 5B). While washout at high forskolin concentrations first lead to a significant ECAR stimulation before the return to basal values, the OCR immediately returned to basal (100%) values. The shift to higher forskolin concentrations observed for all effects in the Bionas Discovery® 2500 compared to the Cytosensor® measurements, respectively, could be attributed to a loss of substance in the longer tubing system. The effects of CPT-cAMP did not shift compared to the Cytosensor, as CPT-cAMP is less hydrophobic than forskolin and therefore does not stick to the hydrophobic surface of the medium supply tubes.

Fig. 5 A, B

Sensitivity of CPT-cAMP and forskolin induced effects to PK A inhibition

To investigate whether changes in lactate efflux were mediated by a PKA dependent pathway, we applied two different protein kinase inhibitors, the myristoylated PKA inhibitor peptide PKI(14-22) (K_i = 36 nM) and the PKA inhibitor H-89 (K_i = 135 nM). Cells were first incubated with an inhibitor concentration of 10 µM or 20 µM as these concentrations had previously been shown to inhibit PKA in living cells (27-29). Both inhibitors influenced the ECAR and thus the cell metabolism. PKI(14-22) at a concentration of 20 µM transiently enhanced the ECAR to about 190 % most likely due to a detergent-like nature. However, the signal reverted to basal values during the incubation period. H-89 instead increased the ECAR of all cell lines to about 180 % and stabilized at a higher level. Therefore all observations were normalized to this altered basal activity in the latter case. The observed inhibition is summarized in Table 1. At a concentration of 20 µM both inhibitors clearly reduce the effect of maximal stimulation with either forskolin or CPT-cAMP to about 20 %. However the strong unspecific inhibitory effect of high concentrations of forskolin C(fsk)>10 µM was not influenced by H-89.

Tab. 1

Iodide efflux measurements

Iodide efflux measurements were carried out, to elucidate how the changes in ECAR might correlate to the channel function of CFTR. We could show that CHO-CFTR cells respond equally in Cytosensor® experiments when MEMα was replaced by a slightly modified (2 mM HEPES vs. 20 mM HEPES) iodide efflux buffer. This should allow comparing ATP consumption with iodide efflux. For iodide efflux recordings, cells were incubated for 3 h with loading buffer, where chloride is replaced by iodide. Afterwards efflux was detected by replacing loading buffer with efflux buffer where chloride is replaced by nitrate. Efflux buffer was exchanged every minute, and the collected samples were stored in the dark until detection of the amount of iodide by an iodide selective electrode. In the case of CPT-cAMP, a significant increase in iodide efflux can only be observed at concentrations C(CPT) ≥ 100 µM and increases further at C(CPT) = 200 µM (Fig. 6A) where a decrease of the ECAR starts (Fig. 1 A). In the case of forskolin only small effects could be observed at a concentration C(fsk) = 0.5 µM, where ECAR is already clearly increased. A maximum seems to be reached at C(fsk) = 5 µM and does not decrease at higher concentrations. (Fig. 6B).

Fig. 6 A,B

Assessment of membrane partitioning of CPT-cAMP and forskolin

Because the dielectric constant of air ($\varepsilon \approx 1$) and the lipid core region ($\varepsilon \approx 2$) are similar, the air-water interface is an ideal model system for estimating the behavior of molecules entering the lipid-water interface. Amphiphilic drugs orient with their axis of amphiphilicity perpendicular to the air-water or lipid-water interface, and therefore generally adopt a comparable conformation at the two interfaces (23,30). To elucidate the properties of the present compounds at the lipid-water interface we measured the surface pressure, π, as a function of the solute concentration, C, (Gibbs adsorption isotherm) at pH 7.4 and room temperature. The surface pressure, π, increased with the concentration up to a limiting value which reflects the critical micelle concentration, CMC_D (not shown). The maximal surface pressure, π_{max}, reached at the CMC_D was determined as π_{max} (CPT) = 5.2 mN / m and π_{max} (fsk) = 14.1 mN / m and the air-water partition coefficients were $K_{aw}(CPT)$ = $2.61 \cdot 10^5$ M^{-1} and K_{aw}(fsk) = $5 \cdot 10^5$ M^{-1}. Due to the low surface pressure, the cross-sectional area for CPT-cAMP could not be inferred from these measurements. Therefore, cross-sectional areas A_D for lipid membrane insertion where predicted with the software Pgpredix (30) resulting in A_D(CPT) = 49 Å^2 and A_D(fsk) = 66 Å^2. It has to be noted, that the latter value is in reasonable agreement with measured cross-sectional area at the air-water interface A_D(fsk) = 73 Å^2. Lipid-water partitioning coefficients where therefore calculated with eq. 1 as K_{lw}(CPT) = $8.4 \cdot 10^3$ M^{-1} (without taking into account charge effects) and K_{lw}(fsk) = $4.9 \cdot 10^3$ M^{-1}.

Discussion

Changes in ECAR correspond to ATP consumption

Using a Cytosensor we have shown that the stimulation of CFTR by the phosphorylation agents CPT-cAMP and forskolin leads to a concentration dependent ECAR increase due to the export of the glycolytic waste product lactic acid. An analogous increase in the ECAR was previously observed upon stimulation of the ATPase activity of Pgp (16). Cells under anaerobic and high glucose conditions produce most of the ATP required for metabolism by glycolysis. Hence, ATP synthesis directly correlates with the production of lactic acid. As ATP is only produced when required, the changes in ATP synthesis correspond directly to alterations in ATP consumption. In the case of CFTR, at least two ATP consuming processes have to be considered: consumption of ATP for phosphorylation of CFTR by cAMP activated protein kinase A and ATP hydrolysis by the nucleotide binding domains of CFTR as described above. Whether only one reaction or both are observed is discussed in the following.

Effects of CPT-cAMP on ECAR are specific for functional CFTR

Increasing concentrations of CPT-cAMP (up to concentrations C(CPT-cAMP) < 100 µM) enhanced the ECAR indicating ATP consumption in cells expressing functional *CFTR*, whereas CHO-K1 control cells showed no effect in this concentration range. CHO-ΔF behaved in a similar manner as CHO-K1 cells. This is likely due to the fact that measurements were carried out at the temperature of 37 °C at which this mutant is unstable in various cell lines (31-33). Microphysiometry experiments at lower temperature which may stabilize CFTRΔF508, yielded very low basal activities and hence unreliable results. Therefore experiments with CHO-ΔF cells were considered as a control, showing that the effects observed were not due to transfection as such or the presence of misfolded CFTR. Effects due to growth in methotrexate containing medium could also be excluded. We therefore concluded that the increase in ATP consumption at concentrations C(CPT-cAMP) < 100 µM was specific for the presence of functional CFTR in the membrane.

The slow reduction in ECAR at concentrations observed at C(CPT-cAMP) > 100 µM (Fig. 1C) could be due to several effects. Although suggested primarily for forskolin (34), high concentrations of CPT-cAMP might also be influenced by upregulated phosphodiesterase as it has been shown that CPT-cAMP can be hydrolyzed by

phosphodiesterases (35). Interestingly the inhibitory effects correlate with an unspecific stimulation of ATP hydrolysis in control cells and stimulation of iodide efflux, that could not be observed at concentrations C(CPT-cAMP) < 100 µM. The unspecific response in control cells might indicate that additional processes in the cell are stimulated that might account for the feedback. The clearly increased channel conductance could additionally cause direct effects of ion export on ECAR to become visible in this concentration range. This assumption is supported by findings, that stimulation of CFTR in C127 cells by C(CPT-cAMP) = 100 µM resulted in a relative alkalinization compared to control cells that might be caused by an increased efflux of bicarbonate ions (36). We can exclude an effect of inhibitory phosphorylation sites in CFTR (37) as iodide efflux does not decrease.

ATP consumption reflects activation of CFTR by protein kinase A

The ATP consumption was shown to be significantly inhibited by protein kinase A inhibitors. We fitted the ECAR vs. C(CPT-cAMP) curves in CHO-CFTR (Fig. 1D) and BHK-CFTR cells (Fig. 3A) with an equation (Eq.1) proposed previously for the activation of protein kinase A. The apparent dissociation constants obtained for CHO-CFTR and BHK-CFTR cells were assessed as $K_{d,app}$(CPT) = 12 µM and $K_{d,app}$(CPT) = 3.7 µM, respectively. The values are in the same order of magnitude as those obtained previously for cAMP binding to purified human PKA (K_d(cAMP) = 2.9 µM) (38). The maximal ECAR of 230 % calculated from that model is also in accordance with the maximal stimulation observed before the start of the slow decrease in the ECAR discussed above (Fig. 1C). The same holds true for BHK cells, although the slow inhibitory effect was less pronounced in that case.

It had been shown that already 2 minutes after stimulation of PKA a steady state of phosphorylation at several sites in the R domain of CFTR was reached (39). Therefore the activation of protein kinase A is probably the rate-limiting step. At the time resolution of Cytosensor® experiments (i.e. 2 min) the phosphorylation state of CFTR should directly correlate to this reaction. This allows us to assume that we are indeed monitoring the activation of CFTR by PKA dependent phosphorylation. The finding that the signal is sensitive to inhibition with PKA inhibitors further supports this assumption. Nevertheless approximately 20 % of maximum ECAR at C(CPT-cAMP) = 100 µM and C(PKI) = 20 µM or C(H-89) = 20 µM remained even after inhibitor application. This residual activity is probably due to incomplete inhibition. However,

we cannot exclude that the remaining increased ECAR reflects a direct interaction between CFTR and CPT-cAMP. This seems possible, because ABCC4, which is most closely related to CFTR among the human ABC transporters, is known to be a cAMP and cGMP exporter (40,41). Furthermore there is even evidence for direct binding of cAMP to CFTR (42). Incomplete inhibition, however, was also seen for stimulation with forskolin. If the remaining activity would be due to direct interactions, forskolin would have to interact with CFTR as well. As it had been shown earlier for other ABC transporters like P-glycoprotein that substrate binding occurs from the inner membrane leaflet, we carried out surface activity measurements for CPT-cAMP and forskolin, to elucidate if such effects would be plausible. We could show that both substances are surface active. It has also been shown, that H-bonds play a major in the substrate-transporter binding in ABC transporters. CPT-cAMP and forskolin would also fulfill this requirement as they possess several H-bond acceptor groups respectively. Therefore direct interactions for both substances would be possible. However, we observed that the concentrations of half-maximum activation for CPT-cAMP are two orders of magnitude greater than the values obtained for forskolin. The similar values for K_{lw} and the higher number of hydrogen bond acceptors in the case of CPT-cAMP would suggest that the effects occur at similar concentrations or even at lower concentrations in the case of CPT-cAMP. Thus, we cannot exclude that direct interactions of phosphorylation agents and CFTR are involved, but these results support again more the assumption that we are mainly monitoring the PKA mediated phosphorylation.

ECAR is decreased in the presence of BHK-E1371S

As discussed above BHK-CFTR cells react in the same manner as CHO-CFTR cells. However, the effect is completely abolished in BHK cells overexpressing *CFTRE1371S,* an ATP hydrolysis deficient mutant (43) and instead even a decrease in ECAR was observed. However, this does not necessarily mean that the observed signal is due to ATP hydrolysis. First of all, we cannot exclude that the expression level might be lower, although earlier findings suggest that *CFTRE1371S* expresses well (44). Moreover, the aforementioned alkalinization might also be responsible for the slight decrease in ECAR observed in BHK-E1371S cells. As this mutant shows prolonged open times compared to wildtype CFTR, it seems plausible that direct effects of ion conductance on ECAR are more pronounced in this mutant and might hide the actual stimulation. In

line with this assumption, we did not observe a decrease in BHK-ΔF cells. Although no additional information for the separation of the involved ATP consuming processes could be inferred from these measurements, we could show again that the observed effects clearly depend on the presence of functional CFTR.

Low forskolin concentrations cause effects on ECAR specific for functional CFTR

Forskolin causes a similar effect on ATP hydrolysis at low concentrations (C(fsk) ≤ 1 µM) as CPT-cAMP in CHO as well as BHK cells overexpressing functional *CFTR*. However, at higher concentrations (C(fsk) ≥ 1 µM) a decrease in ECAR is observed which is distinctly more pronounced than in the presence of CPT-cAMP. A decrease in the ECAR which can be interpreted as an alkalinization has been observed in previous Cytosensor experiments with *CFTR* transfected NIH/3T3 mouse embryo fibroblasts and C127 epithelial cells in the presence of C(fsk) = 1 µM and to an even greater extent in the presence of C(fsk) = 10 µM (45). As seen for CPT-cAMP concentrations C(CPT)≥100 µM this effect again correlates with an unspecific increase of ATP hydrolysis in control cells and also significant stimulation of iodide efflux (Fig. 6) and is only seen at concentrations where inhibition of ECAR can be observed. The decrease in ECAR for BHK-E1371S cells for concentrations C(fsk) <= 10 µM could again be due to the prolonged open time of this mutant and therefore increased efflux of bicarbonate. Altogether these observations strongly support that we are indeed monitoring the activation of CFTR by protein kinase A-dependent phosphorylation. As forskolin and CPT-cAMP cause similar specific effects in *CFTR* expressing cell lines, ATP consumption by adenylate cyclase is probably not contributing to a great extent to the observed signal.

Specific and unspecific effects of high forskolin concentrations can be separated

At concentrations C(fsk) > 10 µM an unspecific decrease of extracellular acidification could be observed in all tested cell lines. Unspecific metabolic effects of high forskolin concentrations C(fsk) > 20 µM have been suggested before (34). We assume that this effect is most likely due to a reduced glucose import that had been observed for forskolin earlier in various cell lines (46-48). This interpretation is in accordance with the increase in oxygen consumption (Fig. 5 B) to compensate for the decrease in glycolysis. As the effect of forskolin on glucose import has been described to start

already at concentrations C(fsk) < 1 µM we cannot exclude, that the decrease in ECAR between C(fsk) = 1 µM and C(fsk) = 10 µM is also at least partially also due to limited glucose supply. The more pronounced decrease of extracellular acidification in CHO-CFTR cells compared to control cells at concentrations C(fsk) > 10 µM might be again due to alkalinization. Whereas stimulation of ATP hydrolysis by CPT-cAMP vanishes shortly after CPT-cAMP withdrawal, stimulation of ATP hydrolysis by forskolin remains for up to 2 hours after withdrawal of forskolin (Fig.2 B and C), but at a lower level than the maximum stimulation. This effect is again specific for the presence of functional CFTR in the membrane and therefore may reflect increased ATP hydrolysis by CFTR. A prolonged activation of CFTR after withdrawal of protein kinase A stimulation has been observed before in excised patches from CHO cells (49).

Conclusions

We could show that microphysiometry monitors the stimulation of CFTR dependent ATP hydrolysis by CPT-cAMP and forskolin in a non-invasive and label-free way in real time. We could furthermore show, that the observed activity reflects the activation of CFTR via phosphorylation. Although the observed ATP hydrolysis cannot be clearly attributed to only PKA or only CFTR yet, the signal is nevertheless specific for cells expressing functional CFTR up to C(CPT) = 100 µM or C(fsk) = 10 µM. In parallel, microphysiometry yields useful information on potential side effects of tested compounds. Unspecific metabolic effects can be observed in real time and can be easily separated from CFTR-specific effects by comparison with wild type cells as demonstrated for high forskolin concentrations. The combination of ECAR and OCR measurements moreover allowed attributing this effect to impaired glucose uptake. The possibility to directly monitor the CFTR activity by microphysiometry may serve as a basis for investigating the influence potentiators and inhibitors on CFTR mediated ATP hydrolysis. Such experiments might in turn also help to distinguish better between ATP consumption by protein kinase A and CFTR.

Our assay may also prove useful in screening for corrector/potentiator combinations. As the experiments are carried out at 37 °C one would only get a signal if stable and functional CFTR is present in the membrane.

Acknowledgments: We gratefully thank Dr. J.R. Riordan (UNC School of Medicine, Biochemistry and Biophysics) and Dr. J. Reinhardt (Novartis, Switzerland) for the gift of CHO-CFTR, CHO-ΔF, BHK-CFTR, BHK-ΔF and BHK-E1371S cells.

Tables

Table 1: Sensitivity of forskolin and CPT-cAMP effects to inhibition of PKA and CFTR

Cells were incubated with H-89 or myristoylated PKI(14-22) fragment before stimulation with 1 µM forskolin, 50 µM forskolin or100 µM CPT-cAMP. Values are given as percent of stimulation without inhibitor application.

	100 µM CPT-cAMP	1 µM forskolin	50 µM forskolin
10 µM PKI	50.5 %	73.1 %	*n.d.*[a]
20 µM PKI	17.0 %	*n.d.*[a]	*n.d.*[a]
20 µM H89	22.3 %	17.2 %	108.4 %

[a] *not determined;*

Figure Legends

Figure 1: ECAR of CHO-K1 and CHO-CFTR cells as a function of CPT-cAMP concentration

Extracellular acidification rates of CHO-K1 (□) and CHO-CFTR (■) cells measured in a Molecular Dynamics Cytosensor® at 37 °C for 30 seconds every 2 minutes. A-C: Examples of raw data. Horizontal bars indicate time range of perfusion with medium containing CPT-cAMP (A: 1 µM; B: 50 µM; C:400 µM). D: The last 4 points of measurements (8 min) during perfusion with CPT-cAMP were averaged, normalized to the basal value before stimulation and plotted against CPT-cAMP concentration. Error bars represent the standard deviation of 3 – 6 measurements. The dotted line represents the best fit to data using Eq. 1 with $K_{d,app}$(CPT) = 12 µM and $ECAR_{max}$ = 230%. ECAR response of CHO-CFTR cells reach a maximum of 166±18 % of basal ECAR at 100 µM. ECAR increases even further at higher concentrations, but cannot be clearly quantified due to the observed slow decrease. CHO-K1 cells only start to respond at concentrations higher than 50 µM resulting in a maximum ECAR of 130 % at 400 µM CPT-cAMP.

Figure 2: ECAR of CHO-K1 and CHO-CFTR cells as a function of forskolin concentration

Extracellular acidification rates of CHO-K1 (□) and CHO-CFTR (■) cells measured in a Molecular Dynamics Cytosensor® at 37 °C for 30 seconds every 2 minutes. A-C: Examples of raw data. Horizontal bars indicate time range of perfusion with medium containing forskolin (A: 0.5 µM; B: 10 µM; C:100 µM). D: The last 4 points of measurements (8 min) during perfusion with forskolin were averaged, normalized to the basal value before stimulation and plotted against forskolin concentration. Error bars represent the standard deviation of 2 – 4 experiments. ECAR response of CHO-CFTR cells showed a increase at low and decrease at higher concentrations with a maximum of 195±19 % of basal ECAR at 1 µM forskolin. CHO-K1 cells only respond at concentrations C(fsk) > 10 µM. A minimal ECAR of 35 % at C(fsk) = 100 µM

Figure 3: Effects of CPT-cAMP and forskolin on extracellular acidification of BHK cells overexpressing *CFTR* variants

Extracellular acidification rates of BHK-E1371S (○) and BHK-CFTR (■) cells measured in a Molecular Dynamics Cytosensor® at 37 °C for 30 seconds every 2 minutes. The last 4 points of measurements (8 min) during perfusion with CPT-cAMP were averaged, normalized to the basal value before stimulation and plotted against concentration. Error bars represent the standard deviation of 2 – 4 experiments. Stimulation with CPT-cAMP (A) results in a maximal ECAR of 123 ± 7 % at C(CPT) = 100 µM for BHK-CFTR cells, while ECAR is slightly reduced in BHK-E1371S cells down to a minimum of 84 ± 4 % at C(CPT) = 50 µM. The dotted line depicts description of our data by Eq. 1 with $K_{d,app}$(CPT) = 3.7 µM and $ECAR_{max}$ = 125%. For forskolin a maximal ECAR of 117 ± 4 % is stably reached for concentrations 0.5 < C(fsk) ≤ 10 µM in BHK-CFTR cells. BHK-E1371S cells show a reduction down to 91 ± 3 % in this concentration range. At concentrations C(fsk) ≥ 10 µM a decrease in ECAR of both cell lines could be observed.

Figure 4: Effects of CPT-cAMP on ECAR and OCR of CHO-K1 and CHO-CFTR cell lines

Effect of 1, 5, 10, 50, 100, 200, 320 µM CPT-cAMP on the ECAR (■) and OCR (Δ) of CHO-K1 (A) and CHO-CFTR cells (B) measured in a Bionas Discovery 2500. Rates were measured for 2 min, followed by 2 min of flushing with flow medium. Therefore a measurement point was generated every 4 minutes. The rates were corrected automatically for sensor drift in the Bionas Data Analyzer® Software. Effects on OCR were parallel but slightly delayed. Horizontal lines indicate the presence of CPT-cAMP in the flow medium.

Figure 5: Effect of forskolin on oxygen consumption rate of CHO-K1 and CHO-CFTR cells

Effect of 0.1, 1, 2, 5, 10, 50, 100 µM forskolin on the ECAR (■) and OCR (Δ) of CHO-K1 (A) and CHO-CFTR cells (B) measured in a Bionas Discovery® 2500. Rates were measured for 2 min, followed by 2 min of flushing with flow medium. Therefore a measurement point was generated every 4 minutes. The rates were corrected automatically for sensor drift in the Bionas Data Analyzer® Software. Horizontal lines indicate the presence of forskolin in the flow medium.

Figure 6: Effects of CPT-cAMP and forskolin on iodide efflux of CHO-CFTR cells

CHO-CFTR cells were loaded with sodium iodide, and the recorded efflux rates were plotted against time. Horizontal bars indicate stimulation with 50 µM (*), 100 µM (○) and 200 µM (■) CPT-cAMP (A) or with 0.5 µM (*), 5 µM (○) and 10 µM (■) forskolin (B)

Figures

Figure 1: Effect of CPT-cAMP on ECAR of CHO-K1 and CHO-CFTR cells

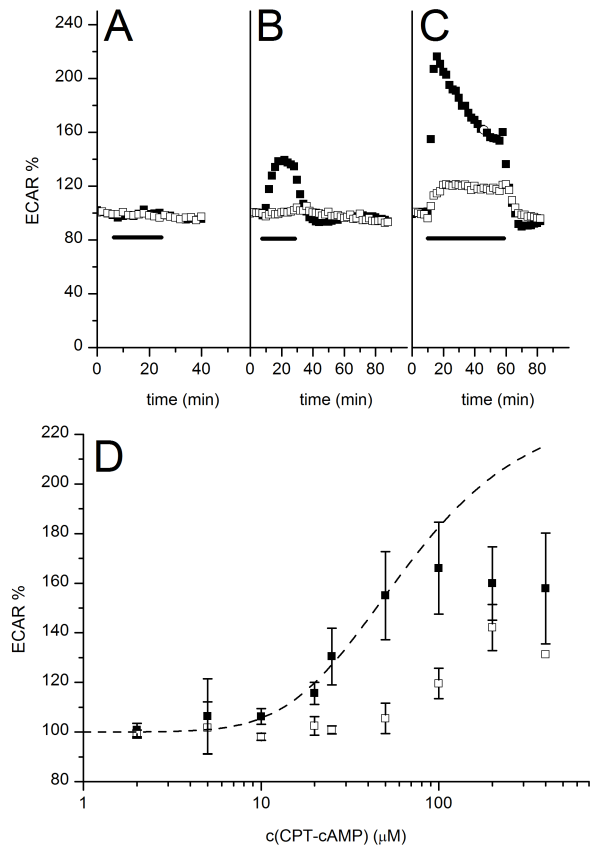

Figure 2: Effect of forskolin on the ECAR of CHO-K1 and CHO-CFTR cells

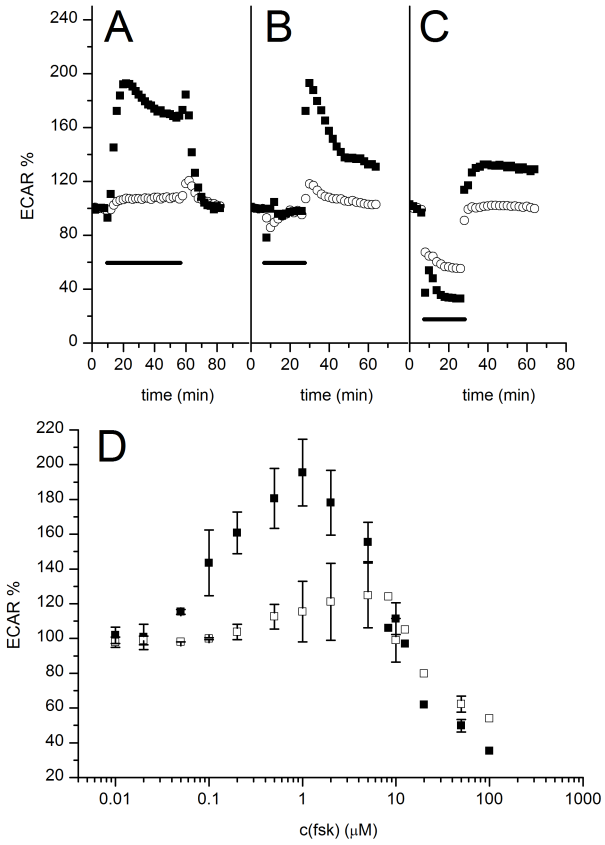

Figure 3: Effects of CPT-cAMP and forskolin on extracellular acidification of BHK cells overexpressing *CFTR* variants

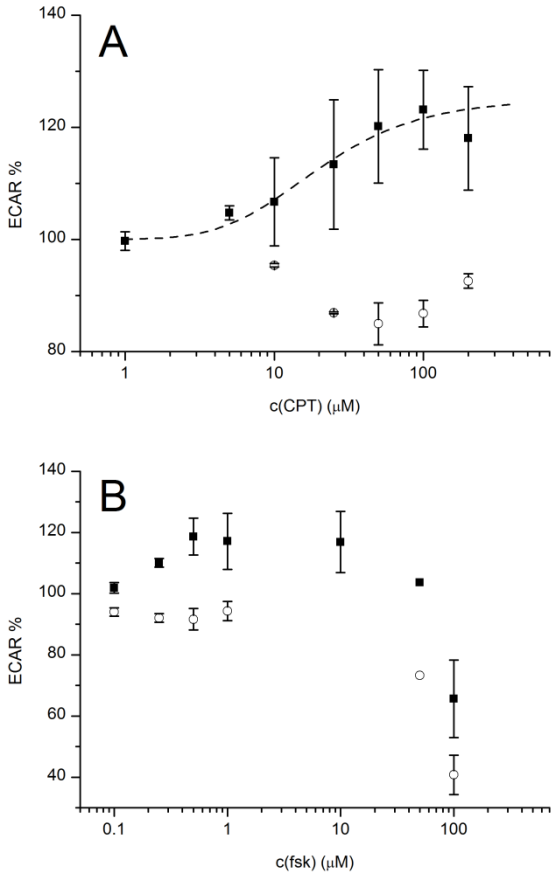

Figure 4: Effect of CPT-cAMP on oxygen consumption rate of CHO-K1 and CHO-CFTR cells

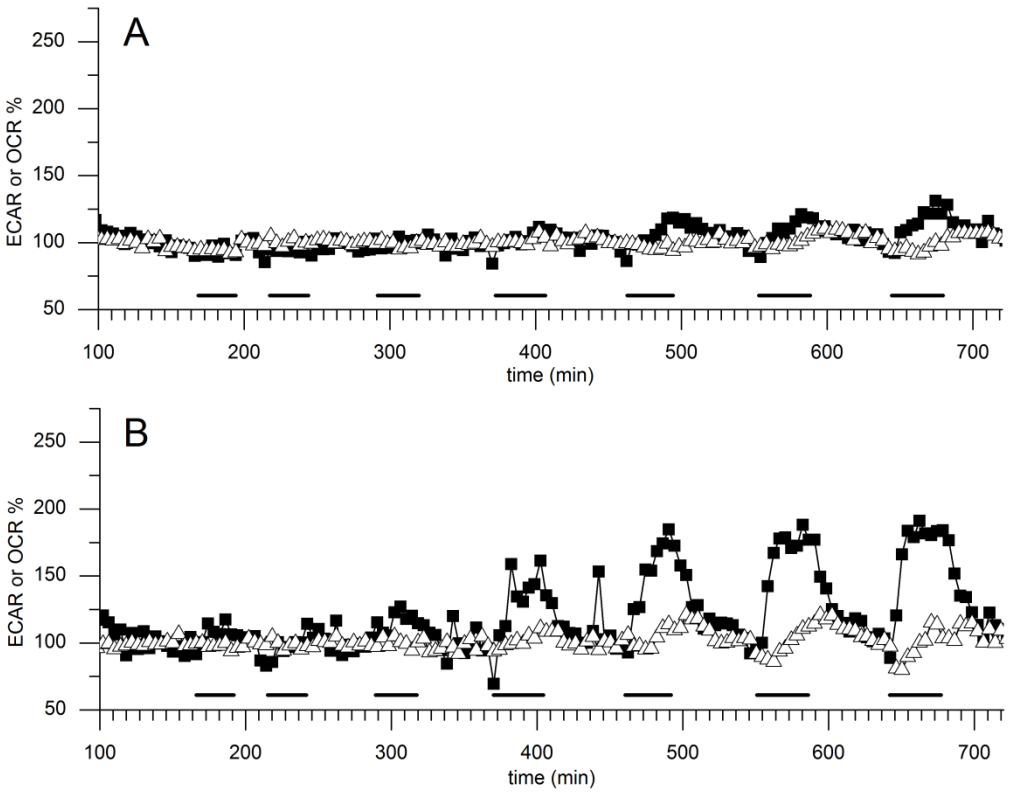

Figure 5: Effect of forskolin on oxygen consumption rate of CHO-K1 and CHO-CFTR cells

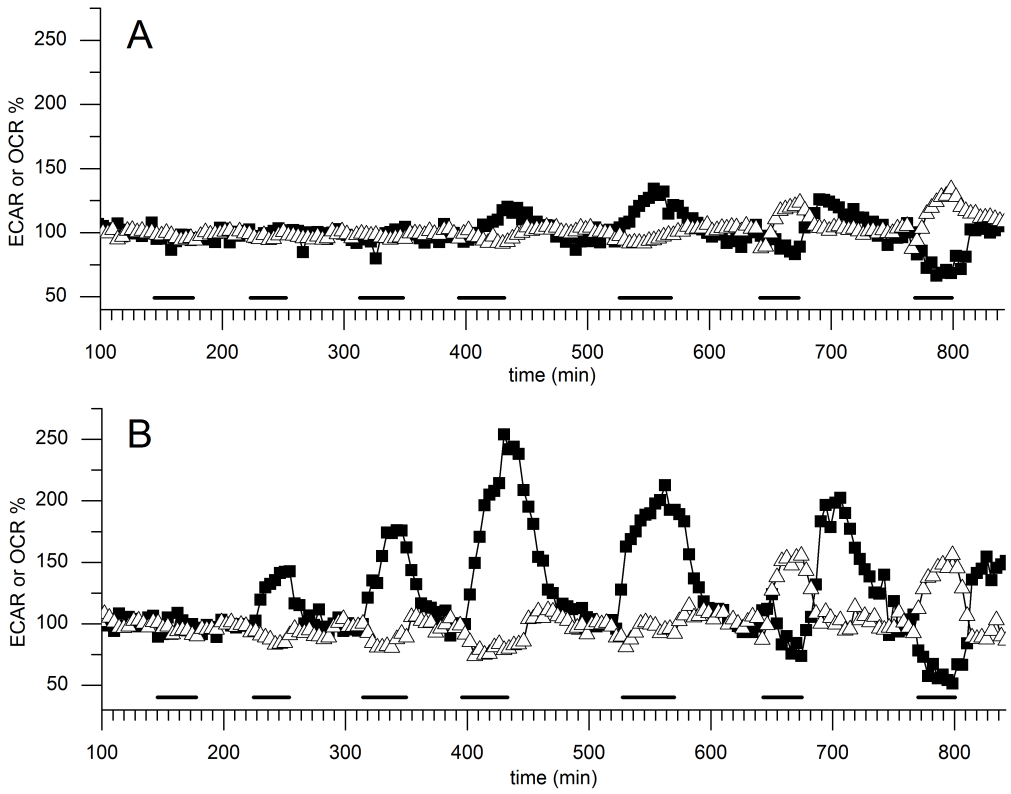

Figure 6: Effects of CPT-cAMP and forskolin on iodide efflux of CHO-CFTR cells

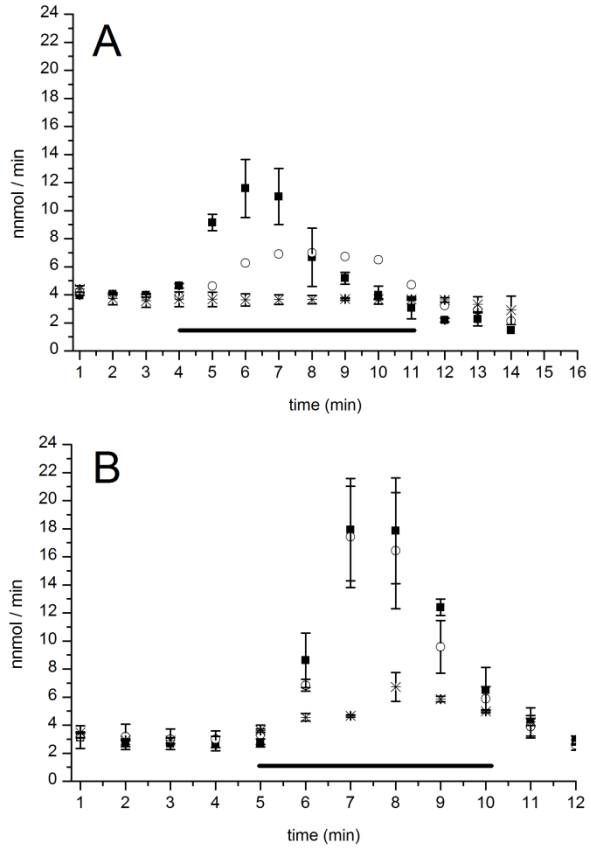

References

1. Riordan, J. R., Rommens, J. M., Kerem, B., Alon, N., Rozmahel, R., Grzelczak, Z., Zielenski, J., Lok, S., Plavsic, N., Chou, J. L., and et al. (1989) *Science* **245**, 1066-1073
2. Li, C., Ramjeesingh, M., Wang, W., Garami, E., Hewryk, M., Lee, D., Rommens, J. M., Galley, K., and Bear, C. E. (1996) *J Biol Chem* **271**, 28463-28468
3. Gunderson, K. L., and Kopito, R. R. (1995) *Cell* **82**, 231-239
4. Vergani, P., Lockless, S. W., Nairn, A. C., and Gadsby, D. C. (2005) *Nature* **433**, 876-880
5. Csanady, L., Nairn, A. C., and Gadsby, D. C. (2006) *J Gen Physiol* **128**, 523-533
6. Bear, C. E., Li, C. H., Kartner, N., Bridges, R. J., Jensen, T. J., Ramjeesingh, M., and Riordan, J. R. (1992) *Cell* **68**, 809-818
7. Csanady, L., Vergani, P., and Gadsby, D. C. (2010) *Proc Natl Acad Sci U S A* **107**, 1241-1246
8. Tabcharani, J. A., Chang, X. B., Riordan, J. R., and Hanrahan, J. W. (1991) *Nature* **352**, 628-631
9. Hegedus, T., Serohijos, A. W., Dokholyan, N. V., He, L., and Riordan, J. R. (2008) *J Mol Biol* **378**, 1052-1063
10. Mense, M., Vergani, P., White, D. M., Altberg, G., Nairn, A. C., and Gadsby, D. C. (2006) *Embo J* **25**, 4728-4739
11. Ketchum, C. J., Rajendrakumar, G. V., and Maloney, P. C. (2004) *Biochemistry* **43**, 1045-1053
12. Kogan, I., Ramjeesingh, M., and Bear, C. E. (2004) *J Cyst Fibros* **3 Suppl 2**, 133-134
13. Li, H., Sheppard, D. N., and Hug, M. J. (2004) *J Cyst Fibros* **3 Suppl 2**, 123-126
14. Taddei, A., Folli, C., Zegarra-Moran, O., Fanen, P., Verkman, A. S., and Galietta, L. J. (2004) *FEBS Lett* **558**, 52-56
15. Landwojtowicz, E., Nervi, P., and Seelig, A. (2002) *Biochemistry* **41**, 8050-8057.
16. Gatlik-Landwojtowicz, E., Aanismaa, P., and Seelig, A. (2004) *Biochemistry* **43**, 14840-14851
17. Gatlik-Landwojtowicz, E., Aanismaa, P., and Seelig, A. (2006) *Biochemistry* **45**, 3020-3032
18. McConnell, H. M., Owicki, J. C., Parce, J. W., Miller, D. L., Baxter, G. T., Wada, H. G., and Pitchford, S. (1992) *Science* **257**, 1906-1912
19. Hafner, F. (2000) *Biosens Bioelectron* **15**, 149-158
20. Aanismaa, P., Gatlik-Landwojtowicz, E., and Seelig, A. (2008) *Biochemistry* **47**, 10197-10207
21. Chen, E. Y., Bartlett, M. C., Loo, T. W., and Clarke, D. M. (2004) *J Biol Chem* **279**, 39620-39627
22. Fromherz, P. (1975) *Rev Sci Instrum* **46**, 1380-1384
23. Fischer, H., Gottschlich, R., and Seelig, A. (1998) *J Membr Biol* **165**, 201-211
24. Gerebtzoff, G., Li-Blatter, X., Fischer, H., Frentzel, A., and Seelig, A. (2004) *Chembiochem* **5**, 676-684
25. Boguslavsky, V., Rebecchi, M., Morris, A. J., Jhon, D. Y., Rhee, S. G., and McLaughlin, S. (1994) *Biochemistry* **33**, 3032-3037.
26. Moran, O. (2010) *J Theor Biol* **262**, 73-79
27. Laohapitakworn, S., Thongbunchoo, J., Nakkrasae, L. I., Krishnamra, N., and Charoenphandhu, N. (2011) *Am J Physiol Cell Physiol* **301**, C137-149
28. Hughes, L. K., Ju, M., and Sheppard, D. N. (2008) *Mol Membr Biol* **25**, 528-538
29. Wu, D., and Hu, Z. (2008) *J Pharmacol Exp Ther* **325**, 256-266
30. Gerebtzoff, G., and Seelig, A. (2006) *J Chem Inf Model* **46**, 2638-2650
31. Heda, G. D., Tanwani, M., and Marino, C. R. (2001) *Am J Physiol Cell Physiol* **280**, C166-174

32. Swiatecka-Urban, A., Brown, A., Moreau-Marquis, S., Renuka, J., Coutermarsh, B., Barnaby, R., Karlson, K. H., Flotte, T. R., Fukuda, M., Langford, G. M., and Stanton, B. A. (2005) *J Biol Chem* **280**, 36762-36772
33. Varga, K., Goldstein, R. F., Jurkuvenaite, A., Chen, L., Matalon, S., Sorscher, E. J., Bebok, Z., and Collawn, J. F. (2008) *Biochem J* **410**, 555-564
34. Moran, O., and Zegarra-Moran, O. (2008) *J Cyst Fibros* **7**, 483-494
35. Connolly, B. J., Willits, P. B., Warrington, B. H., and Murray, K. J. (1992) *Biochem Pharmacol* **44**, 2303-2306
36. Luckie, D. B., Singh, C. N., Wine, J. J., and Wilterding, J. H. (2001) *J Membr Biol* **179**, 275-284
37. Csanady, L., Seto-Young, D., Chan, K. W., Cenciarelli, C., Angel, B. B., Qin, J., McLachlin, D. T., Krutchinsky, A. N., Chait, B. T., Nairn, A. C., and Gadsby, D. C. (2005) *J Gen Physiol* **125**, 171-186
38. Dao, K. K., Teigen, K., Kopperud, R., Hodneland, E., Schwede, F., Christensen, A. E., Martinez, A., and Doskeland, S. O. (2006) *J Biol Chem* **281**, 21500-21511
39. Hegedus, T., Aleksandrov, A., Mengos, A., Cui, L., Jensen, T. J., and Riordan, J. R. (2009) *Biochim Biophys Acta* **1788**, 1341-1349
40. Wielinga, P. R., van der Heijden, I., Reid, G., Beijnen, J. H., Wijnholds, J., and Borst, P. (2003) *J Biol Chem* **278**, 17664-17671
41. Klein, I., Sarkadi, B., and Varadi, A. (1999) *Biochim Biophys Acta* **1461**, 237-262
42. Pereira, M. M., Parker, J., Stratford, F. L., McPherson, M., and Dormer, R. L. (2007) *Biochem J* **405**, 181-189
43. Vergani, P., Nairn, A. C., and Gadsby, D. C. (2003) *J Gen Physiol* **121**, 17-36
44. Bompadre, S. G., Cho, J. H., Wang, X., Zou, X., Sohma, Y., Li, M., and Hwang, T. C. (2005) *J Gen Physiol* **125**, 377-394
45. Luckie, D. B., Singh, C. N., Wine, J. J., and Wilterding, J. H. (2001) *J Membr Biol* **179**, 275-284
46. van Valen, F., and Keck, E. (1988) *Bone* **9**, 89-92
47. Geisbuhler, T. P., Sergeant, S., Miramonti, F. L., Kim, H. D., and Rovetto, M. J. (1987) *Pflugers Arch* **409**, 158-162
48. Sergeant, S., and Kim, H. D. (1985) *J Biol Chem* **260**, 14677-14682
49. Ferrera, L., Pincin, C., and Moran, O. (2007) *J Membr Biol* **220**, 1-9

7.2 CFTR-ATPase Modulation by Inhibitors and Potentiators

Matthias Zwick, Rita Müller, and Anna Seelig*

Submitted to Biochemistry

Biophysical Chemistry, Biozentrum, University of Basel, Klingelbergstrasse 50/70, CH-4056 Basel, Switzerland, Phone: +41-61-267 2206, FAX: +41-61-267 2189, e-mail: anna.seelig@unibas.ch

*Corresponding author

Introduction

Typical ATP binding cassette (ABC) export proteins consist of two transmembrane domains (TMDs), each comprising six transmembrane α-helices, and two cytoplasmic nucleotide binding domains (NBDs), arranged in the order NBD1, TMD1, NBD2, TMD2. In the case of the best investigated transporter P-glycoprotein (Pgp, ABCB1) (1) the four domains form a monomer, whereas in the case of BCRP (ABCG2), discovered more recently (2,3), two domains form a monomer and the protein most likely functions as a homodimer. Binding of two ATP molecules at the interface between the two NBDs is generally assumed to induce dimerization and concomitant opening of the TMDs to the extracellular side as shown for the bacterial Sav1866 (4). Subsequent hydrolysis of at least one ATP molecule leads to NBD dissociation and reopening of the TMDs at the cytosolic side. Due to the concerted opening and closing of the TMDs via ATP binding and hydrolysis (5) translocation becomes unidirectional (6).

Pgp and BCRP function as exporters of membrane soluble compounds that are recognized and bound by the TMDs in the cytosolic membrane leaflet. The recognition elements in compounds are free electron pairs, π-electron systems, i.e. hydrogen bond acceptor groups or cationic groups and the counterparts in the TMDs are the numerous amino acids with hydrogen bond donor groups and π-electron systems. This allows gliding of the compounds along the TMDs via weak electrostatic interactions (7,8)

The rate of ATP hydrolysis increases with the concentration of cargo molecules up to a maximum and then decreases again at higher concentrations yielding a bell-shaped activity curve. The bell-shaped activity vs. concentration curves can be analyzed using a two-site binding model based on uncompetitive inhibition. The two-site binding model is consistent with the two binding sites observed by photoaffinity labeling of Pgp (9) and by crystallization of Pgp in the presence of substrates (10). Substrate transport seems to be the rate-limiting step in the activity cycle of Pgp (11). The rate of ATP hydrolysis is proportional to the rate of effective transport (not to confuse with the rate of net transport) (12). Pgp does not interact with negatively charged compounds but efficiently flops amphiphilic electrically neutral or cationic compounds, and is inhibited by non-amphiphilic compounds (Xiaochun Li-Blatter,, Andreas Beck and Anna Seelig, submitted), whereas BCRP flops amphiphilic negatively charged or zwitterionic compounds and is inhibited by amphiphilic electrically neutral or negatively charged compounds (Estefania Egido, Rita Müller, Xiaochun Li-Blatter and Anna Seelig, in preparation).

The cystic fibrosis transmembrane conductance regulator (CFTR, ABCC7) is special among the ABC proteins in that it contains a unique additional regulatory domain (RD)

with multiple cAMP-dependent protein kinase A (PKA) targets that modulates NBD dimerization. The best known function of the protein is that of an ion channel which allows passive diffusion of chloride and other small anions across the membrane. The channel is supposed to be conductive when TMDs are in a conformation open to the extracellular side. Different classes (I-VI) of mutations in the *CFTR* gene are known which cause malfunction of the chloride flux.

Modulators of CFTR are investigated as drugs against several diseases. Potentiators of anion conductance are developed to treat cystic fibrosis (CF) caused by class III or IV mutations in the *CFTR* gene that lead to channels with impaired gating or chloride conductance. These drugs are often investigated in combination with correctors designed to improve folding and membrane trafficking defective in the most common mutation ΔF508 which belongs to class II (for review see (13)). Hybrid molecules consisting of a potentiator and a corrector moiety have been investigated recently. Apart from CF, the channel is involved in other disorders, including secretory diarrheas where enhanced cAMP or cGMP levels cause increased chloride efflux through CFTR (14), or autosomal dominant polycystic kidney disease where CFTR inhibitors have been shown to be beneficial (15). While it has been shown recently that most correctors act indirectly via upregulation of chaperones or hindered ubiquitinylation in a cell line dependent manner, many potentiators and inhibitors are known to directly interact with CFTR (16). For inhibitors two possible modes of action have been described so far: direct block of the open channel pore from the extracellular side which was seen for GlyH-101 and allosteric block from the cytoplasmic side (17). Interestingly some inhibitors of CFTR are transported by other ABC transporters. An example is glibenclamide which was found to bind to the ABC transporter analog SUR1 (18) and to inhibit Pgp (19). This raises the question whether the same mechanism is responsible for both, substrate transport and modulation of chloride flux.

Inhibitors and potentiators were shown to specifically and directly interact with CFTR and are therefore ideal tools to monitor the effect on CFTR-ATPase activity. For measurements of ATPase activity in living cells as a function of concentration of modulators we used microphysiometry (20). This technique applied to living cells has been shown to be up to ten times more sensitive than classical methods applied to inside-out plasma membrane vesicles or reconstituted systems (Joseph Zolnerciks, Kenneth Linton, submitted). Using CFTR inhibitors and potentiators we could measure the CFTR-ATPase activity in *CFTR*-transfected CHO and BHK cells in real time.

We detected bell-shaped activity profiles that resemble the behavior seen for other ABC transporters and therefore conclude that ATPase activity of CFTR is indeed

regulated in the same way. Based on these findings we propose a model for inhibitor and potentiator action based on known effects of these compounds on other ABC transporters. We also found some evidence that at least some potentiators might act in a way similar to inhibitors, though leading to a different effect. Furthermore we found that most of the investigated inhibitors of CFTR, including CFTRinh-172 and PPQ-102, are also BCRP or Pgp substrates respectively.

Materials and Methods

Compound preparation

Glibenclamide, glipizide, CFTRinh-172, 8-(4-Chlorophenylthio)adenosine-3',5'-cyclic monophosphate (CPT-CAMP), capsaicin and flavonoids were purchased from Sigma-Aldrich (St. Louis, Missouri, USA). PPQ-102 was bought from Merck (Darmstadt, Germany), curcumin from Extrasynthese (Genay, France). Cell culture media, heat inactivated fetal bovine serum (FBS) and other chemicals used for cell culture were purchased from LuBioSciences (Luzern, Switzerland).

Cell lines

CHO-K1, CHO cells stably transfected with the human *CFTR* gene (CHO-CFTR) or the mutant *CFTRΔF508* (CHO-ΔF) were a generous gift from Dr. J. R. Riordan (University of North Carolina, USA) and Dr. Jürgen Reinhardt (Novartis, Switzerland). NIH3T3 and *MDR1*-transfected mouse embryo fibroblasts (NIH-MDR1-G185) were a generous gift from Dr. M. M. Gottesman and Dr. S. V. Ambudkar (National Institutes of Health, Bethesda, MD).

Cell culture

Untransfected CHO cells were grown in minimum essential medium alpha (MEMα) without ribonucleosides/deoxyribonucleosides containing 10 % FBS at 37 °C and 5 % CO_2. CHO-CFTR and CHO-ΔF cells were cultured in the same medium supplemented with 50 µM methotrexate (MTX). The cells were split 1:10 or 1:15 and passaged every 2 - 3 days. Transfected mouse embryo fibroblasts were grown in the presence of 0.15 µM colchicine and were maintained as described previously (21).

Microphysiometry

The Cytosensor® microphysiometer (Molecular Devices) consists of 8 light-addressable potentiometric sensors. Cells are grown as a layer on 3.0 µm polycarbonate membranes (Ø 12 mm, Corning) on the bottom of a flow chamber. This flow chamber is placed above the sensors which can measure voltage changes that are linearly correlated to pH changes. Calibration experiments showed that 61 mV correspond to 1 pH unit (21). Cells were seeded to reach a final number of $5 \cdot 10^5$ cells / membrane and incubated either for 4 hours or overnight. Commercially available dry powder MEMα without sodium bicarbonate was used for flow medium preparation. The absence of sodium bicarbonate is necessary to maintain a very low

buffer capacity and to avoid bubble formation during the measurements. Sodium chloride was used as a substitute to preserve osmotic balance. The pH was always adjusted to 7.4 at 37 °C. Cells were continuously flushed with fresh flow medium at a flow rate of 100 µl/min. Pumps were stopped every 2 minutes for 30 seconds to allow detection of acidification. Extracellular acidification rates were calculated using Molecular Devices Cytosoft® and the slope between 5 seconds after stopping and 2 seconds before restarting the pump was evaluated to avoid artifacts caused by pump switching. The Cytosensor® offers a second tubing system that was filled with drug containing medium prior to application. The stimulating agents could be therefore applied with little delay, as a valve close to the measurement chamber can be switched between the two channels. All measurements were carried out at 37 °C.

Compound concentrations were corrected for adsorption to the tubing system. The loss was monitored by UV spectroscopy. Compound concentration was detected in a Spectramax M2 (Molecular Devices, Sunnyvale, CA) spectrophotometer at the following wavelengths: apigenin and genistein at 261 nm; glibenclamide and glipizide at 300 nm; CFTRinh-172 at 380 nm; PPQ-102 at 320 nm.

Colorimetric assay of vanadate sensitive ATPase activity of Pgp and BCRP

For Pgp, inside-out vesicles from NIH-MDR-G185 cells were prepared as described elsewhere (11). In the case of BCRP, inside-out vesicles were bought from Solvo Biotechnologies (Budapest, Hungary). ATPase activity was measured in 96-well microtiter plates (Nunc F96 MicroWell plate, nontreated) as described earlier by Litman et al. (22). Membrane vesicles containing Pgp were diluted to a protein concentration of 0.1 mg/mL in ice-cold phosphate release assay buffer (25 mM Tris-HCl pH7.0, 50 mM KCl, 3 mM ATP, 2.5 mM MgSO4, 3 mM DTT, 0.5 mM EGTA, 2 mM ouabain and 3 mM sodium azide). Assay volume was 60 µL and drugs were added on ice. Reaction was started by transferring the plate to a water bath (37 °C) and terminated after 1h by rapidly cooling the plate on ice. To quantify the released inorganic phosphate 200 µL of an ice-cold solution containing ammonium molybdate (0.2% (w/v)), sulfuric acid (1.43% (v/v)), freshly prepared ascorbic acid (1% (w/v)) and SDS (0.9% (w/v)) was added to each well. Plates were incubated at room temperature for 30 minutes and the formed complex was quantified by measuring absorption at 820 nm in a Spectramax M2 (Molecular Device, Sunnyvale, CA) spectrophotometer. For calibration, samples containing known phosphate concentration were included in each plate. Measurements with samples containing 0.5 mM were carried out in parallel and subtracted from the obtained results.

Kinetics of ABC transporter ATPase

The activity curves yielded by ECAR measurements and ATPase assays in inside-out vesicles were fitted with an equation based on a two-site binding model described in eq. 1 (23). This model is based on the principles of uncompetitive or substrate inhibition and allows for basal activity. Therefore the observed velocity V, reflecting the change in ATPase activity or ECAR, was described by

$$V = \frac{K_1 K_2 V_0 + K_2 V_1 C + V_2 C^2}{K_1 K_2 + K_2 C + C^2}, \quad (1)$$

where K_1 is the concentration of half-maximum activation, K_2 the concentration of half-maximum inhibition, V_0 the normalized basal activity, V_1 is the maximum activity, V_2 the minimum activity, and C the substrate concentration in aqueous solution. Since experiments were performed under steady state conditions and the binding steps were much faster than the catalytic step, the concentration of half-maximum activation, K_1, could be assumed to correspond to the dissociation constant of the drug from the transporter. The inverse ($1/K_1$) then corresponds to the transporter-water binding constant, K_{tw} (24) to a first approximation,

$$K_{tw} = \frac{1}{K_1}. \quad (2)$$

Iodide efflux assay

The protocol described by Chen et al. (25) was slightly modified do determine iodide efflux from living cells. CHO cells were grown to 90 % confluency in 60 mm culture dishes. After washing three times with 2.5 ml loading buffer (136 mM NaI, 3 mM KNO_3, 2 mM $Ca(NO_3)$, 11 mM Glucose, 20 mM HEPES/NaOH pH 7.4) cells were incubated for 2 – 3 hours on 37 °C. The incubation was followed by 30 washing steps with 2.5 ml efflux buffer (136 mM $NaNO_3$, 3 mM KNO_3, 2 mM $Ca(NO_3)$, 11 mM Glucose, 20 mM HEPES/NaOH pH 7.4) containing 5 – 50 µM CPT-cAMP to remove excess iodide without removing the cells. Afterwards efflux buffer was exchanged every minute and collected. The first five samples were used to determine basal iodide efflux. Afterwards, efflux buffer was replaced by stimulation buffer containing CPT-cAMP and tested drugs. Samples were collected and stored in the dark at room temperature. An iodide selective electrode (Mettler Toledo, perfectIon® combination I^-) was used to

determine iodide concentrations based on a calibration curve recorded with various NaI concentrations in efflux buffer. All experiments were carried out at 37 °C.

Determination of lipid-membrane partitioning coefficients

The surface pressure, π, was measured as a function of drug concentration employing either a 3 ml or 20 ml Fromherz Teflon trough connected to a Wilhelmi balance (26). If not stated otherwise the same drug stock solutions as described above were used. Measurements were carried out in 50 mM Tris/HCl pH 7.4 containing 114 mM NaCl. Changes in π upon drug addition to the buffer in the trough were recorded as a function of time until equilibrium was reached. If stock solutions in DMSO where used an upper limit of 5 % DMSO was not exceeded as effects of DMSO can be neglected below. Measurements were carried out at room temperature.

To determine the air-water partition coefficient K_{aw}, the cross-sectional area at the air-water interface A_{D} and the critical micelle concentration CMC_{D} or solubility limit C_{sol} respectively, we measured a Gibbs adsorption isotherm. Therefore the surface pressure at equilibrium was recorded as a function of drug concentration C(drug). Data evaluation was performed as described earlier (27,28).

The actual lipid-water partition coefficient K_{lw} relevant for membrane binding was derived from K_{aw} according to

$$K_{\mathrm{lw}} = K_{\mathrm{aw}} \cdot e^{\frac{-\pi_{\mathrm{M}} A_{\mathrm{D}}}{k_{\mathrm{B}} T}} \qquad (3)$$

where k_{B} is the Boltzmann constant and T the temperature. The term $\pi_{\mathrm{M}} \cdot A_{\mathrm{D}}$ represents the work required to create a hole in the lipid membrane with a given packing density π_{M} that is wide enough to accommodate a molecule with the cross-sectional area A_{D}.

Calculation of Free Energy of Modulator Binding to the Transporter and Free Energy of Lipid-Water Partitioning. Binding of a modulator from the extracellular aqueous phase to an ABC transporter is a two-step binding mechanism, comprising a lipid-water partitioning step followed by a binding step from the lipid membrane to the transporter. The free energy of binding of a modulator from water to the first binding site of an ABC transporter, $\Delta G^0_{\mathrm{tw}(1)}$, can thus be expressed as the sum of the free energy of lipid-water partitioning, ΔG^0_{lw}, and the free energy of binding from the lipid membrane to an ABC transporter, $\Delta G^0_{\mathrm{tl}(1)}$, as shown previously for Pgp (24),

$$\Delta G_{tw}^{0} = \Delta G_{lw}^{0} + \Delta G_{tl}^{0}. \quad (4)$$

The free energy of transporter-water binding is

$$\Delta G_{tw}^{0} = -RT \ln\left(C_w K_{tw}\right), \quad (5)$$

where RT is the thermal energy and C_{w} is the molar concentration of water (C_{w} = 55.3 mol/L at 37°C). An analogous equation can be formulated for the second binding site. The free energy of the lipid-water partitioning, $\Delta G_{\mathrm{lw}}^{0}$ is

$$\Delta G_{lw}^{0} = -RT \ln\left(C_w K_{lw}\right). \quad (6)$$

Results

Sulfonylurea compounds increase ECAR of cells expressing functional CFTR

Cytosensor experiments were carried out as described above. The cells were allowed to accommodate to the flow medium for 2 hours. After this initial phase, basal activity was normalized to 100 % and the cells were stimulated with varying concentrations of CPT-cAMP between C(CPT) = 5 µM and C(CPT) = 100 µM. Cells were again allowed to accommodate and a stable increased activity was usually reached after 2 hours. ECAR of CHO-CFTR cells was increased, while control cells expressing no *CFTR* or defective *CFTRΔF508* remained close to basal levels as observed earlier (Matthias Zwick, Manuel Hellstern, Anna Seelig in preparation). Subsequently cells were perfused with increasing concentrations of glibenclamide or glipizide for 20 minutes per concentration tested. The interval length was chosen to assure that a stable ECAR was reached and steady-state conditions could be assumed. For quantification, the difference between the average of four measurements prior to compound application and the average of 3 – 4 measurement points at the end of each stimulation interval was evaluated. After each stimulation period cells were flushed with medium containing only CPT-cAMP until the ECAR returned to baseline showing that ECAR changes were reversible at all conditions tested. ECAR of CHO-K1 cells increased to a maximum of approximately 125 % at C(glib) = 25 µM and decreased again for higher concentrations (Fig. 1A–C). The effect was not dependent on the CPT-cAMP concentration. ECAR of CHO-CFTR cells instead increased up to 210±27% for C(glib) = 10 µM and C(CPT) = 25 µM (Fig. 1B), resulting in a bell-shaped activity profile. As shown in Figure 1A–C, maximum ECAR is reached at lower concentrations with increasing CPT-cAMP concentrations. CHO-ΔF cells showed a behavior similar to CHO-K1 cells (not shown). The effects were corrected for altered basal activity after CPT-cAMP stimulation and could subsequently be described by eq. 1 (Fig. 1A-C). The calculated concentrations of half-maximal activation, K_1, were shifted to lower glibenclamide concentrations with increasing CPT-cAMP concentrations, i.e. K_1(glib) = 25 µM for C(CPT) = 5 µM and K_1(glib) = 1 µM for C(CPT) = 50 µM. A further increase of CPT-cAMP to C(CPT) = 100 µM did not result in a further decrease in K_1 values. The calculated parameters for various conditions are summarized in Table 1.

Fig. 1

Titrations with glipizide yielded a similar bell-shaped ECAR activity profile. The K_1 values were shifted to higher concentrations compared to glibenclamide at identical prestimulation conditions with CPT-cAMP concentrations C(CPT) = 25 µM or C(CPT) = 50 µM (Fig. 2 A and B) and are summarized in Table 1. Maximum ECAR was slightly lower (161±16%) compared to glibenclamide. The effect of glipizide on CHO-K1 cells was comparable to the effect caused by glibenclamide but again shifted to higher concentrations, i.e. maximum ECAR of 121 % was reached at C(glipz) = 80 µM and C(CPT) = 25 µM.

Fig. 2

CFTRinh-172 and PPQ-102 have similar effects on ECAR as sulfonylurea compounds

The two high affinity CFTR inhibitors identified in high-throughput screens, the thiazolidinone CFTRinh-172 and the pyrimido-pyrrolo-quinoxalinedione compound PPQ-102 induced similar bell-shaped activity curves in CHO-CFTR cells as seen above for the sulfonylurea drugs. The ECAR was increased by CFTRinh-172 to a maximum of 189±28 % for C(inh172) = 1 µM and C(CPT) = 25 µM. However, only small shifts for K_1 values with CPT-cAMP concentration were observed, i.e. K_1(inh172) = 1.0 µM for C(CPT) = 5 µM and K_1(inh172) = 4.0 µM for C(CPT) = 50 µM. CFTRinh-172 also induced an unspecific effect on CHO-K1 cells. In contrast to glibenclamide, the unspecific effect was dependent on the CPT-cAMP concentration used for prestimulation and maximal unspecific stimulation increased up to 138±11 % for C(inh172) = 10 µM and C(CPT) = 50 µM (Fig. 3A-C).

Fig. 3

PPQ-102 was only tested following stimulation with CPT-cAMP at a concentration of C(CPT) = 50 µM. A bell-shaped concentration dependent ECAR profile could be seen again with a maximum of 137±12% at a concentration C(PPQ) = 0.45 µM (Fig. 4A). CHO-K1 cells were affected in a similar way and the ECAR reached a maximum of 114±8% at the same conditions. Describing the observed effect by eq. 1 resulted in K_1(PPQ) = 0.5 µM. Due to the small difference between control and transfected cells, the results for PPQ-102 can only be considered as an estimate. Adsorption to the tubing system was monitored by UV spectroscopy. (MM) It has to be noted, that adsorption to the tubing system was much higher in the case of PPQ-102 compared to all other compounds tested. A loss of almost 80 % was detected for concentrations C(PPQ-102)

≥ 1 µM. Reliable corrections could only be made at concentrations C(PPQ-102) ≥ 0.22 µM , lower concentrations may therefore be even lower.

Fig. 4

Table 1

Flavonoids

The influence of the flavonoids apigenin and genistein on the ECAR of CHO-CFTR cells is shown in Fig. 5 and 6. Following prestimulation with 5 µM CPT-cAMP, apigenin reduced the ECAR of control cells with increasing concentration down to 73±2 % at a concentration C(api) = 8 µM. However, the ECAR of CHO-CFTR increased for concentrations C(api) ≥ 1 µM and reached a maximum of 112±3% for C(api) = 2 µM (Fig. 5A). Higher concentrations reduced ECAR again down to 91±13 %. Nevertheless the ECAR of transfected cells always remained at a higher level than that of control cells. A similar effect could be seen for prestimulation with 25 µM CPT-cAMP. ECAR of control cells was again reduced with increasing apigenin concentrations. Activating effects on CHO-CFTR cells were more pronounced and reached a maximum of 135±11% at a concentration of C(api) = 2 µM (Fig. 5B). At higher concentrations the ECAR decreased again but remained on higher levels compared to control cells. Furthermore apigenin concentrations C(api) > 1 µM caused a second effect. Upon withdrawal of apigenin and replacement by flow medium ECAR of CHO-CFTR cells increased clearly and returned to baseline within 20 minutes (Fig. 5 G). This effect again was more pronounced for higher CPT-cAMP concentrations. After prestimulation with 5 µM or 25 µM CPT-cAMP the ECAR peak upon washout reached a maximum of 118±12% or 153±22% respectively. The effect did not decrease significantly with increasing concentrations C(api) > 1 µM. The ECAR increase upon withdrawal of apigenin in control cells, prestimulated with 25 µM CPT-cAMP was comparably small, and the ECAR returned to baseline levels already after 6 minutes. As apigenin started to aggregate at a concentration C(api) = 10 µM no higher concentrations were tested.

Fig. 5

Genistein (Fig. 6) was tested under several prestimulation conditions. Below C(CPT) = 50 µM CHO-K1 and CHO-CFTR cells behaved identically. No effect on ECAR could be seen for genistein concentrations C(gen) ≤ 1 µM. Higher concentrations reduced ECAR of both cell lines down to a minimum of approximately 50 %. An example for C(CPT)=5 µM is given in Figure 6A. When CPT-cAMP concentrations C(CPT) ≥ 50 µM were used for prestimulation, a small increase in ECAR of CHO-CFTR cells could be observed caused by genistein concentrations between C(gen) = 0.08 µM and C(gen) = 4 µM. Figure 6B shows these effects in presence of 100 µM CPT-cAMP. Inhibitory effects on ECAR of CHO-K1 cells resemble the effects seen for CPT-cAMP concentrations C(CPT) < 50 µM. In contrast, genistein concentrations C(gen) > 4 µM reduce ECAR of CHO-CFTR cells even more strongly under these conditions (Fig. 6B). ECAR in this cell line is reduced to approximately 30 % at a genistein concentration C(gen) = 20 µM and prestimulation with 100 µM CPT-cAMP. ECAR is only reduced to roughly 70 % in CHO-K1 under the same conditions (Fig. 6B) or CHO-K1 and CHO-CFTR cells prestimulated with only 5 µM CPT-cAMP (Fig. 6A). The ECAR decrease in both cell lines was fully reversible under all conditions and no ECAR increase upon withdrawal as seen for apigenin could be observed.

Fig. 6

As the measurements with flavonoids are dominated by the observed unspecific inhibitory effects, data could not be evaluated quantitatively. We also investigated the flavonoid daidzein which did not induce any ECAR change in CHO-K1 or CHO-CFTR cells (not shown) for concentrations in the range 0.1 µM ≤ C(daidzein) ≤ 50 µM. Except for apigenin flavonoids seem not to stimulate CFTR significantly.

Curcumin

Cytosensor experiments with curcumin revealed a similar CFTR dependent stimulation of the ECAR as seen for apigenin. Again a specific increase in ECAR in CHO-CFTR cells for curcumin concentrations C(curc) ≥ 5 µM and C(curc) ≤ 10 µM was observed in the presence of 25 µM CPT-cAMP (Fig. 7A). ECAR of CHO-K1 remained unaffected by curcumin concentrations C(curc) ≤ 10 µM. At C(curc) = 20 µM, however, an unspecific ECAR decrease was observed in both cell lines. Similar to apigenin a strong effect upon washout of drug was monitored. While ECAR increased to a maximum of only 130% during perfusion with 5 µM curcumin and decreased at higher concentrations, the washout peak following application of curcumin at a concentration of

C(curc) = 10 µM increased transiently to 200%. Application of 20 µM curcumin resulted in a similar washout peak. An example of raw data is shown in Fig. 7C. A washout peak could as well be observed with CHO-K1 cells following stimulation with 20 µM. However the ECAR increased only up to 130% and returned to baseline levels within 10 minutes, while ECAR of CHO-CFTR cells transiently reached levels of more than 200 %. Additionally the acidification did not revert to baseline immediately. It only decreased to approximately 150 % and remained on that level for 80 minutes before a slow decrease back to baseline level set in (Fig. 7C).

Fig. 7

Capsaicin

No specific ECAR increase was observed for capsaicin concentrations 1.65 µM ≤ C(caps) ≤ 52.8 µM. In CHO-CFTR and CHO-K1 cells an unspecific decrease in ECAR was observed for concentrations C(caps) ≥ 6.6 µM (Fig. 8A). Results were comparable in the presence of either 5, 25, or 50 µM CPT-cAMP (Fig. 8A). No ECAR increase was observed upon withdrawal of capsaicin.

Fig. 8

Substrate stimulated ATPase activity of Pgp and BCRP

Colorimetric phosphate assays were carried out to clarify whether CFTR modulators influence the ATPase activity of the well characterized ABC transporters Pgp and BCRP. For Pgp, inside-out membrane vesicles were prepared from NIH/3T3 mouse fibroblasts as described above. BCRP ATPase assays were performed with BCRP M ATPase membranes from Solvo Biotech. Results of these ATPase assays are shown in Figure 9. Glibenclamide (Fig. 9A), PPQ-102 (Fig. 9C) and capsaicin (Fig. 9D) clearly stimulated Pgp-ATPase at low concentrations and inhibited at high concentrations. Therefore, eq. 1 was fitted to data yielding concentrations of half-maximum activation K_1(glib) = 116.1 µM, K_1(PPQ) = 1.1 µM and K_1(caps)= 141.1 µM respectively. Glipizide (Fig. 9B) increased Pgp-ATPase only slightly at concentrations C(glipz) ≥ 120 µM. As the solubility limit of glipizide was reached, the concentration of half-maximum activation has to be considered as a rough estimate. CFTRinh-172 (Fig. 9F) and the potentiators apigenin (Fig 9G) and genistein (Fig. 9H) did not influence Pgp-ATPase. The kinetic parameters for the modulation of Pgp-ATPase are summarized in Table 2.

Table 2

For BCRP only inhibition of ATPase activity by glibenclamide (Fig. 9A) and PPQ-102 (Fig. 9C) was observed. The results were fitted with eq.1 yielding concentrations of half-maximum inhibition K_2(glib) = 29.3 µM and K_2(PPQ) = 2.27 µM. We did not detect any significant influence of glipizide on BCRP activity within the accessible concentration range. CFTRinh-172 concentrations between C(inh172) = 0.01 µM and C(inh172) = 120 µM resulted in a bell-shaped ATPase activity profile (Fig. 9C) with K_1(inh172) = 0.42 µM and K_2(inh172) = 98.2 µM. The tested flavonoids genistein and apigenin (Fig. 9E and F) influence BCRP in a similar way. However, the effects of apigenin occur at approximately 10 times lower concentrations compared to genistein, as reflected in the derived K_1 values K_1(genistein)= 0.18 µM and K_1(apigenin) = 0.02 µM. All calculated and estimated parameters are summarized in Table 3.

Table 3

Fig. 9

Estimation of lipid-water partitioning of the tested compounds

We measured the air-water partition coefficient, K_{aw}, for several tested compounds. Therefore the surface pressure, π, was recorded as a function of the solute concentration, C, at pH 7.4 and room temperature. The surface pressure, π, increased with the concentration up to a limiting value which reflects the critical micelle concentration, CMC_D (not shown). The results are summarized in Tab. 4. While glibenclamide, PPQ-102 and CFTRinh-172 are rather amphiphilic compounds yielding K_{aw} values between $1.5 \cdot 10^5$ M^{-1} and $7.9 \cdot 10^5$ M^{-1}, glipizide does hardly partition into the air-water interface, as it is more hydrophilic compared to glibenclamide. This is reflected in the low value determined for π_{max} = 3 mN/m compared to values around 20 mN/m for the other inhibitors. The air-water partition coefficient for apigenin and genistein could not be determined due to the low surface activity of the two compounds. For curcumin and capsaicin K_{aw}(curc) = $2.1 \cdot 10^6$ M^{-1} and K_{aw}(caps) = $1.8 \cdot 10^5$ M^{-1} was measured and the cross-sectional area for insertion into the air-water interface was determined as 172 $Å^2$ and 47 $Å^2$ respectively. The K_{aw} values can be used to estimate the lipid-water partition coefficient, K_{lw}, using eq. 2. The cross-sectional areas A_D of the molecules relevant for entering a lipid membrane were calculated using the algorithm implemented in Pgpredix (29). It has to be noted, that especially for glipizide and curcumin a huge difference in cross-sectional areas from surface activity measurements and calculated cross-sectional areas was observed. In

the case of glipizide, this is due to the low surface activity. For curcumin, however, this might indicate that it enters the air-water interface in a more or less flat conformation, while it probably enters the lipid-membrane along its axis. The results are included in Tab. 4. Additionally we identified possible hydrogen bond acceptor patterns (HBA) according to Seelig *et al. (7)*

Table 4.

Iodide efflux experiments

We carried out iodide efflux experiments to get insight into a potential correlation between ECAR changes and channel function. Conditions similar to microphysiometry, i.e. preincubation with CPT-cAMP and subsequent application of the tested compound were only accessible for CPT-cAMP concentrations C(CPT) ≤ 50 µM. As shown earlier (Matthias Zwick, Manuel Hellstern, Anna Seelig in preparation), higher CPT-cAMP concentrations increase efflux drastically but decreases quickly after 3 minutes due to the reduced intracellular iodide concentration. Glibenclamide concentrations between C(glib) = 2 µM and C(glib) = 50 µM (Fig. 1D) and glipizide concentrations between C(glipz) = 1 µM and C(glipz) = 20 µM (Fig. 2C) did not specifically potentiate CFTR dependent iodide efflux in CHO-CFTR cells in presence of 25 µM CPT-cAMP. It has to be noted, however, that both compounds had unspecific stimulating effects on iodide efflux on both, CHO-CFTR and CHO-K1 cells. Similar, no potentiation of iodide efflux could be detected for CFTRinh-172 concentrations between C(inh172) = 0.1 µM and C(inh172) = 1 µM (Fig. 3D) under the same conditions. No unspecific effects were detected in that case.

Apigenin had no effect on iodide efflux at concentrations below C(api) = 5 µM (Fig. 5C). Higher concentrations up to C(api) = 100 µM potentiated iodide efflux. It has to be noted that apigenin concentrations C(api) ≥ 10 µM contained aggregates and results might be influenced by these aggregates. Genistein concentrations C(gen) ≥ 10 µM increased iodide efflux in presence of 25 µM CPT-cAMP (Fig. 6C).

Discussion

ECAR corresponds to ATPase activity

Titration of CHO-CFTR cells as a function of inhibitor concentration yielded bell-shaped activity curves (Fig. 1-4). As inhibitors we used the sulfonylurea compounds glibenclamide and glipizide as well as CFTRinh-172 and PPQ-102. It has been shown earlier that sulfonylurea drugs (30) and CFTRinh-172 (31) interact directly with CFTR. Moreover it has been shown that CFTR dependent changes in the ECAR reflect either the ATPase activity of CFTR or ATP consumption by protein kinase A during CFTR phosphorylation (Matthias Zwick, Manuel Hellstern, Anna Seelig in preparation). The latter would require an increase in cellular cAMP. We cannot fully exclude such indirect effects for the tested sulfonylurea compounds. However, CFTRinh-172 and PPQ-102 have been demonstrated not to alter cAMP levels in FRT or CHO cells (15,32). We can thus conclude that the modulation of ATP consumption as a function of inhibitor concentration in the presence of functional CFTR is essentially due to the CFTR-ATPase activity.

CFTR modulators are ABC transporter substrate

The bell-shaped activity curves observed for ECAR and thus probably CFTR-ATPase furthermore resemble those observed previously for ATPase activity of other ABC transporters (23,24). To test, whether there exist common principles substrate-transporter interactions we investigated the ability of CFTR modulators to alter the ATPase activity of Pgp and BCRP. We indeed observed bell-shaped ATPase activity curves for Pgp and BCRP by glibenclamide (Fig. 9A). Thereby it has to be noted that the inhibitory branch dominated in the case of BCRP. These findings are not surprising as both transporters have been shown to transport glibenclamide (19,33). For Pgp, a bell-shaped behavior for ATPase activity as a function of glibenclamide concentrations was recently also described by Bessadok and colleagues (34). Glipizide also activated the Pgp-ATPase (Fig. 9B), although at clearly higher concentrations. While these compounds were known before to interact with multiple ABC transporters, CFTRinh-172 was so far assumed to interact exclusively with CFTR. The present data show that CFTRinh-172 is not specific for CFTR among the ABC transporter family, as it influences BCRP-ATPase (Fig. 9C) in a similar way as sulfasalazine, a well characterized BCRP substrate (35). This finding is not totally unexpected, as the thiazolinediones rosiglitazone und pioglitazone have been shown recently to interact with BCRP (36) and share structural elements with CFTRinh-172. Due to their cationic charge these compounds also interact with Pgp while the anionic CFTRinh-172 does not. The

electrically neutral compound PPQ-102 behaves like the sulfonylurea compounds and causes bell-shaped ATPase activity curves for Pgp and inhibitory curves for BCRP (Fig. 9D).

We also tested the CFTR potentiators investigated in this study on their ability to alter ATPase activity. The flavonoids apigenin and genistein do not interact with Pgp due to a lack of amphiphilicity. However they activate BCRP whereby apigenin acts already at concentrations C(api) at least 10 fold lower than genistein (Fig. 9E-F). This corresponds nicely with the 10 fold difference in EC_{50} for BCRP inhibition detected by increased mitoxantrone import by Zhang et al. (37). The absence of effects on Pgp detected in our ATPase assays is in accordance with earlier findings that apigenin could reverse BCRP mediated drug resistance but had no influence on Pgp mediated resistance (38). Our observations suggest that these effects on BCRP mediated transport are not caused by simple inhibition of ATP hydrolysis due to binding to the nucleotide binding domains as suggested earlier (39). As apigenin and genistein behave like transport substrates, they are most likely actively flopped by BCRP. The effect on Pgp-ATPase caused by capsaicin (Fig. 9G) can explain earlier findings (40) that capsaicin was involved in Pgp mediated drug-food interactions. In the same study, curcumin was also identified as a Pgp inhibitor and it has been shown that Pgp-ATPase as a function of curcumin concentration shows a bell-shaped behavior with stimulation below 1 µM and inhibition for higher concentrations (41). A similar effect has been seen also for curcumin, but at even lower concentrations (David Eyholzer, unpublished results). The kinetic parameters from these measurements are appended in Tab. 2 and 3 respectively.

Therefore we can conclude that all of the investigated CFTR inhibitors and modulators are indeed either substrates of Pgp, BCRP or even both and that the same factors determining binding to these transporters might also play a role for CFTR.

K_1 values for CFTR-modulator interaction shift dependent on CPT-cAMP concentration

We found that the K_1 values obtained from fitting eq. 1 to data depend on the CPT-cAMP concentration present in our measurements. While drastic shifts could be seen for glibenclamide and glipizide, only a comparably small effect was seen for CFTRinh-172. Such shifts in kinetic constants dependent on the CPT-cAMP concentration have been described before for the interaction of the potentiator genistein with CFTR (39). Our observations therefore support the idea that, the same binding sites might be involved in both, potentiator and inhibitor binding. However, the shift could be probably explained in two ways, which are both in favor of our

assumption that the detected ATPase activity is due to direct modulation of CFTR. One explanation could be that CPT-cAMP might also bind directly to CFTR in addition to its effects on protein kinase A. Thus the shift would be due to competition between CPT-cAMP and the modulator for the binding sites. This would be plausible, as we could show earlier that the K_{lw}(CPT) = $8.02 \cdot 10^3$ M^{-1} and therefore is in a similar range as for most of the modulators (Matthias Zwick, Manuel Hellstern, Anna Seelig in preparation) and that there is evidence for direct interaction of cAMP and CFTR (42). Nevertheless the shift might be also due to conformational changes in the regulatory domain of CFTR induced by phosphorylation. It was speculated, that these rearrangements affect the transmembrane domains and shift the configuration of CFTR towards the open state (43). As the binding sites proposed in our model lie within the TMDs, they would be most likely affected by such structural changes. As shown in Fig. 10 the K_1 values and therefore also $\Delta G^0_{tw(1)}$ do not shift any further for CPT-cAMP concentrations C(CPT) > 50 µM. This coincides with the concentration range, where maximal stimulation of ECAR by CPT-cAMP was found. However, this does not favor one of the two models over the other. Independent of the explanation for these phenomena, a comparison of $\Delta G^0_{tw(1)}$ between the three investigated ABC transporters, supports again nicely the idea of a common binding mechanism. While $\Delta G^0_{tw(1)}$ for CFTRinh-172 and PPQ-102 are in the same range as seen for BCRP or Pgp respectively, $\Delta G^0_{tw(1)}$ for glibenclamide seem to differ clearly between CFTR and Pgp. Extrapolation of the observed shift to zero CPT-cAMP, however, results in a value resembling the one observed for Pgp (Fig. 11). A similar conclusion can be drawn for glipizide, as the measured $\Delta G^0_{tw(1)}$ value can be extrapolated to roughly -30 kJ / mol for C(CPT) = 0 µM, which would correspond to a K_1 value around 400 µM, which is in good correlation with our estimate of K_1(glipz) > 300 µM.

Fig. 10

Correlation of ATPase activity and channel block

We found that the neutral inhibitor PPQ-102, the slightly negatively charged sulfonylurea compounds and the acidic CFTRinh-172 affect ATPase activity of CFTR in the same way. Therefore ATPase activity modulation or the underlying binding to two binding sites might be the common reason for their inhibitory function. While channel block by negatively charged compounds could be plausibly explained by simple block of the pore and charge repulsion in the pore, such a mechanism cannot explain the

effect of PPQ-102 In the case of glibenclamide and glipizide, published results on CFTR channel block correspond more or less to the inhibitory part of the ATPase activity profile. Nevertheless chloride channel data is generated under different conditions. Our data is generated upon prestimulation with only CPT-cAMP. Therefore the observation, that glibenclamide blocks iodide influx into FRT cells in the presence of 100 µM CPT-cAMP only at concentrations C(glib) > 10 µM (32) (Fig. 1E) might be best to compare with our results. Comparable results showing CFTR block by concentrations C(glib) ≥ 10 µM have been also seen in excised patches from C127 cells (44) (Fig. 1F) or *Xenopus* oocytes (30,45) (Fig. 1G-H). In the latter case no inhibition could be observed for C(glib) = 5 µM. The latter kind of experiments has been done as well for glipizide showing inhibition for glipizide concentrations C(glipz) ≥ 10 µM (45). Nevertheless, the concentration range effective in whole cells or excised patches is hard to compare. First, it is not clear if the phosphorylation state of CFTR achieved by protein kinase A catalytic subunit in patch-clamp experiments corresponds to the phosphorylation induced by CPT-cAMP. As patch-clamp studies for inhibitors are mostly done under conditions assuming complete phosphorylation of CFTR, they should be somewhat comparable to our results for 50 µM CPT-cAMP as we did not observe any further shift in K_1 values for higher glibenclamide concentrations and phosphorylation induced ECAR reaches a plateau between 50 and 100 µM (Matthias Zwick, Manuel Hellstern, Anna Seelig in preparation). Furthermore, our results suggest that binding from the inner membrane leaflet might play a role. Therefore the local concentrations will be higher if compounds are supplied from the inside, as they do not have to be flipped over the membrane first. This phenomenon has been observed earlier for the comparison between microphysiometry measurements and ATPase assays in inside-out vesicles for Pgp (11).

For CFTRinh-172 and PPQ-102 the correlation with the decreasing branch is less obvious. For CFTRinh-172 channel block has been observed for concentrations C(inh172) ≥ 0.2 µM in iodide influx measurements in FRT cells in the presence of an activating cocktail containing 5 µM forskolin, 25 µM apigenin and 100 µM apigenin (Fig. 3E) as well as for short circuit current measurements in the presence of 100 µM CPT-cAMP (32) (Fig. 3F). These findings have been confirmed by patch-clamp recordings in excised patches from NIH/3T3 mouse fibroblasts as shown in Fig. 3G (46). Unfortunately CFTRinh-172 has CPT-cAMP dependent effects on extracellular acidification. Therefore our results for high CPT-cAMP concentrations are most likely influenced by these unspecific effects. In the case of PPQ-102, inhibition of short circuit current in FRT cells has been reported to occur for concentrations in the range

0.05 µM ≤ C(PPQ) ≤ 2 µM in the presence of 100 µM CPT-cAMP (Fig. 4B) (15). In the same study short circuit current block in T84 cells has been shown to occur at higher concentrations C(PPQ) ≥ 1 µM in the presence of 10 µM forskolin and 100 µM CPT-cAMP (Fig. 4C). This shows another problem in correlating our results with published work as the results might be additionally influenced also by the cell type used. Therefore we cannot exclude that PPQ-102 might be inhibiting already at lower concentrations, although the results for T84 cells would suggest a similar correlation as seen for sulfonylurea drugs. In summary, the inhibitory part of the bell-shaped ATPase activity profile always corresponds to channel block. The ascending branch, however, cannot be clearly attributed to an inhibitory effect. We therefore investigated if increasing ATPase activity might in turn cause potentiation. Iodide efflux in the presence of 25 µM CPT-cAMP was not stimulated by either glibenclamide (Fig. 1D), glipizide (Fig. 2C) or CFTRinh-172 (Fig 3D) at concentrations causing submaximal effects on ECAR. As iodide efflux measurements were not suitable to detect inhibition under these conditions, the overlap between observed inhibition and no effects in our experiments is not contradictory and we can conclude that stimulation of ATPase activity by inhibitors does not cause potentiation.

Channel potentiation and ECAR changes

The effects on ECAR caused by potentiators were less consistent and reproducible compared to inhibitors. A common feature of all tested compounds apigenin, genistein, curcumin and capsaicin was an unspecific decrease of extracellular acidification in both, CHO-CFTR and CHO-K1 cell lines. A similar effect has been observed earlier for forskolin and was attributed to decreased glucose import (Matthias Zwick, Manuel Hellstern and Anna Seelig in preparation). Strikingly, apigenin, genistein and several other flavonoids have been shown to inhibit glucose import at concentrations C(flavonoid) > 1 µM in U937 cells (47), which corresponds with the observed inhibitory effects. For genistein, there exists also evidence that glucose import in CHO cells is inhibited in the same concentration range (48). For capsaicin and curcumin, however, no influence on glucose metabolism has been described so far. A comparison with data on channel function shows, that potentiation is mostly observed in the range, where unspecific effects on ECAR occur. We could show that iodide efflux from CHO-CFTR cells in the presence of 25 µM CPT-cAMP is increased for concentrations C(api) > 5 µM (Fig. 6C). This is in good correlation with stimulating effects of apigenin observed for concentrations C(api) ≥ 3 µM on CFTR dependent short circuit currents in Calu-3 cells in the presence or absence of 10 µM forskolin (Fig. 5E and F) (49).

A slightly earlier onset was observed for iodide influx in FRT cells in the presence of 0.1 µM forskolin, but it has to be noted, that the effects were small (<20%) for concentrations C(api) < 1 µM (50). Concentrations apparently causing an inhibition of chloride currents were unfortunately not accessible due to insolubility under Cytosensor conditions. Published data on potentiation of CFTR by genistein shows that the effects of both flavonoids are quite similar. Concentrations C(gen) ≥ 1 µM were shown to potentiate CFTR in excised patches from mouse fibroblasts and similar to apigenin an inhibition was seen for high concentrations C(gen) ≥ 35 µM (Fig. 7G) (51). Similar potentiating and inhibitory effects of genistein where observed in short-circuit current measurements with FRT cells for concentrations C(gen) < 10 µM (39). These experiments also reported that the concentrations causing potentiation or inhibition depend on the CPT-cAMP concentration used for stimulation. Fig. 6E and F summarize these effects for C(CPT) = 30 µM and C(CPT) = 100 µM corresponding to our measurement conditions. However, effects might start at lower concentrations, though not tested, as iodide influx experiments in FRT cell lines revealed potentiation at concentrations C(gen) ≥ 5 µM (Fig. 6D) (52). The good correlation between results from FRT cells and the CHO cells used in this study as described above was confirmed again in this case by iodide efflux measurements (Fig. 6C). For capsaicin the concentration range 10 µM ≤ C(caps) ≤ 200 µM was reported to have potentiating effects on CFTR in whole cell patch-clamp experiments in the presence of 100 µM CPT-cAMP and 10 µM forskolin (53) (Fig. 8B). While a common mechanism for genistein, apigenin and capsaicin was suggested before (53), we only detected a CFTR dependent ECAR increase for apigenin. The increase seemed to be CPT-cAMP dependent as it started at lower apigenin concentrations in presence of 25 µM CPT-cAMP compared to 5 µM. The CFTR dependent washout peaks at concentrations C(api) > 1 µM suggest that the effect might persist there and could be hidden under the unspecific decrease. However, if this was a direct effect on CFTR ATPase one would expect the same effect at least in the case of genistein and probably also capsaicin. As no clear evidence for such effects could be found, we assume that the effect of apigenin might reflect an indirect, yet CFTR dependent effect. As flavonoids have been identified as inhibitors of various phosphodiesterases (54) an increase in cAMP and therefore stimulation of protein kinase A could be a plausible explanation. For curcumin, we also observed a similar comparably small activating effect, unspecific inhibition at higher concentration and a drastic CFTR dependent washout peak. Upon stimulation with 20 µM curcumin, this washout peak was even followed by an increased baseline that remained for up to 80 minutes (Fig. 7C). This observation resembles the effect we had seen before for

forskolin and would similarly be in accordance with an explanation involving upregulated cAMP and again point to indirect effects. In the case of curcumin, moreover, reported channel potentiation in excised patches from HEK cells (55) shows neither clear correlation with this ECAR stimulation nor with the unspecific decrease (Fig. 7B). In summary, the investigation of CFTR potentiators by microphysiometry leads to less consistent results compared to the inhibitors, which might be mainly due to the fact that all of the investigated compounds affect cell metabolism in many different ways. Nevertheless, we can draw the conclusion that most likely no specific stimulation of ATPase activity or only much lower stimulation in comparison with CFTR inhibitors plays a role in CFTR potentiation.

Implications from a comparison of ABC transporters

We found that CFTR modulators are substrates for either Pgp, BCRP or both. Therefore the question arises whether CFTR shares more similarities with one of them. Our results show that drug modulation of CFTR-ATPase resembles that of Pgp-ATPase in terms of activation by amphiphilic compounds and inhibition by non-amphiphilic compounds. However, as a member of the ABCC subfamily, CFTR also resembles the behavior of MRP4, the nearest relative of CFTR among ABC transporters in terms of activation by amphiphilic anionic compounds. These assumptions require a similar binding principle as described for Pgp, i.e. binding from the membrane due to hydrogen bonds, as described above. We could show that all of the tested compounds can bind to the membrane and that the lipid-water partition coefficient of glipizide is significantly lower compared to the other inhibitors (Tab. 2). This correlates with the finding that K_1(glipz) is about 18 fold higher than K_1(glib) although glipizide and glibenclamide have a similar structure. Calculation of $\Delta G^0_{\mathrm{tl}(1)}$ according to eq. 2 indeed revealed a free binding enthalpy for glipizide in the same order of magnitude as observed for the other inhibitors. This supports the idea of binding to the TMDs from the membrane, which would be in accordance to the proposed interaction of sulfonylurea compounds with a site within the membrane, close to the cytoplasmic face but distinct from the pore (56).

As the tested inhibitors and the potentiator capsaicin are rather amphiphilic compounds, one would thus expect bell-shaped activation profiles, while the non-amphiphilic flavonoids and curcumin should cause ATPase inhibition. Although the latter assumption cannot be directly inferred from our data due to the large metabolic effects of the potentiators, it is not contradictory. The ATPase activation by inhibitors on the other hand is in line with our data. Only the effect of capsaicin remains puzzling,

as its amphiphilicity would suggest ATPase activation, which was not observed. However, it was shown for Pgp that a certain balance between amphiphilicity and lipid binding is necessary for ATPase activation and that compounds with too high lipid affinity relative to transporter affinity are transported only at a low rate (Xiaochun Li-Blatter, Andreas Beck and Anna Seelig, submitted). It could well be, that capsaicin still fulfills the requirements of Pgp, but not those of CFTR.

According to our assumption inhibition would correlate with bell-shaped activity profiles, while potentiation would be caused by ATPase inhibition. These findings can be well explained with the two-site binding model (22). Inhibitors would bind to the binding-competent and thus closed state of CFTR. At low concentrations only the first binding site is occupied and a typical transporter cycle is initiated. Therefore inhibitor binding would facilitate dimerization of the NBDs and therefore opening of the channel. However, amphiphilic molecules can easily flop, as shown for Pgp, and will therefore dissociate rapidly from this conformation allowing CFTR to return to the closed state. However, the rate of return might be different for various inhibitors depending on their binding constants, and thus the balance between open time and closed time could be slightly different. This would explain why no effects on macroscopic currents for low sulfonylurea concentrations were observed, despite clearly enhanced ATPase activity, while CFTRinh-172 and PPQ-102 seem to inhibit already at that concentrations range. At high concentrations of inhibitors, however, the second binding site gets occupied, which seems to clearly correlate to inhibition for all tested compounds. According to our model, this could be explained by a simple steric effect caused by protrusion of a molecule at the second binding site into the pore as well as by stalling CFTR in the binding competent and thus closed state. The latter assumption would be in agreement with the observed decrease in ATPase activity. Similarly, binding of a potentiator at low concentrations would induce dimerization of the NBDs and therefore induce the conformational change to the release competent or open conformation. The non-amphiphilic potentiators, however, do not easily flop over the membrane, thus CFTR remains open longer. Binding to the second binding site at high concentration could again lead to protrusion of the bound molecule into the pore or stabilization of CFTR in the binding competent and thus closed conformation.

Conclusions

We demonstrated that the bell-shaped ECAR changes measured as a function of inhibitor concentration were due exclusively to CFTR-ATPase activity. Inhibitors thus enhance the ATPase activity of CFTR at low concentrations and reduce it at high concentrations. CFTR inhibitors are electrically neutral or anionic amphiphilic compounds and thus resemble Pgp activating substrates in the former and MRP4 activating substrates in the latter case. The bell-shaped ATPase activity curves can be well interpreted with a kinetic two-site binding model based on un-competitive inhibition. Therefore, we propose a model that CFTR-ATPase activation at low inhibitor concentrations reduces the time in which the chloride channel is open relative to the time in which it is closed and thus inhibits the chloride flux. At high concentrations where both binding sites are occupied the channel is most likely occluded. The negative charge of many inhibitors may have an additional repulsive effect for chloride ions. Quite in contrast, potentiators barely enhanced the ATPase activity of CFTR at low concentrations but reduced it at high concentrations. High concentrations of most potentiators show additional metabolic effects as evidenced by comparison with control cells. The observation of chloride flux inhibition at high potentiator concentrations nevertheless, supports the two-site binding model. In analogy to Pgp we assume that molecules with a lack of amphiphilicity such as flavonoids or curcumin bind to CFTR but are flopped only slowly and thus stabilize the open conformation. The fact that very amphiphilic molecules such as capsaicin can also act as potentiators may be explained in analogy to Pgp where it has been demonstrated that the flopping rate is also reduced for compounds which exhibit a too large lipid affinity relative to the transporter affinity.

Tables

Table 1: Kinetic constants derived from microphysiometry experiments with CHO-CFTR cells in MEMα at pH 7.4 and T = 37°C. The concentration of half-maximum activation (inhibition) K_1 (K_2) and the rate of activation (inhibition) v_1 (v_2) were obtained by fitting eq. 1 to data.

Compound	C(CPT) [µM]	K_1 [µM]	K_2 [µM]	v_1 [%]	v_2 [%]	$ECAR_{max}$ [%]
Glibenclamide	5	25.0	105.1	315	0	192±19
Glibenclamide	10	9.9	67.3	332	0	214±32
Glibenclamide	12.5	3.7	96.8	204	0	163±4
Glibenclamide	25	3.0	68.8	275	0	210±27
Glibenclamide	50	1.0	85.3	192	0	165±16
Glibenclamide	100	1.5	63.4	207	0	166±16
Glipizide	25	56.4	80	231	100	148±10
Glipizide	50	6.25	80	198	100	161±16
CFTRinh-172	5	1.0	2.4	190	130	145
CFTRinh-172	25	0.5	3.8	250	150	189±27
CFTRinh-172	50	0.4	12.7	210	80	175±10
PPQ-102	50	0.5	3.1	180	0	137±12

Table 2: Kinetic constants derived from Pgp ATPase assays in inside-out membrane vesicles. The concentration of half-maximum activation (inhibition) K_1 (K_2) and the rate of activation (inhibition) v_1 (v_2) were obtained by fitting eq. 1 to data

Compound	K_1 [μM]	K_2 [μM]	v_1 [%]	v_2 [%]	v_{max} [%]
Glibenclamide	116.1	314.5	627	0	325±2
PPQ-102	1.1	4.2	260	83	174±9
Capsaicin	114.1	127.3	624	0	257±12
Glipizide	≥300[1]	n.i. [2]	≥164[1]	n.i. [2]	164±24
Curcumin[3]	< 1	> 10	≥ 150	< 100	≈150

[1] *Estimated from the increase at concentrations C(glipz) > 100 μM before reaching the solubility limit;* [2] *n.i.: no inhibition detected;* [3] Estimated from Anuchapreeda et al. (41)

Table 3: Kinetic constants derived from BCRP ATPase assays in inside-out membrane vesicles. The concentration of half-maximum activation (inhibition) K_1 (K_2) and the rate of activation (inhibition) v_1 (v_2) were obtained by fitting eq. 1 to data

Compound	K_1 [µM]	K_2 [µM]	v_1 [%]	v_2 [%]	v_{max} [%]
glibenclamide	n.a. (1)	29.3	n.a. (1)	17	n.a. (1)
CFTRinh-172	0.42	98.2	216	147	224±15
PPQ-102	n.a. (1)	2.27	n.a. (1)	19	n.a. (1)
genistein	0.18	551.5	191	0	195±4
apigenin	0.02	8.0	214	195	214±2
curcumin(2)	0.01	10.3	206	30	

(1) n.a. no activation detected; (2) D. Eyholzer, unpublished results;

Table 4: Inhibitor binding to lipid membrane and CFTR in the presence of 50 µM CPT-cAMP

Compound	π_{max} [mN/m]	K_{aw} [1/M]	A_D(1) [Å²]	K_{lw} [1/M]	$\Delta G^0_{tw(1)}$ [kJ/mol]	$\Delta G^0_{tl(1)}$ [kJ/mol]	HBA(2)	$\Delta\Delta G^0_H$ [kJ/mol]
glibenclamide	17.8	$7.9 \cdot 10^5$	71	$4.5 \cdot 10^3$	-44.0	-13.9	4	-3.5
glipizide	3.1	10^3 - 10^4	64 -97	< 110	-41.2	≤ -18.7	3	≤ -6.4
CFTRinh-172	21.4	$1.5 \cdot 10^5$	58	$2.8 \cdot 10^3$	-49.4	-18.6	4	-4.7
PPQ-102	21.6	$1.9 \cdot 10^5$	71	$1.3 \cdot 10^3$	-47.4	-18.9	4	-6.3

(1) Calculated with Pgpredix (29); (2) number of possible hydrogen bond acceptor patterns

Figure Legends

Figure 1: Effects of glibenclamide on ECAR and iodide efflux in comparison to published results on channel function

A - C: ECAR as a function of glibenclamide concentration in CHO-K1 (open squares) and CHO-CFTR (filled squares) cells after stimulation with CPT-cAMP concentrations C(CPT) =5 µM (A), C(CPT) = 25 µM (B) or C(CPT) = 50 µM (C). D: Concentration range where no effects (cross-hatched bars) on iodide efflux after stimulation with C(CPT) = 25 µM were observed. It has to be noted that an unspecific increase of iodide efflux in control cells and transfected cells was observed for concentrations C(glibenclamide) ≥ 10 µM. E: Glibenclamide concentrations causing no effect (cross-hatched) or inhibition (filled bars) of short-circuit current stimulated by 100 µM CPT-cAMP in *CFTR* expressing FRT cells described in literature (32). F: Inhibitory concentrations of glibenclamide detected in analysis of single-channel patch-clamp experiments in stably transfected C127 cells in the presence of PKA (44). G and H: Concentration range reported to cause channel block by glibenclamide in excised patches from *Xenopus* oocytes in the presence of 50 U/ml PKA (30,45).

Figure 2: Effects of glipizide on ECAR and iodide efflux in comparison to published results on channel function

A and B: ECAR as a function of glipizide concentration in CHO-K1 (open squares) and CHO-CFTR (filled squares) cells after stimulation with C(CPT) =25 µM (A) or C(CPT) = 50 µM (B). C: Concentration range where no effects on iodide efflux after stimulation with C(CPT) =25 µM were observed. D: Concentration range reported to cause channel block by glipizide in excised patches from *Xenopus* oocytes in the presence of PKA (45).

Figure 3: Effects of CFTRinh-172 on ECAR and iodide efflux in comparison to published results on channel function

A -C: ECAR as a function of CFTRinh-172 concentration in CHO K1 (open squares) and CHO-CFTR (filled squares) cells after stimulation with C(CPT) = 5 µM (A), C(CPT) = 25 µM (B) or C(CPT)=50 µM.

D: Concentration range where no potentiation of channel function was observed in iodide efflux experiments after stimulation with C(CPT) =25 µM. E: Inhibition of channel function described in literature for iodide influx after stimulation with an CFTR activating cocktail containing 5 µM forskolin, 100 µM IBMX and 25 µM apigenin (32) F: Concentration range reported to cause inhibition of CFTR dependent short-circuit current after stimulation with 100 µM CPT-cAMP (32). G: Concentration range described to block CFTR in excised patches from transfected mouse embryo fibroblasts (46).

Figure 4: Effects of PPQ-102 on ECAR in comparison to published results on channel function

A: ECAR as a function of PPQ-102 concentration in CHO K1 (open squares) and CHO-CFTR (filled squares) cells after stimulation with C(CPT) = 50 µM. B: Concentration range reported to inhibit CFTR dependent short-circuit currents after stimulation with either 100 µM CPT-cAMP, 100 µM apigenin or 100 µM IBMX respectively in FRT cells (15). C: PPQ-102 concentrations shown to cause inhibition of short-circuit current in T84 or human airway epithelial cells upon stimulation with 10 µM forskolin and 100 µM IBMX (15).

Figure 5: Effects of apigenin on ECAR in comparison to published results on channel function

A and B: ECAR as a function of apigenin concentration in CHO K1 (open squares) and CHO-CFTR (filled squares) cells after stimulation with C(CPT) = 5 µM (A) or C(CPT) = 25 µM (B). C: Concentration ranges where no effect (cross-hatched), potentiation (hatched) or inhibition (filled bars) of channel function was observed in iodide efflux experiments after stimulation with C(CPT) =25 µM D-F: Effects on channel function described in literature for iodide influx after stimulation with 0.25 µM forskolin (D) (50) or short-circuit current measurements without (E) or with preliminary stimulation with 10 µM forskolin (F) (49). Symbols have the same meaning as in C. G: Example of raw data. Time dependence of application of 2 µM apigenin on CHO K1 (open squares) and CHO-CFTR (filled squares) cells; the gray bar indicates the 20 minutes incubation time with apigenin.

Figure 6: Effects of genistein on ECAR and iodide efflux in comparison to published results on channel function

A and B: ECAR as a function of genistein concentration in CHO K1 (open squares) and CHO-CFTR (filled squares) cells after stimulation with C(CPT) = 5 µM (A) or C(CPT) = 100 µM (B) C: Concentration ranges where no effect (cross-hatched), potentiation (hatched) or inhibition (filled bars) of channel function was observed in iodide efflux experiments after stimulation with C(CPT) =25 µM; D-H: Effects on channel function described in literature for iodide influx in FRT cells after stimulation with 0.1 µM forskolin (D) (52), short-circuit current measurements in the presence of 5 µM (E) or 100 µM CPT-cAMP (F) (39) or patch-clamp measurements in excised patches after stimulation with 0.05 µM forskolin (H) (51). Symbols have the same meaning as in C.

Figure 7: Effects of curcumin on ECAR in comparison to published results on channel function

A: ECAR as a function of curcumin concentration in CHO K1 (open squares) and CHO-CFTR (filled squares) cells after stimulation with C(CPT) = 25 µM. B: Concentration range reported to cause potentiation by curcumin in excised patches in the presence of protein kinase A (55). C: Example of raw data. Time dependence of application of 20 µM curcumin on CHO K1 (open squares) and CHO-CFTR (filled squares) cells; the gray bar indicates the 20 minutes incubation time with curcumin.

Figure 8: Effects of Capsaicin on ECAR in comparison to published results on channel function

A: ECAR as a function of capsaicin concentration in CHO K1 (open squares) in the presence of 50 µM CPT-cAMP and CHO-CFTR cells in the presence of C(CPT) = 50 µM (filled squares), C(CPT) = 25 µM (open triangles) or C(CPT)=5 µM (stars). B: Concentration range reported to cause potentiation by capsaicin whole cell patch-clamp experiments in the presence of 10 µM forskolin (53).

Figure 9: Modulation of Pgp- and BCRP-ATPase activity by CFTR modulators

ATPase activity of BCRP (stars) and Pgp (open triangles) as function substrate concentration for A: glibenclamide, B: glipizide, C: CFTRinh-172, D: PPQ-102, E: genistein; F: apigenin; G: capsaicin. Error bars indicate deviation of 2-4 measurements.

Figure 10: $\Delta G^0_{\mathrm{tw}(1)}$ *for glibenclamide and glipizide as a function of CPT-cAMP concentration*

$\Delta G^0_{\mathrm{tw}(1)}$ calculated from apparent K_1 values from ECAR measurements in CHO-CFTR cells with glibenclamide (filled squares) or glipizide (filled triangle). The value calculated from Pgp-ATPase measurements with glibenclamide is also shown (open squares)

Figures

Figure 1: Effects of glibenclamide on ECAR and iodide efflux in comparison to published results on channel function

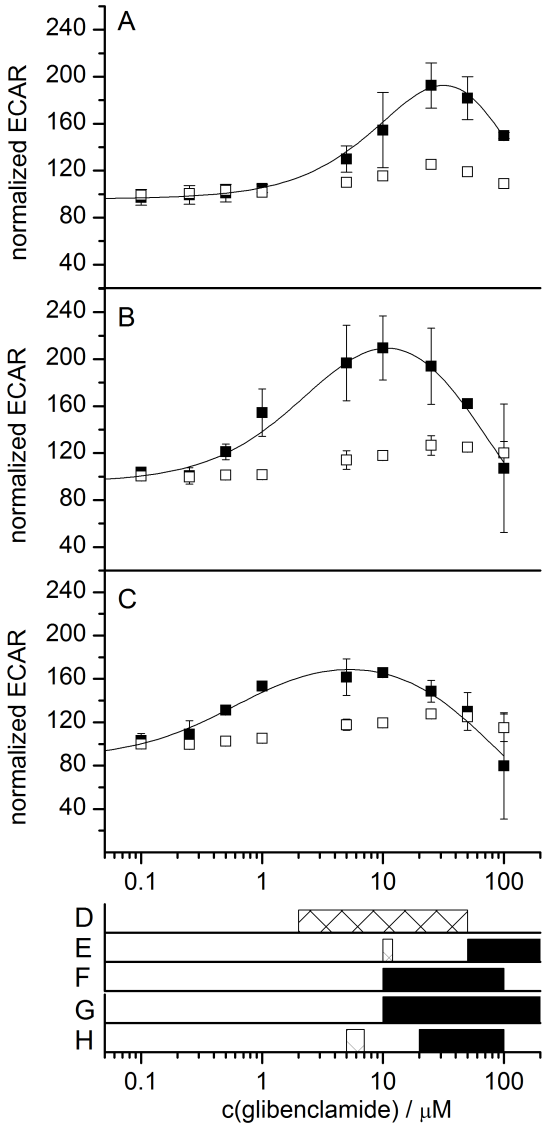

Figure 2: Effects of glipizide on ECAR and iodide efflux in comparison to published results on channel function

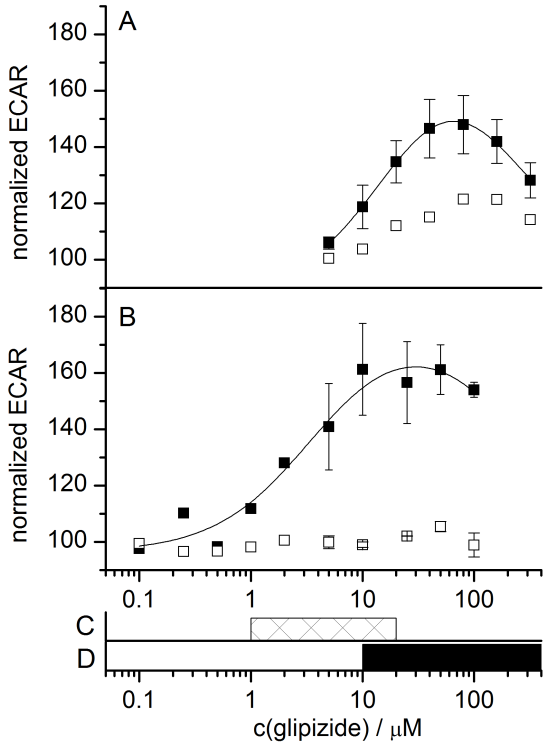

Figure 3: Effects of CFTRinh-172 on ECAR and iodide efflux in comparison to published results on channel function

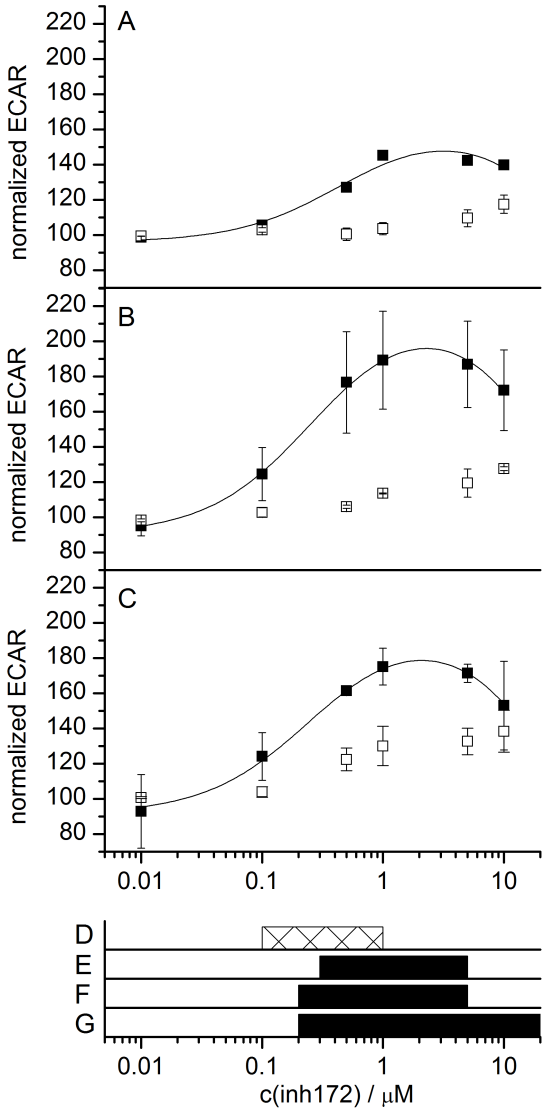

Figure 4: Effects of PPQ-102 on ECAR in comparison to published results on channel function

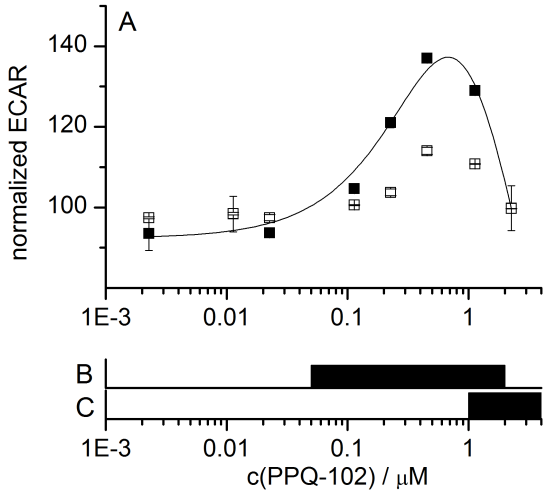

Figure 5: Effects of apigenin on ECAR in comparison to published results on channel function

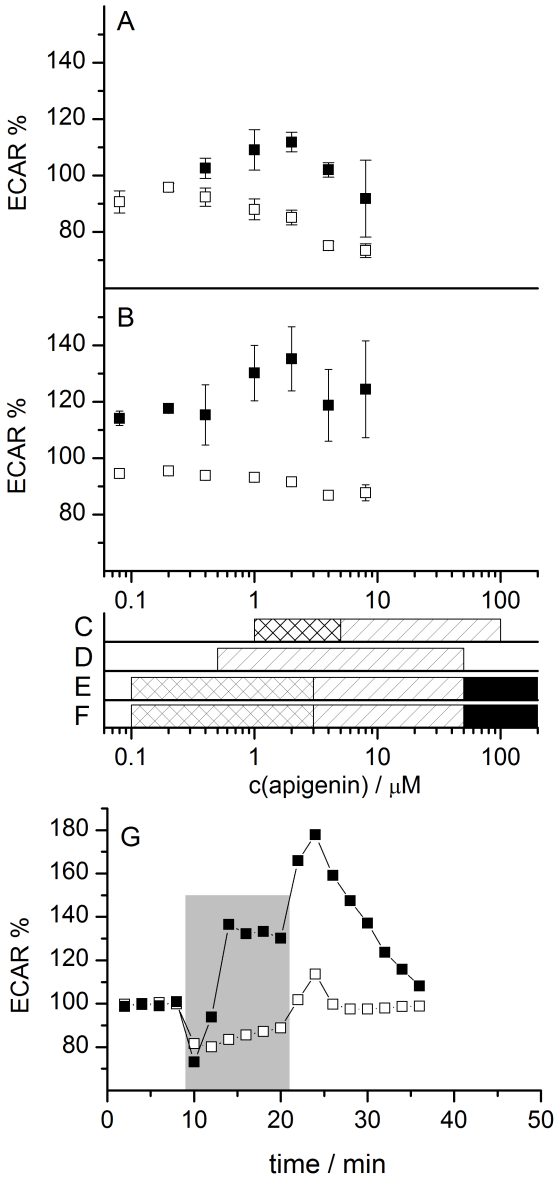

Figure 6: Effects of genistein on ECAR in comparison to published results on channel function

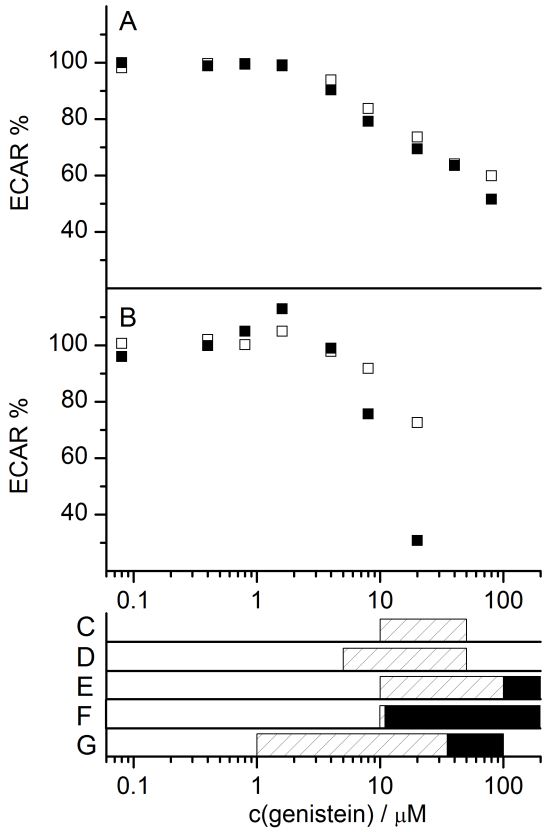

Figure 7: Effects of curcumin on ECAR in comparison to published results on channel function

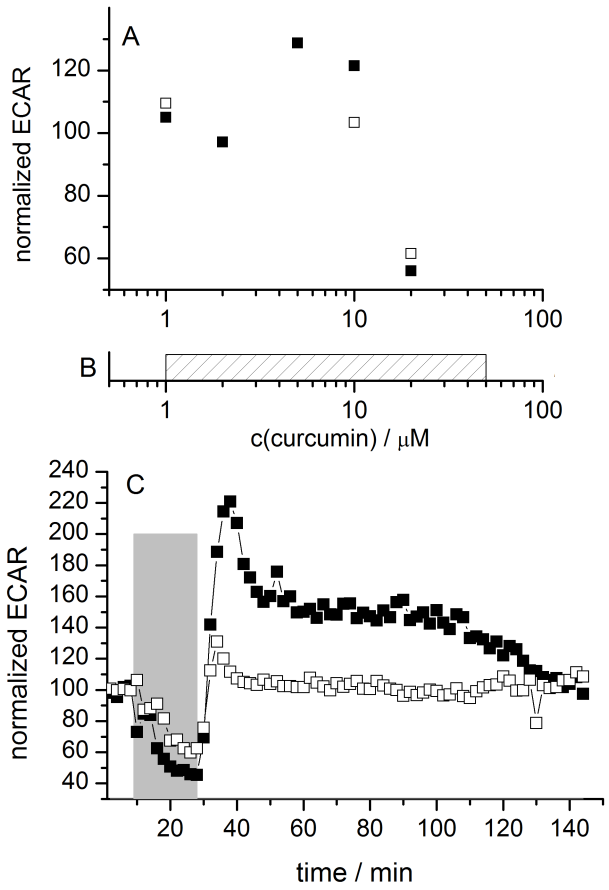

Figure 8: Effects of Capsaicin on ECAR in comparison to published results on channel function

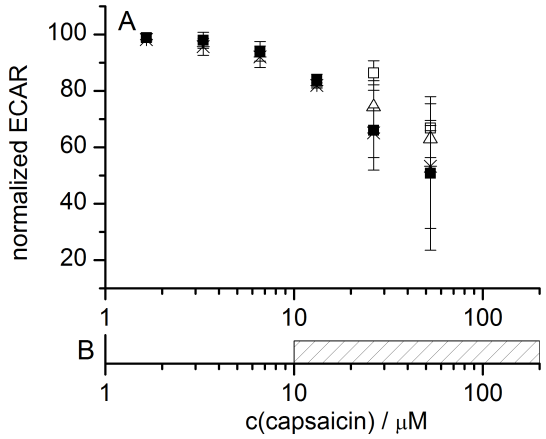

Figure 9: Comparison of substrate modulated ATPase activity of Pgp and BCRP

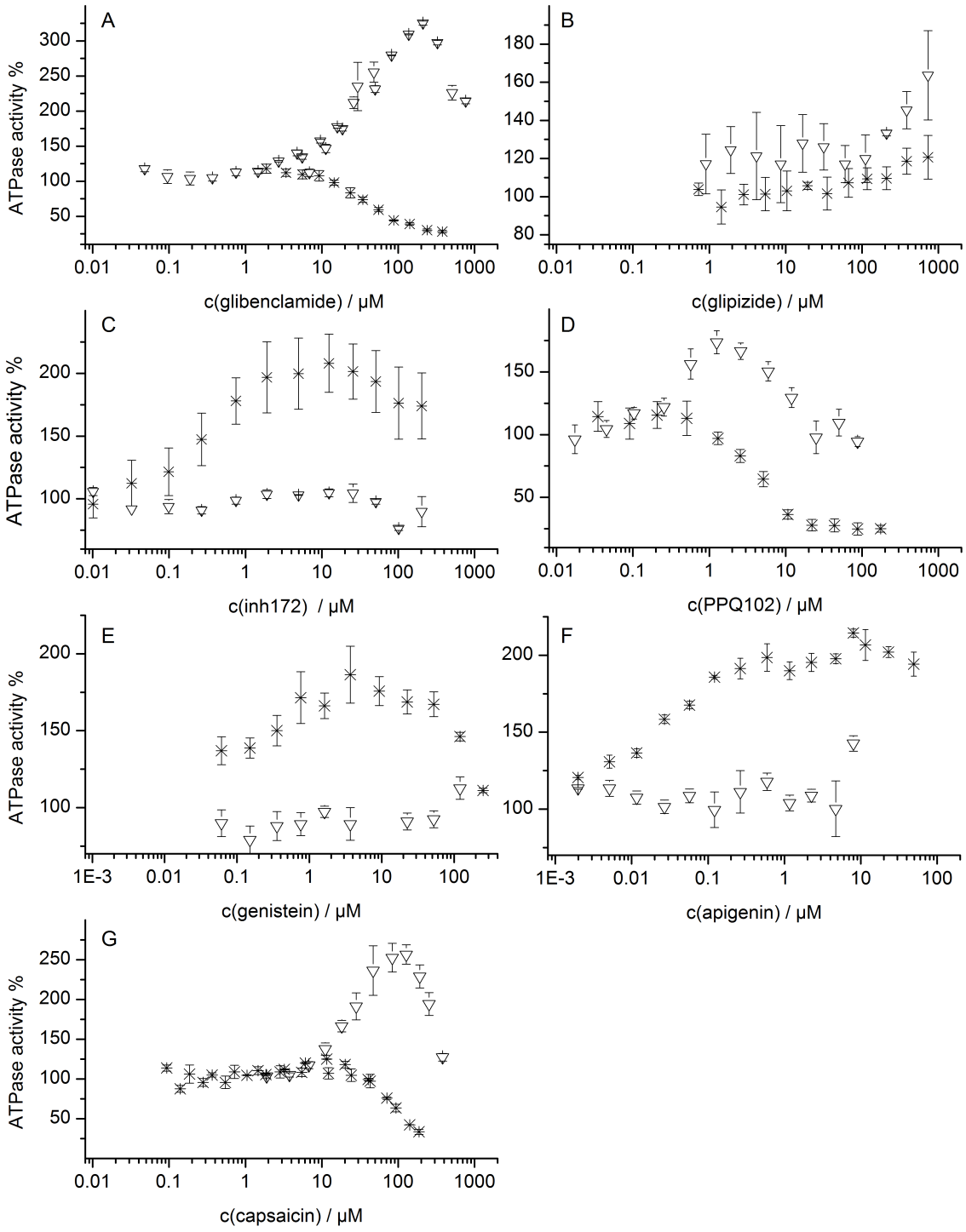

Figure 10: $\Delta G^0_{\mathrm{tw}(1)}$ for glibenclamide and glipizide as a function of CPT-cAMP concentration

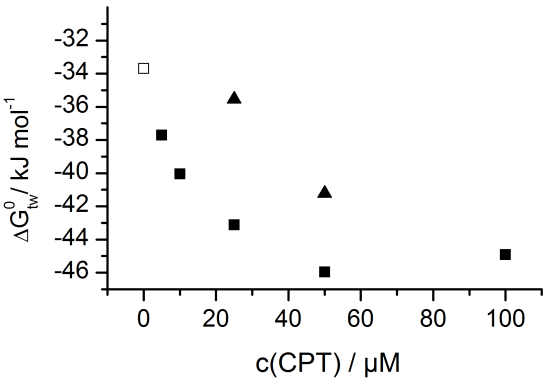

References

1. Riordan, J. R., and Ling, V. (1979) *The Journal of biological chemistry* **254**, 12701-12705
2. Allikmets, R., Schriml, L. M., Hutchinson, A., Romano-Spica, V., and Dean, M. (1998) *Cancer Res* **58**, 5337-5339
3. Doyle, L. A., Yang, W., Abruzzo, L. V., Krogmann, T., Gao, Y., Rishi, A. K., and Ross, D. D. (1998) *Proc Natl Acad Sci U S A* **95**, 15665-15670
4. Dawson, R. J., and Locher, K. P. (2006) *Nature* **443**, 180-185
5. Zolnerciks, J. K., Andress, E. J., Nicolaou, M., and Linton, K. J. (2011) *Essays Biochem* **50**, 43-61
6. Astumian, R. D., and Derenyi, I. (1998) *Eur Biophys J* **27**, 474-489
7. Seelig, A. (1998) *Eur J Biochem* **251**, 252-261.
8. Seelig, A., Blatter, X. L., and Wohnsland, F. (2000) *Int J Clin Pharmacol Ther* **38**, 111-121
9. Dey, S., Ramachandra, M., Pastan, I., Gottesman, M. M., and Ambudkar, S. V. (1997) *Proc Natl Acad Sci U S A* **94**, 10594-10599
10. Aller, S. G., Yu, J., Ward, A., Weng, Y., Chittaboina, S., Zhuo, R., Harrell, P. M., Trinh, Y. T., Zhang, Q., Urbatsch, I. L., and Chang, G. (2009) *Science* **323**, 1718-1722
11. Aanismaa, P., and Seelig, A. (2007) *Biochemistry* **46**, 3394-3404
12. Seelig, A. (2007) *J Mol Neurosci* **33**, 32-41
13. Amaral, M. D., and Kunzelmann, K. (2007) *Trends Pharmacol Sci* **28**, 334-341
14. Verkman, A. S., Lukacs, G. L., and Galietta, L. J. (2006) *Curr Pharm Des* **12**, 2235-2247
15. Tradtrantip, L., Sonawane, N. D., Namkung, W., and Verkman, A. S. (2009) *J Med Chem* **52**, 6447-6455
16. Pedemonte, N., Tomati, V., Sondo, E., and Galietta, L. J. (2010) *American journal of physiology. Cell physiology* **298**, C866-874
17. Muanprasat, C., Sonawane, N. D., Salinas, D., Taddei, A., Galietta, L. J., and Verkman, A. S. (2004) *The Journal of general physiology* **124**, 125-137
18. Moreau, C., Jacquet, H., Prost, A.-L., D'Hahan, N., and Vivaudou, M. (2000) *Embo J* **19**, 6644-6651
19. Golstein, P. E., Boom, A., van Geffel, J., Jacobs, P., Masereel, B., and Beauwens, R. (1999) *Pflugers Arch* **437**, 652-660
20. McConnell, H. M., Owicki, J. C., Parce, J. W., Miller, D. L., Baxter, G. T., Wada, H. G., and Pitchford, S. (1992) *Science* **257**, 1906-1912
21. Gatlik-Landwojtowicz, E., Aanismaa, P., and Seelig, A. (2004) *Biochemistry* **43**, 14840-14851
22. Litman, T., Zeuthen, T., Skovsgaard, T., and Stein, W. D. (1997) *Biochim Biophys Acta* **1361**, 169-176
23. Litman, T., Zeuthen, T., Skovsgaard, T., and Stein, W. D. (1997) *Biochim Biophys Acta* **1361**, 159-168.
24. Gatlik-Landwojtowicz, E., Aanismaa, P., and Seelig, A. (2006) *Biochemistry* **45**, 3020-3032
25. Chen, E. Y., Bartlett, M. C., Loo, T. W., and Clarke, D. M. (2004) *J Biol Chem* **279**, 39620-39627
26. Fromherz, P. (1975) *Rev Sci Instrum* **46**, 1380-1384
27. Fischer, H., Gottschlich, R., and Seelig, A. (1998) *J Membr Biol* **165**, 201-211
28. Gerebtzoff, G., Li-Blatter, X., Fischer, H., Frentzel, A., and Seelig, A. (2004) *Chembiochem* **5**, 676-684
29. Gerebtzoff, G., and Seelig, A. (2006) *J Chem Inf Model* **46**, 2638-2650
30. Zhang, Z. R., Zeltwanger, S., and McCarty, N. A. (2004) *J Membr Biol* **199**, 15-28

31. Caci, E., Caputo, A., Hinzpeter, A., Arous, N., Fanen, P., Sonawane, N., Verkman, A. S., Ravazzolo, R., Zegarra-Moran, O., and Galietta, L. J. (2008) *Biochem J* **413**, 135-142
32. Ma, T., Thiagarajah, J. R., Yang, H., Sonawane, N. D., Folli, C., Galietta, L. J., and Verkman, A. S. (2002) *J Clin Invest* **110**, 1651-1658
33. Gedeon, C., Anger, G., Piquette-Miller, M., and Koren, G. (2008) *Placenta* **29**, 39-43
34. Bessadok, A., Garcia, E., Jacquet, H., Martin, S., Garrigues, A., Loiseau, N., Andre, F., Orlowski, S., and Vivaudou, M. (2011) *J Biol Chem* **286**, 3552-3569
35. Jani, M., Szabo, P., Kis, E., Molnar, E., Glavinas, H., and Krajcsi, P. (2009) *Biol Pharm Bull* **32**, 497-499
36. Weiss, J., Sauer, A., Herzog, M., Boger, R. H., Haefeli, W. E., and Benndorf, R. A. (2009) *Pharmacology* **84**, 264-270
37. Zhang, S., Yang, X., and Morris, M. E. (2004) *Pharm Res* **21**, 1263-1273
38. Katayama, K., Masuyama, K., Yoshioka, S., Hasegawa, H., Mitsuhashi, J., and Sugimoto, Y. (2007) *Cancer Chemother Pharmacol* **60**, 789-797
39. Moran, O., and Zegarra-Moran, O. (2005) *FEBS Lett* **579**, 3979-3983
40. Nabekura, T., Kamiyama, S., and Kitagawa, S. (2005) *Biochem Biophys Res Commun* **327**, 866-870
41. Anuchapreeda, S., Leechanachai, P., Smith, M. M., Ambudkar, S. V., and Limtrakul, P. N. (2002) *Biochem Pharmacol* **64**, 573-582
42. Pereira, M. M., Parker, J., Stratford, F. L., McPherson, M., and Dormer, R. L. (2007) *The Biochemical journal* **405**, 181-189
43. Hegedus, T., Serohijos, A. W., Dokholyan, N. V., He, L., and Riordan, J. R. (2008) *J Mol Biol* **378**, 1052-1063
44. Sheppard, D. N., and Robinson, K. A. (1997) *J Physiol* **503 (Pt 2)**, 333-346
45. Cui, G., Song, B., Turki, H. W., and McCarty, N. A. (2011) *Pflugers Arch*
46. Kopeikin, Z., Sohma, Y., Li, M., and Hwang, T. C. (2010) *J Gen Physiol* **136**, 659-671
47. Park, J. B. (1999) *Biochem Biophys Res Commun* **260**, 568-574
48. Vera, J. C., Reyes, A. M., Carcamo, J. G., Velasquez, F. V., Rivas, C. I., Zhang, R. H., Strobel, P., Iribarren, R., Scher, H. I., Slebe, J. C., and et al. (1996) *J Biol Chem* **271**, 8719-8724
49. Illek, B., Lizarzaburu, M. E., Lee, V., Nantz, M. H., Kurth, M. J., and Fischer, H. (2000) *Am J Physiol Cell Physiol* **279**, C1838-1846
50. Springsteel, M. F., Galietta, L. J., Ma, T., By, K., Berger, G. O., Yang, H., Dicus, C. W., Choung, W., Quan, C., Shelat, A. A., Guy, R. K., Verkman, A. S., Kurth, M. J., and Nantz, M. H. (2003) *Bioorg Med Chem* **11**, 4113-4120
51. Wang, F., Zeltwanger, S., Yang, I. C., Nairn, A. C., and Hwang, T. C. (1998) *J Gen Physiol* **111**, 477-490
52. Galietta, L. V., Jayaraman, S., and Verkman, A. S. (2001) *Am J Physiol Cell Physiol* **281**, C1734-1742
53. Ai, T., Bompadre, S. G., Wang, X., Hu, S., Li, M., and Hwang, T. C. (2004) *Mol Pharmacol* **65**, 1415-1426
54. Ko, W. C., Shih, C. M., Lai, Y. H., Chen, J. H., and Huang, H. L. (2004) *Biochem Pharmacol* **68**, 2087-2094
55. Wang, W., Bernard, K., Li, G., and Kirk, K. L. (2007) *J Biol Chem* **282**, 4533-4544
56. Li, H., and Sheppard, D. N. (2009) *BioDrugs* **23**, 203-216

8 Additional Manuscripts

8.1 Steroid Hormones Modulate the ATPase activity of CFTR

8.1 Steroid Hormones Modulate the ATPase Activity of CFTR

Manuel Hellstern, Matthias Zwick and Anna Seelig*

Biophysical Chemistry, Biozentrum, University of Basel, Klingelbergstrasse 50/70, CH-4056 Basel, Switzerland, Phone: +41-61-267 2206, FAX: +41-61-267 2189, e-mail: anna.seelig@unibas.ch

*Corresponding author

Abstract

Steroid hormones have been discussed controversially as activators and inhibitors of the cystic fibrosis transmembrane conductance regulator (CFTR, ABCC7). To unravel the seeming contradiction we measured the CFTR-ATPase activity stimulated by cortisol, progesterone, 17β-estradiol, and the estradiol inhibitor tamoxifen at different concentrations. Measurements were performed in *CFTR* over-expressing Chinese hamster ovary (CHO-CFTR) cells using a microphysiometer that monitors the extracellular acidification rate (ECAR) changes due to ATP consumption in real time. ATP consumption was due to CFTR phosphorylation by protein kinase A upon stimulation with CPT-cAMP or forskolin and subsequent hormone-induced ATP hydrolysis by the CFTR-ATPase. Titration of CHO-CFTR cells with steroid hormones over a broad concentration range in the presence of phosphorylation agents yielded bell-shaped ATPase activity curves, while titrations of the corresponding control (CHO-K1) cells induced no effects at low hormone concentrations. At high concentrations progesterone and especially 17β-estradiol reduced the ECAR due to a reduction of glucose uptake. Tamoxifen showed no CFTR-specific effects but irreversibly reduced the ECAR at high concentrations. The possibility to unambiguously differentiate between CFTR-specific, general metabolic, and cytotoxic effects, respectively, shows that the CFTR-ATPase activity is enhanced at low and reduced at high concentrations of steroid hormones. The correlation between ATP hydrolysis and chloride flux is discussed.

Introduction

The cystic fibrosis transmembrane conductance regulator CFTR (ABCC7) is a homolog of the adenosine triphosphate (ATP) binding cassette (ABC) transporter, P-glycoprotein (ABCB1, Pgp). The best investigated function of CFTR is that of a chloride (Cl^-) channel which plays an essential role in maintaining the fluid balance in several tissues including the lung airways, the intestine, and many exocrine glands. Like Pgp, it is composed of two transmembrane domains (TMD), comprising six putative transmembrane α-helices each, and two nucleotide binding domains (NBD1 and NBD2). In CFTR the two homologous halves are linked by a unique, regulatory domain (RD) which leads to the overall domain organization TMD1-NBD1-RD-TMD2-NBD2. Phosphorylation of the RD by protein kinases facilitates NBD association and formation of an open chloride channel (*1*). *In vitro* phosphorylation by protein kinase A (PKA) can be induced by the membrane permeating cAMP analogon CPT-cAMP or the adenylate cyclase activator forskolin.

Genetic mutations can lead to CFTR proteins that are defective in trafficking and folding. As a consequence the functional activity of CFTR is reduced, which causes cystic fibrosis (CF). To rescue folding or enhance activity of defective CFTR in CF patients small molecule correctors and modulators are sought (for review see (*2*)). Modulators of CFTR tend to be electrically neutral or anionic compounds belonging to most diverse chemical classes. Steroid hormones have been shown to directly interact with CFTR and to reduce chloride flux in excised inside-out patches of L-cells expressing *CFTR* in the presence of forskolin (*3*) or BHK cells (*4*). The above results seem consistent with the aggravation of CF symptoms with increasing levels of 17β-estradiol. Alleviation of the gender-specific effects of CF was therefore expected from a treatment with the steroid receptor antagonist tamoxifen (for review see (*5*)). However, other investigations report opposite effects, namely stimulation of the chloride flux (*6*) and correction of aberrant CFTR localization by steroid hormones (*7*). In this context it should be noted that steroid hormones moreover influence CFTR gene expression (see e.g (*8*)).

The aim of the present analysis was to further elucidate how steroid hormones (cortisol, progesterone, and 17β-estradiol) and the 17β-estradiol inhibitor tamoxifen interact with CFTR and how these, at first sight, contradictory observations can be understood at the molecular level. So far CFTR activity has been investigated mainly by means of patch clamp techniques and only little information is available on concentration-dependent ATPase activity measurements (*9*). Here we measured the

ATPase activity in CHO-CFTR and CHO-K1 cells induced by the different steroid hormones and tamoxifen over a broad concentration range by monitoring the ECAR in real time by means of a μpH meter based on silicon chip technology dubbed Cytosensor® microphysiometer (*10*). ECAR measurements in living cells are non-invasive, highly sensitive and allow titrations over a broad concentration range using the same batch of cells during several hours. The basal ECAR reflects the sum of all metabolic processes of the cell. Cells, transfected with a specific ABC transporter such as Pgp show transporter-specific signals (*11*). Under the anaerobic conditions of the Cytosensor the ECAR is due entirely to the efflux of lactic acid which is a product of glycolytic ATP synthesis. As one molecule of lactic acid exported corresponds to one molecule of ATP synthesized, ATP synthesis directly correlates with ATP hydrolysis. Measurement of the ECAR therefore reveals the rate of ATP hydrolysis of the ABC transporter overexpressed in a specific cell line as demonstrated for Pgp (*12*). We have shown that ATP consumption required for phosphorylation of CFTR by protein kinase A (PKA) (Matthias Zwick, Manuel Hellstern and Anna Seelig, in preparation) as well as modulator induced CFTR-ATPase activity (Matthias Zwick, Rita Müller and Anna Seelig, in preparation) can be measured via changes in the ECAR. As modulators we tested inhibitors and potentiators that both directly interacted with CFTR. The former activated the CFTR-ATPase at low and inhibited it a high concentrations, respectively, yielding bell-shaped activity curves while the latter generally barely activated at low but also inhibited at high concentrations, respectively. In the following we use the information gained on CFTR-ATPase modulation to get more insight into the complex interplay between steroid hormones and CFTR.

For this purpose, we first measured the basal ATPase activity of CHO-K1 and CHO-CFTR cells in phosphate buffer and in MEMα containing the pH indicator phenol red. Second, we stimulated PKA to different extents to induce CFTR phosphorylation using the membrane permeating phosphorylation agents, CPT-cAMP and forskolin. Third, we titrated the two cell lines with the different steroid hormones in the presence of a constant concentration of the phosphorylation agents in buffer and in medium. CHO-CFTR cells showed CFTR-specific changes while control cells showed no effects at low hormone concentrations and only small effects at high concentrations. The effects at high steroid hormone concentrations were more pronounced in medium due to the presence of phenol red. The bell-shaped CFTR-ATPase activity vs. concentration curves obtained for cortisol, progesterone, and 17β-estradiol suggest that all three compounds block the chloride channel at high concentrations. Comparison of the present data with previous patch clamp measurements obtained under identical phosphorylation

conditions (*3*) agree with this conclusion. At lower concentrations the activity enhancing cortisol and progesterone may be inhibitors of the chloride flux while 17β-estradiol is most likely an activator again in agreement with patch-clamp measurements (*6*). To moreover test whether modulators first partition into the lipid membrane before binding to the TMDs of CFTR within the lipid membrane as observed previously for Pgp (*12-14*), we estimated the lipid-water partition coefficient of the different compounds based on surface activity measurements. The analysis suggests that modulator binding indeed occurs in the lipid membrane via hydrogen bond formation between hydrogen bond acceptors in modulators and hydrogen bond donors in the TMDs of CFTR. However, in contrast to Pgp, hydrogen bond donors (i.e., hydroxyl groups) seem also to play a significant role for modulator binding to CFTR.

Materials and Methods

Compounds. Cortisol, progesterone, 17β-estradiol, tamoxifen, 8-(4-Chlorophenylthio)-adenosine-3',5'-cyclic monophosphate sodium salt (CPT-cAMP), forskolin and methotrexate (MTX) were purchased from Sigma Aldrich (St. Louis, Missouri, USA). Minimum essential medium alpha (MEMα), Dulbecco's phosphate buffered saline (DPBS) and fetal bovine serum (FBS) was obtained from Invitrogen (Carlsbad, CA, USA). MTX for cell culture was prepared as a 100 mg/ml stock solution in sterile 1 N NaOH.

Cell Culture. Chinese hamster ovary (CHO) cells, stably transfected with the human *CFTR* gene (CHO-CFTR) or the defective mutant *CFTRΔF508* (CHO-ΔF) were a generous gift from Dr. J. R. Riordan (University of North Carolina, USA). Cells were grown as monolayer cultures in sterile cell culture flasks (Costar, 25-75 cm^2) at 37 °C. A Heraeus incubator with an air atmosphere supplemented with 5 % CO_2 and humidity saturation of 100% was used. MEMα containing 1% streptomycin/penicillin and 10 % FBS was used as medium. Transfected cells were kept under growth selection with MTX solution (50 µM). Passages (1:15) were performed three times a week.

Flow Medium and Flow Buffer. For ECAR measurements MEMα or phosphate buffer both with low buffer capacity were used. MEMα contained no sodium bicarbonate to reduce the buffer capacity. To preserve the osmotic balance NaCl was added (26.4 mM NaCl) and the solution was adjusted to pH 7.4. MEMα contains phenol red which at one hand most likely stimulates CFTR as it exhibits all the relevant recognition elements (see below) and at the other hand is known to interact with the estrogen receptor (*15*). The phosphate buffer contained glucose (10 mM), calcium chloride (0.3 mM), magnesium chloride (0.6 mM) and sodium chloride (130 mM), potassium dihydrogenphosphate (0.5 mM), potassium chloride (3 mM), disodium hydrogen phosphate (0.5 mM) adjusted to pH 7.4.

Cytosensor Measurements. The extracellular acidification rate (ECAR) was measured as a function of time using an eight-channel Cytosensor® microphysiometer (Molecular Devices, Menlo Park, CA, U.S.A.). The measurement is based on silicon chip technology and allows detection of small pH changes by means of a light addressable potentiometric sensor (LAPS). Protons excreted by the cell come into contact with the

LAPS and induce changes in the order of a few μV·s $^{-1}$. According to the calibration 61 mV correspond to 1 pH unit (*11*).

Cells (~$3 \cdot 10^5$) were seeded on 12 mm diameter plates with a microporous polycarbonate membrane bottom (capsule cups) in cell culture medium (MEMα) without MTX and were left in the incubator over night for attachment. For measurements, capsule cups were transferred into the sensor chamber, covered with capsule spacers and inserts in order to form a tight chamber of 2.8 μl which comprised about ¼ of the original number of cells. To keep a constant CFTR phosphorylation during measurements CPT-cAMP or forskolin was added to the medium. The peristaltic pumps were programmed to flush the cells with medium for 1 min 30 s. During the stop period of 30 sec the acidification was measured under steady state condition. Before CFTR stimulation the system was stabilized at 37 °C for at least two hours.

For stock solutions, drugs were dissolved in DMSO and were then diluted with MEMα to the concentrations applied to the Cytosensor. Before reaching the cells the medium passed through a heated debubbler membrane which removed oxygen from the solution and created anaerobic conditions in the measuring chamber. To quantify possible adsorption of the compounds to the tubing and the debubbler membrane their concentration in the solutions leaving the measuring cells was quantified by UV-VIS spectroscopy. The extinction coefficient of progesterone and cortisol was measured at 248 nm and was determined as ε = 15244 M^{-1} cm^{-1} and ε = 15874 M^{-1} cm^{-1}, respectively. The extinction coefficient of 17β-estradiol could not be determined due to the low solubility and the low absorbance. As the absorbance of a 17β-estradiol solution (200 μM) before and after application to the Cytosensor was practically identical we concluded that the adsorption was negligibly small.

Kinetics of the CFTR-ATPase. The ECAR measured as a function of concentration yielded activity curves which were fitted with an equation based on a two-site binding model described in eq. 1 (*16*). The model is based on the principles of uncompetitive or substrate inhibition and allows for basal activity. The rate of ATP hydrolysis which corresponds to the rate of ATP synthesis corresponds to the ECAR which is described as,

$$ECAR = \frac{K_1 K_2 V_0 + K_2 V_1 C + V_2 C^2}{K_1 K_2 + K_2 C + C^2}, \qquad (1)$$

where K_1 is the concentration of half-maximum activation, K_2 the concentration of half-maximum inhibition, V_0 the basal activity after stimulation with CPT-cAMP, V_1 is the maximum activity, V_2 the minimum activity, and C the substrate concentration in aqueous solution. Since experiments were performed under steady state conditions and the binding steps were much faster than the catalytic step, the concentration of half-maximum activation, K_1, could be assumed to correspond to the dissociation constant of the drug from the transporter. The inverse ($1/K_1$) then corresponds to the transporter-water binding constant, K_{tw} (*12*) to a first approximation,

$$K_{tw} = \frac{1}{K_1}. \qquad (2)$$

Air-Water and Lipid- Water Partition Coefficient. Measurements of the surface pressure, π, as a function of solute concentration, C, were performed with a Fromherz Teflon trough (20 mL) connected to a Wilhelmi balance (*17*). The buffer (50 mM Tris and 114 mM NaCl) was adjusted to pH 7.4. Stock solutions were in the range of 3-6 mg per mL DMSO. The final solvent concentration was below 5%. Under these conditions the surface activity of DMSO is negligibly small. Serial aliquots of the stock solution were added to the monolayer trough filled with buffer. The surface pressure, π, was recorded as a function of time at T = 27 °C until equilibrium was reached. The Gibbs adsorption isotherm i.e. the surface pressure at equilibrium as a function of the concentration, C, of the steroid hormones was measured. This allowed assessing the air-water partition coefficient, K_{aw}, the cross-sectional area of the molecule at the air-water interface, A_D, and the critical micelle concentration, CMC_D, which coincides with the concentration at the solubility limit, C_{sol}, for many drugs (*18*). Data were evaluated as described in detail elsewhere (*18, 19*).

The lipid-water partition coefficient, K_{lw}, was derived from the air-water partition coefficient, K_{aw},

$$K_{lw} = K_{aw} * e^{\frac{-\pi_M A_D}{kT}}, \qquad (3)$$

where $\pi_M \cdot A_D = \Delta W$ corresponds to the work required to create a hole in the lipid membrane with a given packing density, π_M, that is large enough to accommodate the molecule with the cross-sectional area A_D (*20*), and k is the Boltzmann constant.

Free Energy of Modulator Binding to the Transporter and Free Energy of Lipid-Water Partitioning. Binding of a modulator from the extracellular aqueous phase to CFTR is a two-step binding mechanism, comprising a lipid-water partitioning step followed by a binding step from the lipid membrane to the transporter. The free energy of binding of a modulator from water to the first binding site of CFTR, $\Delta G^0_{tw(1)}$, can thus be expressed as the sum of the free energy of lipid-water partitioning, ΔG^0_{lw}, and the free energy of binding from the lipid membrane to CFTR, $\Delta G^0_{tl(1)}$, as shown previously for Pgp (*12*),

$$\Delta G^0_{tw(1)} = \Delta G^0_{lw} + \Delta G^0_{tl(1)}. \tag{4}$$

The free energy of transporter-water binding is

$$\Delta G^0_{tw(1)} = -RT \ln\left(C_w K_{tw(1)}\right), \tag{5}$$

where RT is the thermal energy and C_w is the molar concentration of water (C_w = 55.3 mol/L at 37°C). Analogous equations can be formulated for the second binding site. The free energy of the lipid-water partitioning, ΔG^0_{lw} is

$$\Delta G^0_{lw} = -RT \ln\left(C_w K_{lw}\right). \tag{6}$$

Results

The ECAR of CHO-CFTR and CHO-K1 Cells. First, the basal ECAR of CHO-CFTR and CHO-K1, respectively, was measured as a function of time under essentially anaerobic conditions using a Cytosensor microphysiometer (*10*). Measurements were performed in phosphate buffer (Fig. 1A-C) and MEMα medium containing phenol red (Fig. 2A-C) at pH 7.4 and T = 37°C. After the exchange of the culture medium for the flow buffer (Fig. 1A-C) or flow medium (Fig. 2A-C) cells were left to accommodate in the Cytosensor for about two hours until a stable extracellular acidification rate was reached. The first few measuring points in Fig. 1A-C and Fig. 2A-C represent the basal ATPase activity of CHO-CFTR and CHO-K1 cells, respectively, obtained after the accommodation period. The basal ECAR was normalized to 100% taking into account the average of the four pump cycles before stimulation.

In order to induce phosphorylation of CFTR, CHO-CFTR cells were superfused with flow buffer containing CPT-cAMP (25 μM) (Fig. 1A-C). For control, experiments were repeated in CHO-K1 cells. In CHO-CFTR cells CPT-cAMP induced a fast ECAR increase to about 120 ± 10 % followed by a slower increase to about 140 ± 10 %. In CHO-K1 cells no fast effect was observed; the slow effect was also present, however, to a much lower extent. The ECAR increase measured in CHO-CFTR cells upon phosphorylation was shown to be due to lactate extrusion and thus to ATP synthesis which, in turn, correlates directly with ATP hydrolysis (*21*) (Matthias Zwick, Manuel Hellstern and Anna Seelig, in preparation). Despite the fact that the CPT-cAMP level was kept constant during the whole experiment (several hours) the baseline decreased over time. In patch clamp measurements an analogous slow decrease in chloride flux upon longtime phosphorylation was observed and was interpreted as a feedback mechanism due to a reduction in cellular cAMP levels following activation of phosphodiesterases (*22*).

After phosphorylation, CHO-CFTR and CHO-K1 cells were stimulated with increasing concentrations of the steroid hormones cortisol (Fig. 1A), progesterone (Fig. 1B), and 17β-estradiol (Fig. 1C) (in the presence of a constant concentration of phosphorylation agents). Stimulation for 10 to 20 minutes (indicated by gray bars) was sufficient to reach an apparent steady state in CHO-CFTR cells. In CHO-K1 cells the effects were negligibly small. After stimulation with steroid hormones, cells were flushed again with flow buffer without hormones. This reduced the modulator concentration in the lipid bilayer as well as in the cell concomitantly the ECAR returned to basal values, indicating that the ECAR effects in CHO-CFTR cells were reversible.

With increasing steroid hormone concentration the ECAR increased up to a maximum level and decreased again at higher concentrations yielding bell-shaped activity curves. The ECAR increase was higher for cortisol and progesterone than for 17β-estradiol. At high steroid hormone concentrations, washout lead first to an increase in the ECAR before the basal activity was reached again. This effect was more pronounced for progesterone and 17β-estradiol than for cortisol. Small washout effects were also observed in CHO-K1 cells, especially for progesterone and 17β-estradiol, suggesting that the two compounds reduced the basal metabolism (see below).

CFTR stimulations with steroid hormones were repeated in MEMα (Fig. 2A-C). Phosphorylation with CPT-cAMP (25 µM) again induced a fast increase in the ECAR in CHO-CFTR cells, however, ECAR changes were slightly higher (130 ± 10 %) than in buffer. The fast increase was followed by a continuous slow decrease of the ECAR. Control cells again showed no fast CPT-cAMP stimulation but the slow continuous decrease was also observed, although, to a much lower extent than in transfected cells. Steroid hormone stimulation also induced a concentration dependent, fast increase in the ECAR of CHO-CFTR but not in CHO-K1 cells. In contrast to the titrations in buffer, the first measuring point in the stimulation period was generally below basal ECAR and only increased to higher values at the second stimulation point. The fast reversible decrease was most pronounced in the case of 17β-estradiol. After hormone stimulation cells were flushed with modulator-free flow medium containing CPT-cAMP. CHO-K1 cells again showed no steroid-hormone induced effects at low concentrations, however, at higher concentrations an ECAR decrease was also observed, especially in the case of 17β-estradiol which was significantly more pronounced than in buffer.

The decrease of basal activity is most likely due to the interference of 17β-estradiol with the glucose transporter (*23*). The difference in the shape of the ECAR curves as a function of steroid hormone concentration in buffer and medium is clearly due to buffer components, especially, phenol red which is added to media as a pH indicator. Phenol red is known to interact with steroid hormone receptors, particularly with the 17β-estradiol receptor and also with the glucose transporter (*15*). Phenol red may in addition also act as a modulator of CFTR activity. The shape of the ECAR titration curves thus results from the superposition of the effects of CPT-cAMP, steroid hormones, and phenol red on basal activity which is especially pronounced in the case of 17β-estradiol. Despite these additional metabolic effects the CFTR specific effects of 17β-estradiol can still be clearly detected.

Titrations analogous to those of steroid hormones in medium were further performed with tamoxifen in the concentration range of 1-100 µM (not shown). At low

tamoxifen concentrations (1-50 µM) an effect was observed neither in transfected nor in control cells. At higher concentrations (C ≥ 50 µM) tamoxifen induced an ECAR decrease in both, transfected and control cells, which was only partially reversible after washout. At the highest concentration measured (100 µM) the ECAR irreversibly decreased to zero values in both cell types indicating cell death.

Fig. 1A-C

Fig. 2A, B

Fig. 3A-C displays the ECAR curves induced by steroid hormones in CHO-CFTR and CHO-K1 cells under steady state conditions (average of the 5th to 7th stimulation point in Fig. 1A-C and Fig. 2A-C) plotted as a function of steroid hormone concentration in the presence of CPT-cAMP (25 µM) in buffer and MEMα. For all three hormones bell-shaped CFTR-ATPase activity curves as a function of concentration were observed. It has to be noted that the plots reflect the CFTR-specific and not the net changes in the ECARs. The curves were fitted with a two-site binding model based on un-competitive or substrate inhibition (*12, 16*). Solid lines represent fits to the data using eq. 1. The corresponding kinetic constants (i.e., the concentration of half-maximum activation and inhibition, K_1, and K_2, respectively, and the half-maximum and half-minimum activity, V_1 and V_2, respectively) are summarized in Tab. 1. It is interesting to note that the apparent concentrations of half-maximum activation and inhibition, respectively, are shifted to slightly lower values in MEMα compared to buffer which is most likely due to the superposition of the modulator effect of steroid hormones and phenol red. The latter exhibits the structural properties of a CFTR modulator (see below), but unfortunately direct testing is not feasible because phenol red also induces slight metabolic effects.

As we have shown that control cells show only negligibly small effects, the increase in the ECAR in CHO-CFTR cells which is due to lactate efflux (Matthias Zwick, Rita Müller and Anna Seelig, in preparation) can be directly correlated with the increase in ATP hydrolysis of CFTR as shown previously for Pgp (*11, 12*). The ECAR as a function of steroid hormone concentration (Fig. 3A-C) can thus be considered as CFTR-ATPase activity as a function of steroid hormone concentration.

Fig. 3A-C

Tab. 1

Different Phosphorylation Conditions of CFTR. The titrations of CHO-CFTR and CHO-K1 cells with progesterone and 17β-estradiol were repeated in medium under different phosphorylation conditions. Fig. 4 displays the ECAR as a function of the progesterone concentration in the presence of CPT-cAMP (25 μM and 50 μM) and forskolin (0.1 μM and 10 μM). Solid lines in Fig. 4 are fits to the experimentally determined activity curves using eq. 1. The kinetic constants derived from these fits are summarized in Tab. 1. With increasing CPT-cAMP concentration the apparent concentration of half-maximum CFTR-ATPase activation, K_1, induced by progesterone decreased to lower values, and the maximum activity, V_1, increased to higher values. In the presence of forskolin (0.1 μM) the concentration of half-maximum activation, K_1, induced by progesterone was even lower than in the presence of CPT-cAMP and the maximum activity, V_1, decreased to lower values, barely above basal activity, and the inhibitory branch became dominant. At higher concentrations of forskolin (10 μM) the inhibitory effect became even more pronounced.

Fig. 4

Air-Water and Lipid-Water Partition Coefficient of CFTR Modulators. Because the dielectric constant of air ($\varepsilon \sim 1$) and the lipid core region ($\varepsilon \sim 2$) are similar, the air-water interface is an ideal model system for estimating the behavior of molecules entering the lipid-water interface. Amphiphilic drugs orient with their axis of amphiphilicity perpendicular to the air-water or lipid-water interface, and therefore generally adopt a comparable conformation at the two interfaces (*18, 24*). To elucidate the properties of the present compounds at the lipid-water interface we measured the surface pressure, π, as a function of the solute concentration, C, (Gibbs adsorption isotherm) at pH 7.4 and room temperature. The surface pressure, π, increased with the concentration up to a limiting value which reflects the critical micelle concentration, CMC_D (not shown). The CMC_D decreased in the order cortisol > 17β-estradiol > progesterone > tamoxifen. The maximum surface pressure reached at the CMC_D increased in the order, 17β-estradiol ($\pi_{max} \sim 1.8$ mN/m) < cortisol ($\pi_{max} \sim 6$ mN/m) < progesterone ($\pi_{max} \sim 9$ mN/m) < tamoxifen ($\pi_{max} \sim 17$ mN/m). For the steroid hormones the CMC_D coincided with the solubility limit, C_{sol}, which reflects their low amphiphilicity. 17β-estradiol is not amphiphilic and barely surface active. Tamoxifen was the only compound which remained surface active after the CMC_D was reached

which is typical for a highly amphiphilic compound. Further analysis of the Gibbs adsorption isotherms (see (*18, 24*)) yielded the air-water partition coefficient, K_{aw}, and the cross-sectional area, A_D, of the compounds (see Tab. 2). The air-water partition coefficient, K_{aw}, increased in the order, cortisol < 17β-estradiol < progesterone < tamoxifen. Due to the low amphiphilicity, the high tendency to aggregate and precipitate the cross-sectional areas could not be evaluated and were therefore assessed using the molecular modeling algorithm Pgpredix (*24*). Data are summarized in Tab. 2.

Knowledge of the air-water partition coefficient, K_{aw}, and the cross-sectional area, A_D of the compound allows estimation of the lipid-water partition coefficient, K_{lw}, according to eq. 3. The lateral lipid packing density in MDR1-transfected mouse embryo fibroblasts was previously determined as π_M = 30 mN/m at 37°C and was assumed to be identical for the CHO cells, at least to a first approximation. The binding constant of progesterone dissolved in DMSO was also determined by isothermal titration calorimety yielding an approximately twofold higher value (Estefania Egido, Xiaochun Li-Blatter and Anna Seelig, in preparation). Lipid-water partition coefficients, K_{lw}, and the free energies of lipid-water partitioning, ΔG^0_{lw}, (eq. 6) were included in Tab. 2.

Fig. 5

Tab. 2

Discussion

Steroid Hormones Induced Bell-Shaped CFTR-ATPase Activity Curves as a Function of Concentration. Using microphysiometry allowed recording the CFTR-ATPase activity in real time in living cells over a broad concentration range of the steroid hormones, cortisol, progesterone, and 17β-estradiol and the 17β-estradiol inhibitor tamoxifen under different phosphorylation conditions. The resulting bell-shaped CFTR-ATPase activity curves resemble the drug-induced Pgp-ATPase activity curves (*12, 16, 21, 25*). The activity curves were fitted with a binding model assuming activation upon binding of a first molecule and inhibition upon binding of a second molecule to the TMDs of CFTR. The model applied first to describe substrate binding to Pgp (*12, 16*) is based on the concept of uncompetitive or substrate inhibition and takes into account basal activity. The existence of a second, inhibitory binding site in the case of CFTR is supported by the activity increase upon washout at high modulator concentrations which reflects the reversibility of binding upon dilution. The comparison of ECAR changes in control and transfected cells allowed differentiation between steroid hormone-induced CFTR-specific effects, general reversible, metabolic effects due to the interaction of progesterone, 17β-estradiol, and phenol red with the glucose transporter, and irreversible, toxic effects of tamoxifen. Taking these effects into account, we could show that all three steroid hormones induced bell-shaped CFTR-ATPase activity in living cells, whereas no CFTR-specific effect could be detected for tamoxifen.

Correlation with chloride flux. The more amphiphilic cortisol and progesterone showed bell-shaped CFTR-ATPase activity curves and thus resemble typical CFTR inhibitors. This is consistent with a lack of iodide efflux from CFTR-CHO cells upon stimulation with cortisol as measured with an iodide selective electrode (Matthias Zwick, unpublished results). Direct patch-clamp experiments for cortisol seem not to be available in literature. For progesterone in the presence of forskolin (10 μM) a reduction of the Cl^- flux was indeed observed with increasing concentration (*3*). 17β-estradiol showed limited activation at low concentrations and inhibition at high concentrations. The lack of amphiphilicity and the resemblance to the non-amphiphilic polyphenols which are flopped slowly and prolong the open time (Matthias Zwick, Rita Müller and Anna Seelig, preparation) suggest a potentiator function at low concentrations. At high concentrations, where both binding sites are occupied which may block the channel, 17β-estradiol most likely inhibits the channel function as other

potentiators at high concentrations. This is supported by literature data showing an increase (*6*) and decrease (*3*) of the chloride flux, at low and high concentrations, respectively.

Different Phosphorylation Conditions. As seen in Fig. 4 the CFTR-ATPase modulation by steroid hormones depends not only on the concentration of the modulator but also on the concentration and the nature of the phosphorylation agents. As shown earlier, the reason for this could be either a conformational change induced by the PKA dependent phosphorylation of the RD or a direct interaction between the phosphorylation agents and CFTR. As shown elsewhere in more detail (Matthias Zwick, Manuel Hellstern and Anna Seelig, in preparation) data are in favor of the latter interpretation. The concentration of CPT-cAMP used for phosphorylation in the present experiments (25 μM and 50 μM) is below or close to the maximum stimulation of ECAR by CPT-cAMP. A clear decrease in ECAR was observed for high forskolin concentrations (C > 1 μM) (Matthias Zwick, Manuel Hellstern and Anna Seelig in preparation). Iodide efflux measurements, however, confirmed that stimulation and therefore probably also phosphorylation was maximal under these conditions. Forskolin concentrations used here were therefore close to the maximum or close to the minimum of the ECAR curve, respectively. Under these conditions CFTR binding sites could be occupied by a mixed population (hormone and phosphorylation agent). Mixed populations of modulators were also observed in Pgp binding sites (*13, 26*). The concentration dependent effects of CPT-cAMP and forskolin can thus be well explained in the frame of un-competitive activation/inhibition considering that membrane permeating phosphorylation agents act as additional modulators of CFTR, which is consistent with the high number of hydrogen bond donors and acceptors.

Phenol red, a component of the medium, acts most likely as an additional modulator of CFTR besides its effects on glucose metabolism (*15*). CFTR can thus be activated or inhibited by steroid hormones depending on the concentration applied, whereby the presence of additional modulators can further influence the CFTR activity. The present findings suggest that the concentration of the modulators applied for therapeutic purposes has to be monitored carefully, if possible considering additional endogenous modulators, because occupation of both binding sites seems to inhibit CFTR activity.

The Modulator Affinity to the Transporter Depends on the Hydrogen Bonding Capacity of the Modulator. CFTR binds its modulators most likely from the lipid phase. Modulator binding can thus be described as a two-step binding process, and the free energy of modulator binding from the aqueous phase to the first binding site of CFTR (transporter-water binding), $\Delta G^0_{tw(1)}$, can accordingly be expressed as the sum of the free energy of lipid-water partitioning, ΔG^0_{lw}, and the free energy of modulator binding from the lipid membrane to the transporter (transporter-lipid binding), $\Delta G^0_{tl(1)}$, as proposed previously for Pgp (*27*). The free energy of transporter-lipid binding reflects the direct interaction of the substrate with the transporter and its knowledge allows analyzing the specific binding interactions between modulator molecules and the TMDs of the transporter. The free energy of transporter-water binding, $\Delta G^0_{tw(1)}$, was estimated from concentrations of half-maximum activation (*12*). Since the concentration of half-maximum activation, K_1, was measured in the presence of CPT-cAMP which most likely also acts as modulator the values of $\Delta G^0_{tw(1)}$ are somewhat larger than in the absence of phosphorylation agents.

The question then arose as to which modulator elements were recognized by CFTR. As modulator recognition binding occurs most likely in the lipid membrane hydrogen bonding interactions are most probable. Hydrogen bonds are weak electrostatic interactions which, according to Coulomb's law, are up to forty times stronger in a lipid environment (with a dielectric constant, $\varepsilon \approx 2$) than in aqueous solution (with a dielectric constant, $\varepsilon \approx 80$). Binding based on hydrogen bond formation is therefore relatively strong in a lipid environment and weak as soon as water is present. This is ideal for binding in the lipid phase, transport across the lipid phase and release into the aqueous phase (*12-14, 28*).

Tab. 2 lists the number of hydrogen bond acceptors (carboxyl and ether group, respectively) and hydrogen bond donors (hydroxyl group) per molecule. The contribution per hydrogen bonding group, $\Delta\Delta G^0_H$, to the free energy of binding to the transporter was estimated by dividing the free energy of transporter-lipid binding, $\Delta G^0_{tl(1)}$, by the number of hydrogen bonding groups. This suggests that modulator-CFTR interactions also follow a modular binding principle based on hydrogen bonding interactions. The somewhat higher apparent free energy of binding per hydrogen bond in the case of modulator-CFTR interactions compared to modulator-Pgp interactions is most likely due to the small contribution of other

modulators (Tab. 2). In contrast to Pgp which clearly prefers hydrogen bond acceptor groups, CFTR also accepts hydrogen bond donor groups (i.e. hydroxyl groups). The role of hydroxyl groups has also been pointed out in a recent QSAR study of BCRP modulators (*29*). For tamoxifen, the only cationic compound investigated, no specific interaction with CFTR could be observed. Possible interactions may be occluded, however, may be occluded by irreversible effects. Overlapping substrate specificity based on hydrogen bond acceptor groups was not only observed for Pgp and CFTR but also for Pgp and MRP1 (*30*). With this knowledge it will be possible to screen more efficiently for CFTR activators and inhibitors.

Tab. 2

Conclusions. Measuring the steroid-hormone induced ECAR as a function of concentration in living CHO-CFTR and the corresponding CHO-K1 control cells allowed unambiguous differentiation between *CFTR-specific effects* observed for all three steroid hormones, *general metabolic effects* observed for progesterone and 17β-estradiol and tamoxifen, and *irreversible, cytotoxic effects* observed for tamoxifen at high concentrations. The activity versus concentration curves were bell-shaped for all three compounds but the maximum activity decreased in the order cortisol > progesterone >17β-estradiol. In analogy to a previous analysis which revealed that inhibitors are generally amphiphilic compounds that modulate the CFTR-ATPase activity as a function of concentration in a bell-shaped manner with a significant maximum activity, whereas potentiators are often non-amphiphilic barely activating compounds, because of kinetically hindered flopping, the amphiphilic cortisol and progesterone were assumed to act as inhibitors of chloride flux, whereas the non-amphiphilc 17β-estradiol was assumed to be an activator at low concentration and an inhibitor at high concentrations, when both binding sites are occupied leading to channel block. The investigation further revealed that activation and inhibition of CFTR-ATPase activity depends not only on the concentration of a single modulator but also on the concentration and the nature of the co-administered modulators including phosphorylation agents. Like Pgp, CFTR seems to recognize its modulators via hydrogen bond acceptors in the lipid membrane. However, unlike Pgp it also accepts hydroxyl groups. The results warrant further studies to unravel the complexity of CFTR steroid hormone interactions in humans.

Acknowledgments: We gratefully thank Dr. J.R. Riordan (UNC School of Medicine, Biochemistry and Biophysics) for the gift of CHO-CFTR and CHO-ΔF cells. Moreover, we are very grateful to Dr. Beat Zehnder for initiating this work. This work was supported by the Swiss National Science Foundation (Grant Nr. 3100AO-107793).

References

1. Aleksandrov, A. A., and Riordan, J. R. (1998) Regulation of CFTR ion channel gating by MgATP, *FEBS letters 431*, 97-101.
2. Riordan, J. R. (2008) CFTR function and prospects for therapy, *Annu Rev Biochem 77*, 701-726.
3. Singh, A. K., Schultz, B. D., Katzenellenbogen, J. A., Price, E. M., Bridges, R. J., and Bradbury, N. A. (2000) Estrogen inhibition of cystic fibrosis transmembrane conductance regulator-mediated chloride secretion, *The Journal of pharmacology and experimental therapeutics 295*, 195-204.
4. Linsdell, P., and Hanrahan, J. W. (1999) Substrates of multidrug resistance-associated proteins block the cystic fibrosis transmembrane conductance regulator chloride channel, *Br J Pharmacol 126*, 1471-1477.
5. Zeitlin, P. L. (2008) Cystic fibrosis and estrogens: a perfect storm, *J Clin Invest 118*, 3841-3844.
6. Goodstadt, L., Powell, T., and Figtree, G. A. (2006) 17beta-estradiol potentiates the cardiac cystic fibrosis transmembrane conductance regulator chloride current in guinea-pig ventricular myocytes, *J Physiol Sci 56*, 29-37.
7. Ko, S. B., Mizuno, N., Yatabe, Y., Yoshikawa, T., Ishiguro, H., Yamamoto, A., Azuma, S., Naruse, S., Yamao, K., Muallem, S., and Goto, H. (2010) Corticosteroids correct aberrant CFTR localization in the duct and regenerate acinar cells in autoimmune pancreatitis, *Gastroenterology 138*, 1988-1996.
8. Johannesson, M., Ludviksdottir, D., and Janson, C. (2000) Lung function changes in relation to menstrual cycle in females with cystic fibrosis, *Respir Med 94*, 1043-1046.
9. Wellhauser, L., Kim Chiaw, P., Pasyk, S., Li, C., Ramjeesingh, M., and Bear, C. E. (2009) A small-molecule modulator interacts directly with deltaPhe508-CFTR to modify its ATPase activity and conformational stability, *Mol Pharmacol 75*, 1430-1438.
10. McConnell, H. M., Owicki, J. C., Parce, J. W., Miller, D. L., Baxter, G. T., Wada, H. G., and Pitchford, S. (1992) The cytosensor microphysiometer: biological applications of silicon technology, *Science 257*, 1906-1912.
11. Gatlik-Landwojtowicz, E., Aanismaa, P., and Seelig, A. (2004) The rate of P-glycoprotein activation depends on the metabolic state of the cell, *Biochemistry 43*, 14840-14851.
12. Gatlik-Landwojtowicz, E., Aanismaa, P., and Seelig, A. (2006) Quantification and characterization of P-glycoprotein-substrate interactions, *Biochemistry 45*, 3020-3032.
13. Li-Blatter, X., Nervi, P., and Seelig, A. (2009) Detergents as intrinsic P-glycoprotein substrates and inhibitors, *Biochim Biophys Acta 1788*, 2335-2344.
14. Li-Blatter, X., and Seelig, A. (2010) Exploring the P-glycoprotein binding cavity with polyoxyethylene alkyl ethers, *Biophys J 99*, 3589-3598.
15. Berthois, Y., Katzenellenbogen, J. A., and Katzenellenbogen, B. S. (1986) Phenol red in tissue culture media is a weak estrogen: implications concerning the study of estrogen-responsive cells in culture, *Proc Natl Acad Sci U S A 83*, 2496-2500.
16. Litman, T., Zeuthen, T., Skovsgaard, T., and Stein, W. D. (1997) Structure-activity relationships of P-glycoprotein interacting drugs: kinetic characterization of their effects on ATPase activity, *Biochim Biophys Acta 1361*, 159-168.
17. Fromherz, P. (1975) Instrumentation for Handling Monomolecular Films at an Air-Water-Interface, *Rev Sci Instrum 46*, 1380-1384.
18. Fischer, H., Gottschlich, R., and Seelig, A. (1998) Blood-brain barrier permeation: molecular parameters governing passive diffusion, *J Membr Biol 165*, 201-211.

19. Gerebtzoff, G., Li-Blatter, X., Fischer, H., Frentzel, A., and Seelig, A. (2004) Halogenation of drugs enhances membrane binding and permeation, *Chembiochem 5*, 676-684.
20. Boguslavsky, V., Rebecchi, M., Morris, A. J., Jhon, D. Y., Rhee, S. G., and McLaughlin, S. (1994) Effect of monolayer surface pressure on the activities of phosphoinositide-specific phospholipase C-beta 1, -gamma 1, and -delta 1, *Biochemistry 33*, 3032-3037.
21. Aanismaa, P., and Seelig, A. (2007) P-Glycoprotein Kinetics Measured in Plasma Membrane Vesicles and Living Cells, *Biochemistry 46*, 3394-3404.
22. Moran, O., and Zegarra-Moran, O. (2008) On the measurement of the functional properties of the CFTR, *J Cyst Fibros 7*, 483-494.
23. Afzal, I., Cunningham, P., and Naftalin, R. J. (2002) Interactions of ATP, oestradiol, genistein and the anti-oestrogens, faslodex (ICI 182780) and tamoxifen, with the human erythrocyte glucose transporter, GLUT1, *Biochem J 365*, 707-719.
24. Gerebtzoff, G., and Seelig, A. (2006) In silico prediction of blood-brain barrier permeation using the calculated molecular cross-sectional area as main parameter, *J Chem Inf Model 46*, 2638-2650.
25. Al-Shawi, M. K., Polar, M. K., Omote, H., and Figler, R. A. (2003) Transition state analysis of the coupling of drug transport to ATP hydrolysis by P-glycoprotein, *J Biol Chem 278*, 52629-52640.
26. Litman, T., Zeuthen, T., Skovsgaard, T., and Stein, W. D. (1997) Competitive, non-competitive and cooperative interactions between substrates of P-glycoprotein as measured by its ATPase activity, *Biochim Biophys Acta 1361*, 169-176.
27. Seelig, A., Landwojtowicz, E., Fischer, H., and Li Blatter, X. (2003) Towards P-glycoprotein structure-activity relationships, In *Drug Bioavailability/Estimation of Solubility, Permeability and Absorption* (Waterbeemd, v. d., Lennernäs, and Artursson, Eds.), pp 461-492, Wiley/VCH, Weinheim.
28. Seelig, A. (1998) A general pattern for substrate recognition by P-glycoprotein, *Eur J Biochem 251*, 252-261.
29. Saito, H., An, R., Hirano, H., and Ishikawa, T. (2010) Emerging new technology: QSAR analysis and MO Calculation to characterize interactions of protein kinase inhibitors with the human ABC transporter, ABCG2 (BCRP), *Drug Metab Pharmacokinet 25*, 72-83.
30. Seelig, A., Blatter, X. L., and Wohnsland, F. (2000) Substrate recognition by P-glycoprotein and the multidrug resistance-associated protein MRP1: a comparison, *Int J Clin Pharmacol Ther 38*, 111-121.

Tables

Table 1. Kinetic constants derived from ATPase activity measurements in buffer (A) and MEMα (B) at pH 7.4 and T = 37°C. The concentration of half-maximum activation (inhibition) K_1 (K_2) and the rate of activation (inhibition) V_1 (V_2) were obtained by fitting eq. 1 to data.

	Compound	Phosphorylation Agent (PA)	C_{PA} [µM]	ECAR increase [%]	K_1 [µM]	K_2 [µM]	V_1 [%]	V_2 [%]
A	Cortisol	CPT-cAMP	25	150	340	880	185	17
	Progesterone	CPT-cAMP	25	160	-	-	-	-
	17β-Estradiol	CPT-cAMP	25	140	60	265	131	71
B	Cortisol	CPT-cAMP	25	130	201	450	180	17
	17β-Estradiol	CPT-cAMP	25	130	5.9	19.9	80	42
	Progesterone	CPT-cAMP	25	130	5.2	54.3	131	12
	Progesterone	CPT-cAMP	50	180	2.6	24.5	144	8
	Tamoxifen	CPT-cAMP	25	130	-	-	-	-
	Progesterone	Forskolin	0.1	150	0.06	1.1	108	9
	Progesterone	Forskolin	10	170	0.04	4.2	102	6
	17β-Estradiol	Forskolin	10	170	2.5	16	102	9

Table 2. Steroid hormone binding to lipid membrane and CFTR

Compound	π_{max} [mN/m]	K_{aw} [1/M]	A_D [Å^2]	K_{lw} [1/M]	ΔG^0_{lw} [kJ/mol]	$\Delta G^0_{tw(1)}$ [kJ/mol]	HBAs[3]	$\Delta\Delta G^0_H$ [kJ/mol]
Cortisol	6	$2 \cdot 10^3$	73 [1]	12.1	-16.7	-32.3	4	-3.9
17β – Estradiol	1.8	$2 \cdot 10^4$	59 [1]	$3.19 \cdot 10^2$	-25.2	-41.4	2	-6.9
Progesterone	9.5	$1.46 \cdot 10^5$	73 [1]	$8.73 \cdot 10^2$	-27.8	-41.7	2	-8.1
Tamoxifen	17.3	$1.31 \cdot 10^6$	63 [2]	$1.58 \cdot 10^4$	-35.3	--		--

[1] Cross-sectional areas, A_D, calculated with Pgpredix (*24*)

[2] Cross-sectional areas, A_D, derived from measurements of the Gibbs adsorption isotherm.

[3] Hydrogen bond acceptor patterns (HBAs (*6*))

Figure Legends

Fig. 1A-C: ECAR of CHO-CFTR cells (filled symbols) and CHO-K1 (open symbols) as a function of time in phosphate buffer at pH 7.4 and T = 37 °C, respectively. The first few points represent the basal ECAR set to 100%. Stimulated with CPT-cAMP (25 μM) induced a fast increase followed by a somewhat slower ECAR increase, respectively. The concentration of CPT-cAMP was kept constant during the subsequent experiments. Cells were stimulated with increasing concentrations of steroid hormones indicated by gray zones until a steady state was reached (5 - 10 min). Cortisol (■) (A), progesterone (●) (B), and 17β-estradiol (▲) (C).

Fig. 2A-C: ECAR as a function of time for CHO-K1 (open symbols) and CHO-CFTR CHO cells measured in MEMα. Stimulation with CPT-cAMP (25 μM), cortisol (■), progesterone (●) and 17β-estradiol (▲). Measurement were performed at pH 7.4 and T = 37 °C.

Fig. 3A-C: Fig. 3A-C: CFTR activity monitored by ECAR measurements in CHO-CFTR cells stimulated by cortisol (■) (A), progesterone (●) (B) and 17β-estradiol (▲) (C). CHO-CFTR cells were measured in buffer (semi-filled symbols), and in MEMα (filled symbols), and CHO-K1 cells in MEMα (open symbols) at pH 7.4 and T = 37 °C in the presence of 25 μM CPT-cAMP.

Fig. 4A: CFTR activity upon stimulation with (A) progesterone, (B) 17β-estradiol and different phosphorylation agents and concentrations. A: 25 μM CPT-cAMP (●), 50 μM CPT-cAMP (○), 0.1 μM Forskolin (⊗) and 10 μM Forskolin (◗).

Figures

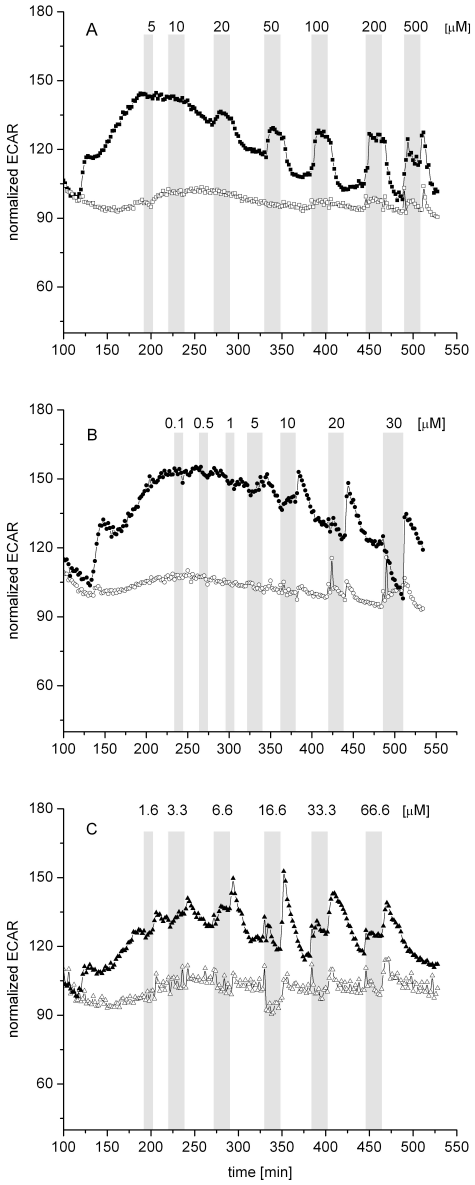

Fig. 1 A-C

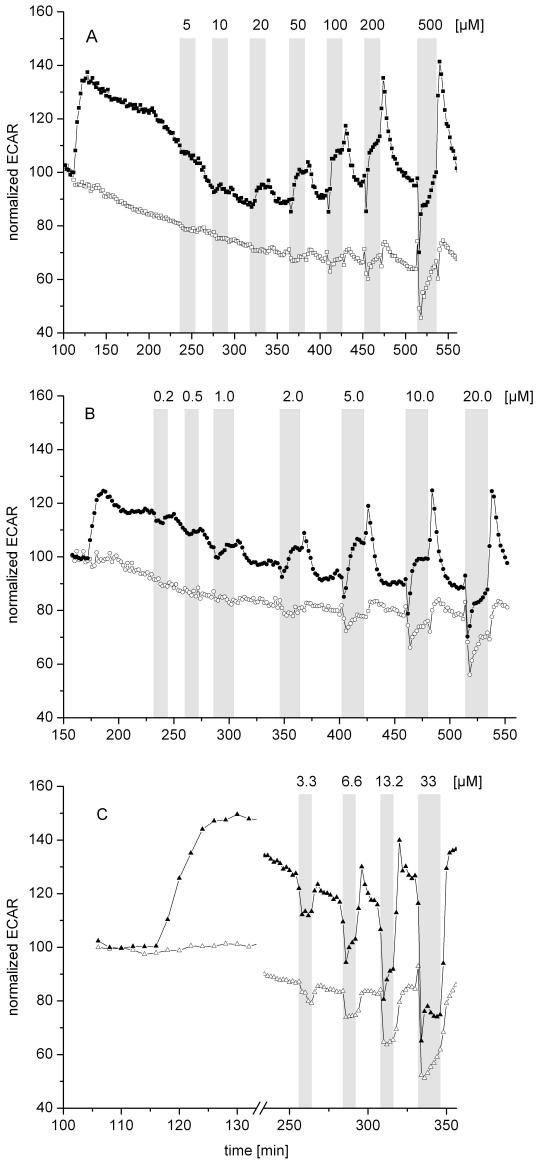
A
5 10 20 50 100 200 500 [µM]
normalized ECAR
B
0.2 0.5 1.0 2.0 5.0 10.0 20.0 [µM]
normalized ECAR
C
3.3 6.6 13.2 33 [µM]
normalized ECAR
time [min]

Fig. 2 A-C

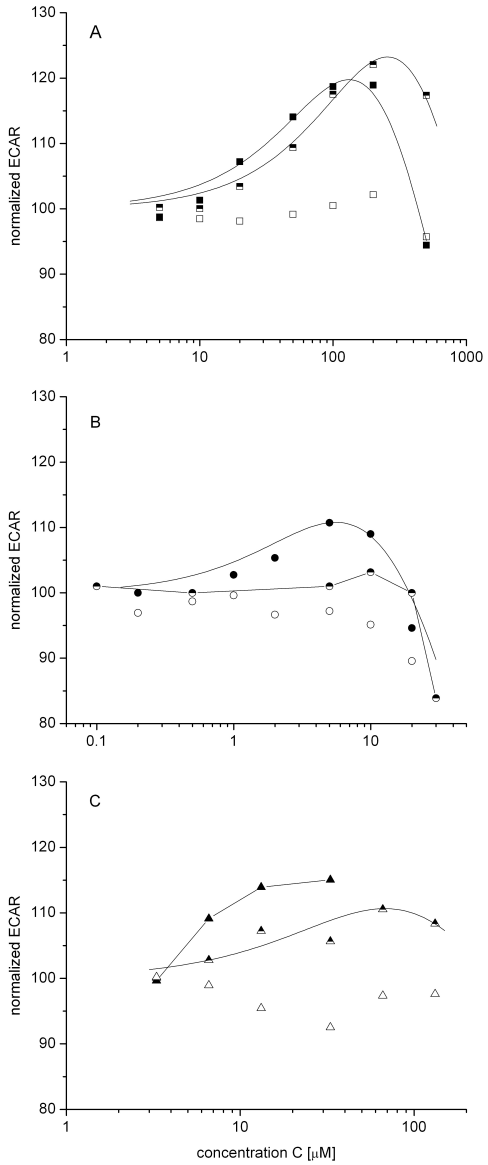
A
B
C
normalized ECAR
normalized ECAR
normalized ECAR
concentration C [µM]

Fig. 3 A-C

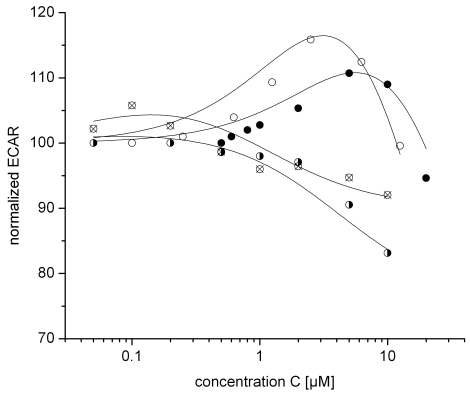
120
110
100
90
80
70
normalized ECAR
0.1
1
10
concentration C [µM]

Fig. 4

9 Declaration

I declare that I have written this thesis “Towards an Understanding of CFTR Regulation by ATP Hydrolysis” with the help indicated and that I have only submitted it to the Faculty of Science of the University of Basel and to no other faculty or university.

Basel, 31.1.2012

_____

Matthias Zwick